FRICTION ANALYSIS IN HOT FORGING PROCESS

A MASTER'S THESIS

In

Manufacturing Engineering

Atılım University

By

SERAP ÇAĞLAR ALKAN

JULY 2012

FRICTION ANALYSIS IN HOT FORGING PROCESS

A THESIS SUBMITTED TO

THE GRADUATE SCHOOL OF NATURAL AND APPLIED SCIENCES

OF

ATILIM UNIVERSITY

BY

SERAP ÇAĞLAR ALKAN

IN PARTIAL FULFILLMENT OF THE REQUIREMENTS FOR THE DEGREE OF

MASTER OF SCIENCE

IN

THE DEPARTMENT OF MANUFACTURING ENGINEERING

JULY 2012

Approval of the Graduate School of Natural and Applied Sciences, Atılım University.

_____

Prof. Dr. İbrahim AKMAN

Director

I certify that this thesis satisfies all the requirements as a thesis for the degree of Master of Science.

_____

Prof. Dr. Bilgin KAFTAOĞLU

Head of Department

This is to certify that we have read the thesis "Friction Analysis in Hot Forging Process" submitted by "Serap ÇAĞLAR ALKAN" and that in our opinion it is fully adequate, in scope and quality, as a thesis for the degree of Master of Science.

_____	_____
Asst. Prof. Dr.Celalettin KARADOĞAN	Prof. Dr. Bilgin KAFTANOĞLU
Co-Supervisor	Supervisor

Examining Committee Members

Prof. Dr. Bilgin KAFTANOĞLU	_____
Assoc. Prof. Dr. Tolga AKIŞ	_____
Asst. Prof. Dr.Celalettin KARADOĞAN	_____
Asst. Prof. Dr. A Hakan ARGEŞO	_____
Asst. Prof. Dr. Besim BARANOĞLU	_____

Date: July 26, 2012

I declare and guarantee that all data, knowledge and information in this document has been obtained, processed and presented in accordance with academic rules and ethical conduct. Based on these rules and conduct, I have fully cited and referenced all material and results that are not original to this work.

Serap ÇAĞLAR ALKAN

Signature:

ABSTRACT

FRICTION ANALYSIS IN HOT FORGING PROCESS

ÇAĞLAR ALKAN, Serap

M.S., Manufacturing Engineering Department

Supervisor: Prof. Dr. Bilgin KAFTANOĞLU

Co-Supervisor: Asst. Prof. Dr. Celalettin KARADOĞAN

July 2012, 92 pages

Forging operations are widely used for manufacturing processes. In forging operations, reducing the friction with changing parameters is quite important to obtain perfectly smooth, frictionless dies. The aim of this study is to evaluate the ring test as a method for determining friction factors for aluminum under hot forging conditions. In the experimental study, several different tests have been improved with different conditions to determine interfacial friction. On the basis of process parameters and die geometry supplied by AYDINLAR Aluminum Company, full scale computational models of the process have been constructed by using MSC Marc v.2010 FEA package. The necessary material characterization has been done by dilatometer test device for different temperatures and strain rates. Mathematical description of flow stress of examined aluminium alloys determined according to optimum match of the shape of the experimental curve. Calibration curves have been obtained with respect to finite element simulations. The measured stress-strain diagrams compared with the computational results. These results indicate that reasonable good agreement between the measured data and computational results can be achieved provided that the Finite Element Method is used.

Keywords: Hot Forging, Aluminum Forging, Ring Compression Test, Metal Forming, Press Forging, Friction, Finite Volume Analysis.

ÖZ

SICAK DÖVME İŞLEMİNDE SÜRTÜNME ANALİZİ

ÇAĞLAR ALKAN, Serap

Yüksek Lisans, İmalat Mühendisliği Bölümü

Tez Yöneticisi: Prof. Dr. Bilgin KAFTANOĞLU

Ortak Tez Yöneticisi: Yrd. Doç. Dr. Celalettin KARADOĞAN

Temmuz 2012, 92 sayfa

Dövme operasyonları yaygın olarak üretim süreçleri için kullanılır. Dövme operasyonlarında, parametreleri değiştirme ile sürtünme azaltmak tamamen pürüzsüz, sürtünmesiz kalıplar elde etmek için çok önemlidir. Bu çalışmanın amacı sıcak dövme koşulları altında alüminyum için sürtünme faktörlerini belirlemek için halka testini değerlendirmektir. Bu deneysel çalışmada, birçok farklı testler ara yüzey sürtünme belirlemek için farklı koşullar ile geliştirilmiştir. İşlem parametreleri ve kalıp geometrisi AYDINLAR Alüminyum tarafından sağlanmış ve model Sonlu Elemanlar Analiz yöntemine dayalı MSC Marc v.2010 yazılım paketinde hazırlanmıştır. Gerekli malzeme karakterizasyonu dilatometre test cihazı tarafından farklı sıcaklık ve gerinme hızlarında elde edilmiştir. İncelenen alüminyum alaşımın akma gerilmesinin matematiksel tanımı deneysel eğrinin şekli ile en yüksek uyum göstermesine bağlı olarak karar verilmiştir. Kalibrasyon eğrileri sonlu elemanlar analizinden elde edilmiştir. Ölçülen gerilim-gerinim grafikleri hesaplanan sonuçlar ile karşılaştırılmıştır. Bu sonuçlar göstermiştir ki, Sonlu Elemanlar yöntemi ile elde edilen sonuçlar gerçek işlemde ölçülen değerlere yakın çıkmaktadır.

Anahtar kelimeler: Sıcak Dövme, Alüminyum Dövme, Halka Basma Testi, Metal Şekillendirme, Dövme Presi, Sürtünme, Sonlu Hacim Analizi.

To My Family

ACKNOWLEDGEMENTS

I would first like to thank my supervisor Prof. Dr. Bilgin KAFTANOĞLU for his continuous guidance and encouragement throughout the duration of this thesis. I was very lucky to work under him as his student.

I would like to express my gratitude to my thesis co-supervisor Asst. Prof. Dr. Celalettin KARADOĞAN for giving me the opportunity to prepare this thesis, and his continuous help, encouragement, valuable discussions, guidance and patience.

This study was carried out at ATILIM Metal Forming Centre of Excellence and I sincerely thank to the engineers and technicians of ATILIM Metal Forming Centre of Excellence especially thank to Deniz DURAN and Yahya TUNÇ. This project was determined according to the needs of the AYDINLAR Company so I would like to thank AYDINLAR Company for providing such a useful topic to work.

I also appreciate for their participation in dissertation committee: Prof. Dr. Bilgin KAFTANOĞLU, Asst. Prof. Dr. Celalettin KARADOĞAN, Asst. Prof. Dr. Ahmet Hakan ARGEŞO, Asst. Prof. Dr. Besim BARANOĞLU and Assoc. Prof. Dr. Tolga AKIŞ.

I wish especially to thank to my dear friend Celal Onur ALKAS for his significant support and encouragement. Special thanks go to my friends, Ceren Merve KARAKAS and Doğan AKSUNGUR for their valuable supports.

Finally; I wish to express my sincere thanks to my family for their support.

TABLE OF CONTENTS

LIST OF TABLES

LIST OF FIGURES

LIST OF ABBREVIATIONS

Al	Aluminum
Cr	Chromium
Cu	Copper
Mg	Magnesium
Mn	Manganese
Si	Silicon
Ti	Titanium
Zn	Zinc
Fe	Ferrous
D	Diameter
FE	Finite Element
FEM	Finite Element Method
FV	Finite Volume
FVM	Finite Volume Method
L	Length
2D	Two Dimensional
3D	Three Dimensional

NOMENCLATURE

σ_f *(u)*	True stress
h_o	Initial height of the specimen
h (u)	Actual height of the specimen
A_0	Initial cross-sectional area
$A_{(u)}$	Current cross-sectional area
$\varepsilon_{(u)}$	True strain
ε_E	Engineering strain
σ_E	Engineering stress
r_0	Original diameter of the specimen
$r_{(u)}$	Current diameter of the specimen
T_d	Die temperature
m	Friction factor
τ	Shear stress
τ_{yield}	Shear yield stress
μ	Coefficient of friction
q	Local normal pressure
k	Shear flow stress
F	Force

CHAPTER 1

INTRODUCTION

1.1 Necessity of This Study

In metal forming operations; friction has a great importance since it affects the forming force, material flow inside the die, product quality and tool lives. Determination of the friction condition is important when obtaining flow curves for the material under formability investigations. One of the most common methods is the free ring compression method. This method, since it is used in determining coefficient /factor of friction in modeling experiments in plastic deformation, will be explained in detail in the following section. Ring compression test will be applied according to four different parameters change and determining friction coefficients according to these parameters. The aim of this study is to evaluate the ring test as a method for determining friction factors for aluminum under hot forging conditions. Graphic dependence between height strain and inner diameter strain, at various influences of friction, gives calibration curves for reading the value of coefficient/ factor of friction. Two dimensional finite element analyses have been performed to simulate the hot forging process of rings. The simulations show how temperature, press velocity, reduction of material and lubrication existence factors affect metal flow and ring geometry. Simulation results of the various tests compared with experimental results and results are consistent with observed results.

1.2 Scope of the Thesis

The outline of the thesis is as follows:

- Chapter 1 gives information about necessity of this study.
- Fundamental definitions of forging with their classifications, forging defects, previous studies and an overview of hot forging process, details of the workpiece material, tools and tool steels will be given in Chapter 2. The

friction theories and friction models in bulk metal forming are introduced and give information about effects of friction on formability. This chapter includes the review of ring compression test.

- The experimental studies related to the analysis of friction in hot forging operations are given in Chapter 3.
- A detailed analysis of forging process of the aluminum 6082 will be performed in Chapter 4. Results of the finite element analyses will also be given in this chapter.
- Finally, discussions and general conclusions will be given in Chapter 5.

CHAPTER 2

LITERATURE SURVEY

2.1 Forging Process

Forging is defined as a bulk, plastic deformation process. Since, there is significant change in the thickness of the workpiece as compared to a sheet metal process; it is called bulk deformation process [1]. In the forging process the metal may either be upset or squeezed in closed impression dies. When metal is compressed, its length increases and its cross section decreases. When metal is upset, it causes increase in length and decrease in section, or if it squeezed in closed impression dies multi directional flow occurs [2].

In forging process, simple billet geometry is turned into a complex geometry by applying required pressure on material with forging machines. It usually produces little or no scrap and produce final part geometry in a very short time. This process causes deformation on the material and this deformation is achieved by hammer, press, upsetter or ring roller. The form is attached with the tools that come into contact with the workpiece and the careful monitoring of the deformation process.

Forging process usually requires expensive tooling. When large number of parts must be produced, the process is economical. However, forging process proposes possible savings in energy and material, especially in medium and large production quantities, where tool costs can be easily amortized [3].

Forging is preferred in industry that because of having some basic advantages as improved mechanical properties, inherent high strength and structural integrity, reduced material waste, cost-efficient production of complex shapes. Combination parts can be forged in one step, optimum grain flow can be obtained and also providing the higher strength- to-weight ratio. The most common applications are in automotive, aerospace, metalworking, power generation industry, space vehicles, electric power generation systems, compressors and construction industry.

2.1.1 Classification of Forging

Forging operation is classified according to type of die set as closed die or open die forging, type of forging temperature as hot forging, cold forging or warm forging and forging machine type as hammer, mechanical press, hydraulic press, screw press or upsetter.

2.1.1.1 Classification of Forging According to Type of Die Set

There are two types of forging operations exists according to die sets which are open die forging and closed die forging. In open-die forging process (common names include upsetting or upset forging), dies do not surround the workpiece. Open die forging process allows grain flow in one or two directions. The workpiece is generally compressed in the axial direction as a result of direction of the movement of the upper die. The operator needs to position the workpiece to get the desired shape. There are several types of dies used in open die forging process such as standard flat, V-shaped, concave or convex dies.

In open die forging process, produced parts have lesser accuracy and dimensional tolerance than those in closed die forging process [3]. According to the rule of material volume conservation the height of the workpiece is decreased and cross-section area is increased [4] as shown in Figure 2.1.

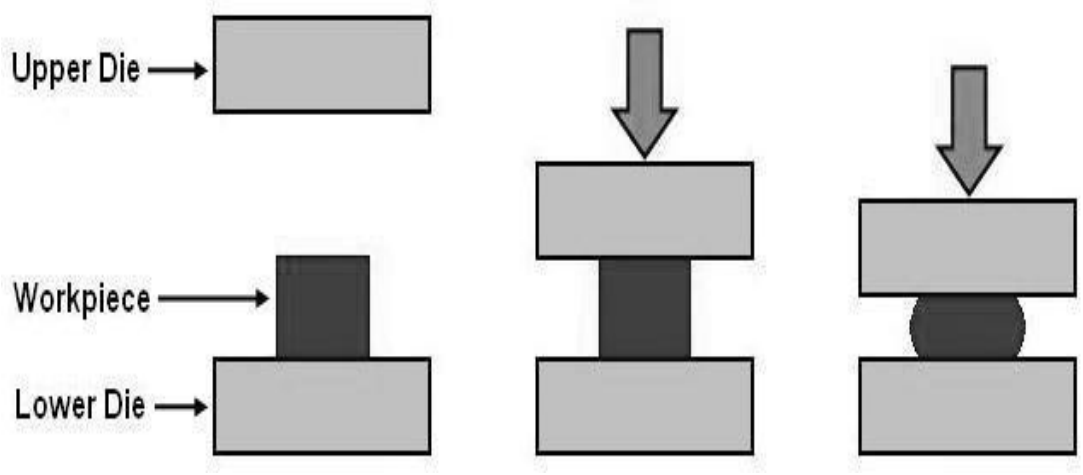

Figure 2.1: Illustration of Open Die Forging Process

Closed die forging is also called impression-die forging. Closed die forging is basically the shaping of metals in between closed die cavities as shown in Figure 2.2. The

forging die is dropped on the workpiece, causing the metal to flow and fill the die cavities. Excess metal is squeezed out of the die cavities which is called flash. According to the size and complexity of the part, the forging machine may be dropped multiple times in quick succession.

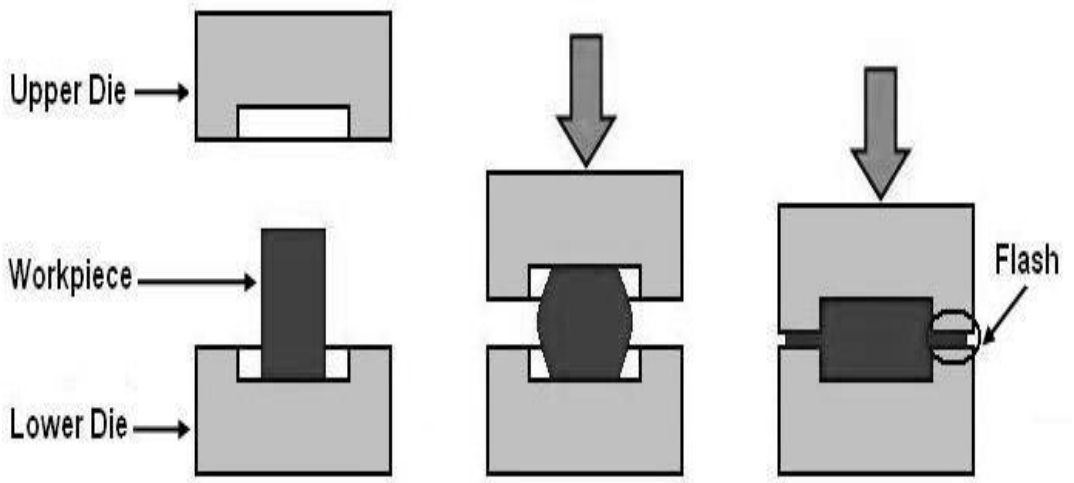

Figure 2.2: Illustration of Closed Die Forging Process

Possible advantages of closed die forging process include:

- More complex shape parts are produced by closed die forging
- Satisfactory improvement in properties
- Quality of material can be improved
- Higher production rates
- Greater strength
- Minimum flash needed for the ideal design

Some possible disadvantages of closed die forging process include:

- Additional cost due to more complex die design
- Better lubrication is necessary
- Not capable of close tolerances
- Mostly needs removal of the flash with a trimming die
- If flash completely fill of the cavity, it will causes extremely high die pressures in the flash area. High pressures reduce die life and require additional power.

2.1.1.2 Classification of Forging According to Temperature

There are three types of forging operations exists according to temperature which are cold, hot and warm forging. Cold forging is done at room temperature or near room temperature. Cold forging is generally used for simple geometries. There are some advantages of cold forging processes which are listed below [5]:

- No heating required
- Improves mechanical properties of the material
- Better surface finish
- Greater dimensional accuracy is achieved.
- Elimination of annealing before forging
- Contamination problems are minimized.
- Superior dimensional control
- Production rates are very high.
- Economic advantages compared to hot forging operation
- Better reproducibility and interchangeability

There are some disadvantages of cold forging processes which are listed below [6]:

- Higher forces are required, so more powerful equipment is necessary.
- Metal is less ductile
- Undesirable residual stress may be produced.

Warm forging is done at intermediate temperature between its recrystallization temperature and work hardening temperature. In warm forging process better dimensional tolerances can be obtained than hot forging process. Warm forging takes the advantages of reduces loads on tooling and increases material ductility than cold forging process.

Hot forging is done at high temperature which is above the recrystallization temperature. Benefits of hot forging processes are listed below [5]:

- Easier to work and requires less force
- Forging complex shapes easily
- Good formability
- Ductility increase

- Elevated temperatures increase diffusion which can remove or reduce chemical inhomogeneity
- Low forming pressures required
- Pores may be reduced in size or closed completely during deformation
- Die wear is reduced and dimensional accuracy is low in hot forging process.

The main disadvantages of hot forging operations are:

- Less precise tolerances due to thermal contraction
- Formation of the scale and causes grain structure to vary throughout the metal.
- Lower dimensional accuracy can be obtained.
- Requirement of heating is necessary.

2.1.1.3 Classification of Forging According to Press Type

Forging processes are classified according to the equipment used and principle of the operation. Various types of forging machines are shown in Figure 2.3. These are [7]:

- Hammer Forging (Board Drop Hammers, Power Drop Hammers, Air-Lift Gravity Drop Hammers, Counterblow Hammers)
- Press Forging (Mechanical Presses, Hydraulic Presses, Multiple Ram Presses, Friction Screw Presses)
- Horizontal Forging Machine
- Roll Forging

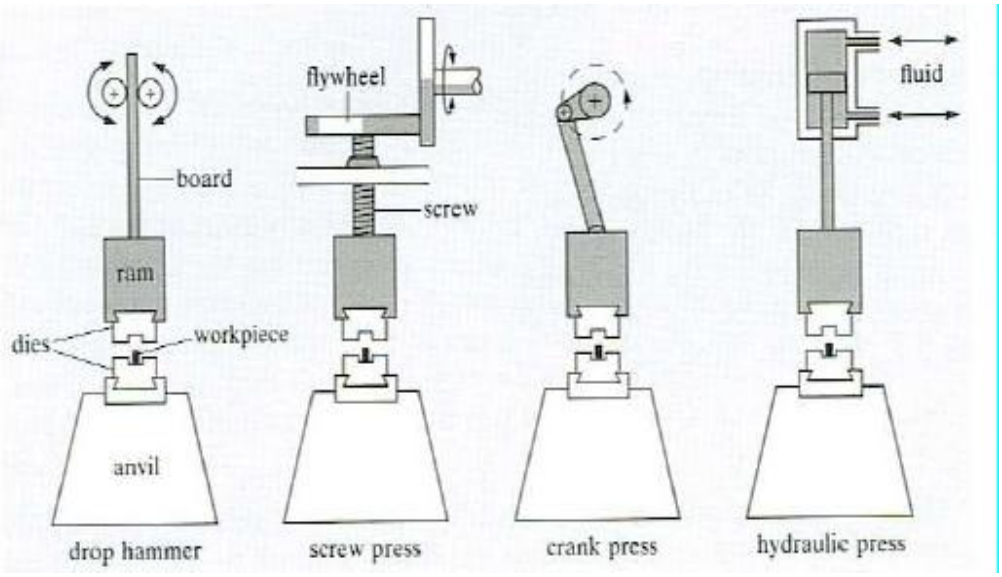

Figure 2.3: Various Types of Forging Machines [8]

Forging hammer (drop hammer) is most widely used forging equipment. Hammer can compresses between 60 and 150 blows per minute depending on size and capacity [9]. Hammers are energy-restricted machines. They are energy limited because it obtains their energy from the potential energy. The maximum nominal energy cannot be completely used for forming. Due to friction at the slides and elastic deformation on the dies, energy loses occur. In hammer forging operation, the workpiece is placed on lower die. The main components of a hammer are ram, frame assembly, anvil and anvil cap. The anvil is directly connected to the frame assembly, the upper die is attached to the ram and lower die is attached to the anvil cap. Forging hammers put in force by the large ram. The ram moves downward and applies force on the anvil. Consequently it causes the workpiece to deform.

Forging hammers can be classified according to the method used to drive the ram. There are two types of hammers, which are board hammer and power hammer. In the board hammer the upper die and ram are raised by friction rolls gripping the board as shown in Figure 2.4. When the board is released, the ram falls under the influence of gravity to produce the blow energy. The board is immediately raised again for another blow.

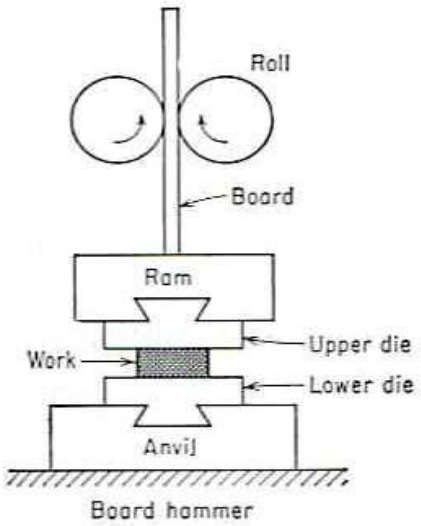

Figure 2.4: Drawing of Board Hammer [8]

Power hammer (Figure 2.5) provides greater capacity. The ram is accelerated on the down stroke by air pressure or stream in addition to gravity. Steam or air pressure is also used to raise the ram on the upstroke. In gravity drop hammer, impact energy is provided from the falling weight of a heavy ram. Die forging hammers are similar in operation to power-drop hammers, but have shorter strokes and more rapid striking rates. The disadvantage of this

process is close dimensional tolerances cannot be obtained also finish machining is often required [9].

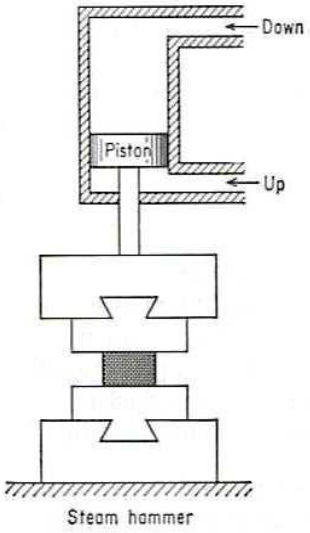

Figure 2.5: Drawing of Power Hammer [8]

Forging presses can produce all types of forging parts produced by hammers. Forging can produce parts nearer the desired shape. In addition, less noise and vibration is developed compared to forging hammers [10]. The other advantage is if large production numbers are needed, press forging is more economical than hammer forging. Forging presses are divided into two types which are mechanical or hydraulic design.

The mechanical forging press is an efficient machine and it is the most widely used equipment for closed-die forging (Figure 2.6). Mechanical presses are displacement-restricted machines. The stroke of mechanical presses is shorter and ram velocity is slower.

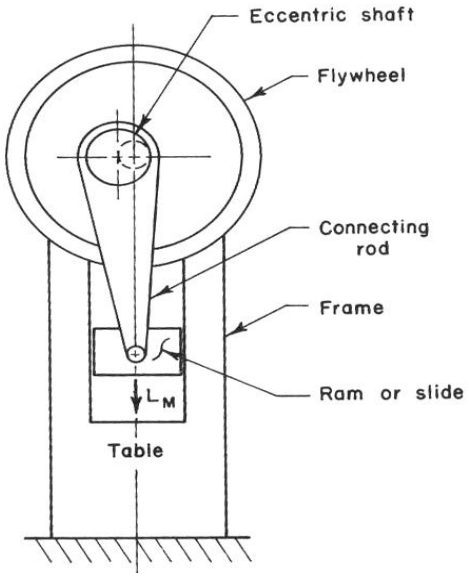

Figure 2.6: Drawing of Mechanical Forging with Eccentric Drive [7]

Hydraulic presses are force-restricted machines. It is capable of deforming the material depending on the maximum force rating of the press. Capacities of hydraulic presses range from 300 to 50000 tons [11]. The hydraulic forging press forges the metal by giving continuous forming at a slower rate. It provides deeper penetration. Contact time is longer at the die-meal interface and pressing speed can be controlled. In hydraulic presses, the maximum press load is useable at any point during the entire ram stroke.

Screw-type presses are classified as energy-restricted machines. Screw presses use energy stored in a flywheel to provide the force for deforming the workpiece. Flywheel's rotational energy is converted to linear motion by a threaded screw attached to the flywheel on one end and to the ram on the other end. Also impact speed is much greater than with mechanical presses.

The crank and eccentric presses are displacement-restricted machines. The slide velocity and the available slide load vary in accordance with the position of the slide before the bottom dead center. Table 2.1 gives some information about energy ratio and load rating of different presses.

Table 2.1: Energy Ratio and Load Rating of Different Presses [8]

Machine Type	Load rating F/kN	Available energy per blow. W/kJ	Ratio W:F/m×10^{-3}
Drop Hammer	12 250	1.6	1.3
Friction Screw Press	12 250	8.0	6.4
Crank Press	12 250	20	16
Hydraulic Press	12 250	250	200

Speed of the ram of the press is also an important factor. This directly influences the strain rates during forming. Velocity ranges for some types of forging machines are given in Table 2.2.

Table 2.2: Some Types of Forging Machines Velocity Range [8]

Forging Machine	Velocity Range, (ms^{-1})
Gravity Drop Hammer	3.6-4.8
Power Drop Hammer	3.0-9.0
HERF Machine	6.0-24.0
Mechanical Press	0.06-1.5
Hydraulic Press	0.06-0.30

The contact time under pressure is especially important for warm and hot forging processes since it determines the cooling amount of the workpiece. Required contact times under pressure for some types of forging machines are given in Table 2.3.

Table 2.3: Required Contact Times Under Pressure for Some Types of Forging Machines [12]

Press Type	Contact Times Under Pressure(s)
Hammers	10^{-3} - 10^{-2}
Screw Press (with Fly-wheel)	10^{-2} - 10^{-1}
Stroke Controlled Presses	10^{-2} - 10^{-1}
Hydraulic Presses	10^{-1} - 1

2.1.2 Forging Defects

The formations of defects are due to many possible reasons and the conditions for defects are quite complex. These defects depend on part designs, tool designs and process conditions such as the state of lubrication, location of the preformed workpiece on the die and formability of materials. Forging engineers always try to eliminate any defects during manufacturing of parts. There are several defects that can occur during forging. These include:

- **Unfilled Section:** The main problem is some sections of the die cavity are not completely filled by the flowing metal. Unfilled Section occurs due to improper design of the forging die or using improper forging techniques.
- **Cold Shut:** Cold shut defect appears as small cracks at the corners of the forging. It occurs due to improper design of die. If metal does not flow properly into the corner when corner and fillet radii are small, cold shut defect appears.
- **Laps and Folds:** This defect occurs due to the improper die design. Forging laps occur onto the final part which is very much undesirable because they distort the surface finish and lead to a weakening of the product due to internal or external cracks.
- **Flakes:** Flakes are very fine internal cracks of circular shape. This defect occurs due to improper cooling of the large forging. Rapid cooling leads to the external cooling quickly causing internal fractures.
- **Scale Pits:** This defect appears as irregular deputations on the surface of the forging. This defect occurs due to improper cleaning of the stock used for forging. The oxide and scale gets embedded in the final forging surface.

- **Centre Bursts:** Centre burst is a rupture that occurs in the central region of a forging. This defect arises due to incorrect forging procedure (e.g. too low temperature or too severe reduction), presence of segregation or brittle phase in the metal being forged.
- **Die Shift:** This defect occurs due to the misalignment of the die halve, making the two halve of the forging to be irregular shape.
- **Improper Grain Flow:** This defect appears due to the improper design of the die which makes the flow of the metal in the wrong direction.
- **Clinks (Thermal Cracks):** Thermal cracks occur due to stresses arising from excessively high temperature gradients within the material.
- **Hot Tears:** This defect appears due to metal being ruptured and pulled apart during forging. The presence of local segregation, seams or brittle phases may cause the defect formation.
- **Seams:** This defect is identified as surface irregularities on the slab or billet which are stretched out during rolling. This defect occurs due to improper rolling which is caused by folding of the metal.

Possible forging defects description and caused problems can be summarized in Table 2.4.

Table 2.4: Possible Forging Defects Description and Caused Problems [13]

Possible Forging Defects		
Defect	**Description**	**Problem**
Segregation	Non-uniform distribution of elements in metal	Non-uniform hardness
High-Hydrogen Content	Forms of hydrogen fissures (flakes)	Embrittlement
Inclusions	Nonmetallic particles in metal	Act as stress-raisers; make machining difficult (tool breakage)
Bursts	Internal tears (effect of forging operations on inclusions, etc.)	Cracking
Poor Grain Structure	Overheating, improper billet size, poor die design, etc.	Poor properties in crucial directions; fatigue failure
Laps (folds)	Hot metal folded over and forged into surface, creating discontinuity	Stress-raisers; may cause machining or heat treat cracking problems
Seams	Hot surface tears in original ingot; embedded scale, etc.	Stress-raisers
Cold Shuts	Defective metal flow	Low strength
Cracks, Tears	Internal discontinuity (poor design; poor practice – metal too cold, etc.)	Cracking

2.1.3 Usage of CAD/CAM/CAE for Analysis of Forging Process

In recent decades Computer Aided Design (CAD), Computer Aided Manufacturing (CAM) and Computer Aided Engineering (CAE) methods have been used in every stage of forging process due to rapid and cost-effective process design and die manufacturing.

CAE programs used in simulation of the forging process are mainly based on Finite Element Method (FEM) and Finite Volume Method (FVM). FEM/FEA is the most widely applied computer simulation method in engineering. FEM is used in problems where analytical solutions are not easily obtained.

Recently, finite element (FE) simulation software has become an integral part of forging process design to develop the die design and conduct die stress analysis, to analyze and optimize the metal flow, preventing flow-induced defects such as laps, predicting temperatures so that part properties, considering the friction conditions can be accomplished. The role of FEM in forging process design is shown in Figure 2.7.

The accuracy of FE simulation depends on dependable input data as follows:

- CAD data of the die geometry,
- Characteristics of the forging equipment used,
- Flow stress of the deforming material to perform strain, strain rate and temperature in the range related to the process being analyzed,
- Friction characteristics at the interface between the workpiece and the die.

The main goal of simulation in manufacturing process design is to reduce part development time and cost considerably, optimizing product design, providing better understanding of material behavior, reduce material waste, improving product quality and increasing die life.

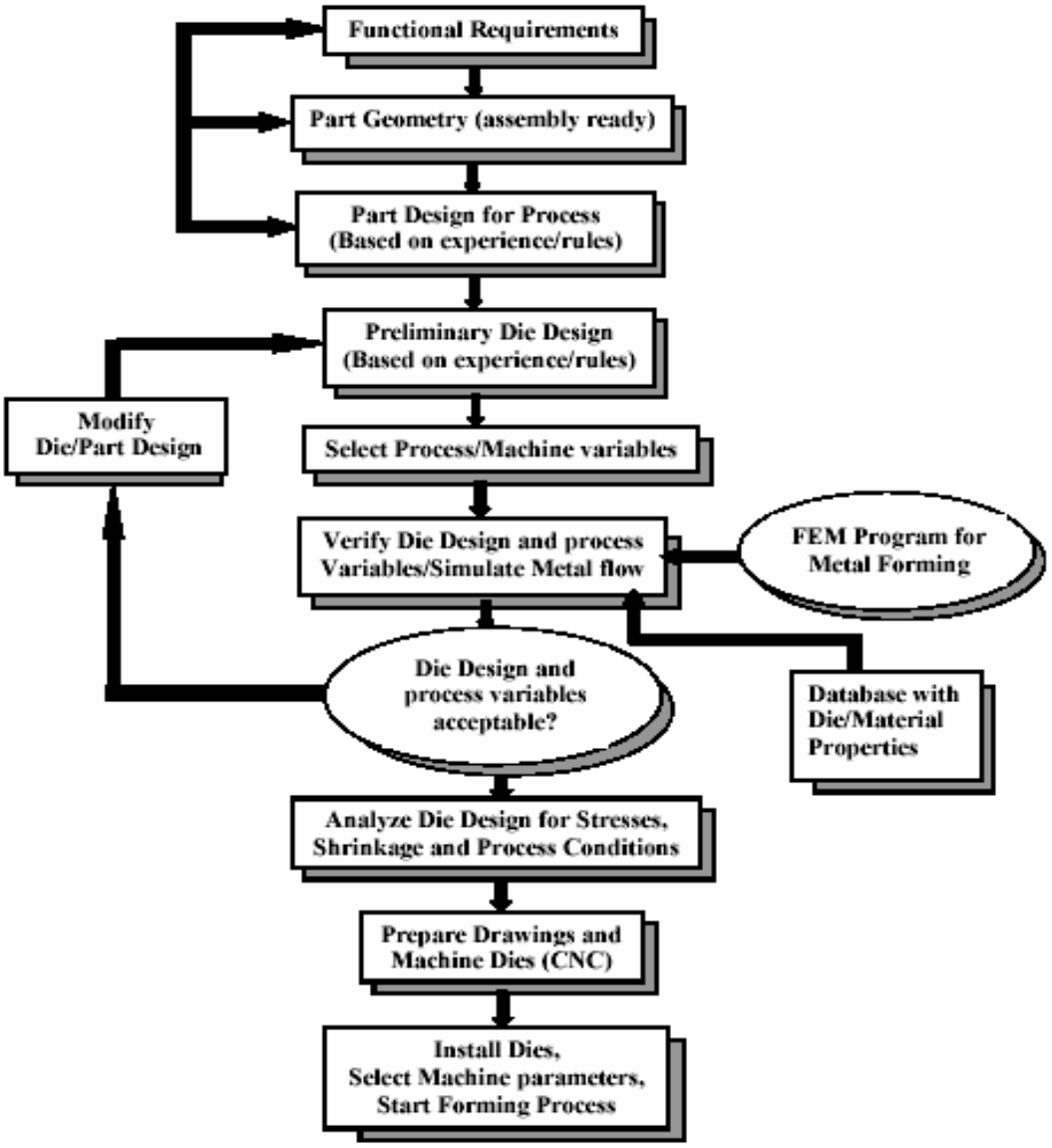

Figure 2.7: The Role of FEM in Forging Process Design [14]

2.1.4 Previous Studies on Forging

A. Thomas, M.El-Wahabi, J.M. Cabrera, J.M. Prado [15] studied on the aging characteristics of Inconel 718 and examined the characterization of the hot forming behavior of this material. Vickers hardness test helped to evaluate presence of precipitation. Experimentally this material annealed from 100 to 600C˚ during different holding times which are 5, 30, 60 and 180 min.

Behrens [16] investigated the thermal effects on the hardness of the tool material and used a finite element model to evaluate the wear. Based on the measured and computed wear

at the mandrel between 1000 and 2000 forging cycles, the curves of measurement and simulation gave results very close to each other.

William R.D. Wilson, Steven R. Schmid, Jiying Liu [17] studied on heat flow which occurred by temperature difference between the workpiece and tooling in forging operations and calculated an effective heat transfer coefficient based on lubricant, material and process types.

M.S. Joun, H.G.Moon, I.S.Choi, M.C.Lee, B.Y.Jun [18] worked on the ring compression test for two different materials and evaluates the two friction laws which are the coulomb friction law and the constant shear friction law. These two friction laws were compared and their effects on metal flow lines using a rigid-plastic finite element method were evaluated.

Hasan Sofuoğlu [19] worked on the effect of material properties, strain-rate sensitivity and barreling on the behavior of friction calibration curves and used ABAQUS finite element code to obtain the necessary material properties. In this experiment he used different materials and showed that friction calibration curves were affected by material properties.

Japanese researchers, Kaguchı, Tezuka, Yoshıno, Ouchı and Watanabe [20] investigated the effectiveness of in si-tu measurement method which is adjusted to ring compression test. In si-tu measurement is data reading method of deformation in height and change the outer diameter of ring work-piece. The test provides the values of the coefficient of friction in the middle of the compressive strain of the ring workpiece.

Ishızuka and Mızutanı [21] studied the mechanism of friction between the hard hemispherical surface and smooth soft surface. Soft surface has been theoretically analyzed in the light of the friction caused by plowing and shearing. The coefficient of friction for the smooth soft surface increases with increasing contact angle which gets from the radius of curvature and the depth of indented hemispherical projection.

Keith P.Savage [22] worked on the ring compression test for determining the friction coefficient for steel under hot forging condition materials and evaluated the test for different lubricants and forging conditions.

Petersen, Martins and Bay [23] studied on the use of general friction model which is developed by Wanheim and Gulf and suggested a significant improvement in the ability to model processes where tool workpiece interface stresses may prevail low.

Y.G An and H.Vegter [24] worked on the frictional behavior of oiled polytetrafluoroethyloene film (PTFE) and the effect of friction has been determined using the compression ring and cylindrical compression tests. The results showed that oiled PTFE film

gives constant friction under compression for the strain interval of about 20%; the shear strength of the film is 10.3MPa, provided that the film is not damaged.

Prof. Dr.-Ing. Bernd-Arno Behrens, Dr.-Ing. Anas, Dipl.-Ing. Falko and André [25] studied using numerical analysis on thermal-mechanical fatigue of hot forging dies. Experimentally, certain areas of the geometry were examined due to the determination of the wear progress. Tempering curves for hot work steel were acquired from technical data of forging experiment. The curves were used in the Finite-Element computational model. Finite-Element (FE) computational model approach for die wear calculation was verified based on real experimental result.

R.S. Lee and J.L. Jou [26] studied on the wear of warm forging die which is predicted by numerical simulation method and verified based on experimental techniques. They used DEFORM which is a FEM code to analyze the warm forging. Also they worked on non-isothermal ring compression test for determining the friction coefficient under warm forging condition materials and evaluated the test for different temperatures and used temperature recording system during the test due to estimated correct heat transfer coefficient of the interface. Therefore, high temperature wear experiments were established to obtain functions varying with temperature. Experimental study and analysis of material showed that if the maximum dimension variable is 1.0 mm, die life is only about 3500 and if the most worn depth is near 1.5 mm, it must be performed after 5000 forging.

Lirio Schaeffer, Alberto M.G.Brito and Martin Geier [27] worked on analyzing two forging processes which are hot and cold forging. The hot forging process is performed at 1200 C° temperature and it is possible to forge the component without flash. This results in a saving of about 5% in material. Also in cold forging process tool failure occurred due to excess load. In both cases, the material DIN 1.7131(16 MnCr5) steel and the commercial software QForm 3D version 3.2.1.1 are used. In both processes, they analyzed the results of simulation and industrial results gave results very close to each other.

Prof.A. Erman Tekkaya [28] studied on possible sources of errors such as modeling errors, numerical errors, and other errors in a finite element analysis of bulk forming processes. This paper gives some suggestions, some useful elementary knowledge like continuum mechanics concepts, plasticity concepts, finite element method concepts and validation of simulation results.

Bouaziz Z.and Zghal A. [29] worked on an analytic model based on slab method obtaining estimation of the forging load of an aluminum work piece. Finite element software

DEFORM™ was used in simulating the process. The results of finite element simulation showed an excellent correlation with the theoretical prediction.

J.Horsinka, J.Kliber, K.Drozd and I.Mamuzıc [30] studied mathematical description of flow stress of examined aluminum alloys. A computer controlled servo hydraulic compression plastometer has been used as a testing machine for the upsetting test. Experiments were carried out at three temperatures: 360 C°, 400 C° and 440 C°and three strain rates: $0.1s^{-1}$, $1\ s^{-1}$, and $10\ s^{-1}$. The result shows that at higher strains (ε > 0. 7) the curves diverge more meaningfully and their shapes cannot be defined by a single equation, at strain intervals of ε < 0. 5 this model investigated to be the most exact one.

Vesna Mandić and Milentije Stefanovıć [31] worked on ring compression test for determination of coefficient/factor of friction in modeling experiments with plasticine. Several kinds of calibration curves were obtained by FEM simulation of ring compression test. Modeling and real process highly depend on the similarities of contact friction conditions.

2.2 Overview of Hot Forging Process

In hot forging process, the temperature reaches above the recrystallization point of the metal. This kind of high temperature is necessary in avoiding strain hardening of the metal during deformation. Average temperatures necessary for hot forging process are:

- Up to 1150 degrees Celsius for Steel
- 360 to 520 degrees Celsius for Al-Alloys
- 700 to 800 degrees Celsius for Cu-Alloys

Hot forging offers forging complex shapes easily, good formability, low to medium accuracy, homogenized grain structure, elimination of chemical incongruities, low stresses or low work hardening, scale formation and increased ductility. A comparison of the process characteristics of hot, warm and cold forging processes are given in Table 2.5.

Table 2.5: A Comparison of Process Characteristics [32]

	Hot Forging (Die Forging)	Warm Forging	Cold Forging (Extrusion)
Shape Spectrum	Arbitrary	Rotationally symmetrical if possible	Mainly rotationally symmetrical
Used Steel Quality	Arbitrary	Arbitrary	Low alloyed steels C<0.45%
Normally Achievable Accuracy	IT 12- IT 16	IT 9 –IT 12	IT 7- IT 11
Normally Achievable Surface Quality R	>100 µm	< 50 µm	< 10 µm
Economic Lot Size	>500 parts	>10 000parts	>3 000parts
Surface Treatment of the Slugs	Generally none	Generally none or graphite layer	Annealing, phosphating
Intermediate Treatments	None	Generally none	Annealing, phosphating
Tool Materials	Hot work tool steels	Hot work tool steels, high speed steels ,hard metals	Cold work tool steels, high speed steels, hard metals
Tool Life	5000 – 10 000 parts	10 000-20 000 parts	20 000-50 000 parts
Material Utilization	60- 80%	Approx. 86%	85- 90%
Energy Required per kg Forged Part	46-49 J/kg	40 - 42J/kg	40 - 42J/kg

2.2.1 Workpiece Material for Hot Forging

2.2.1.1 General Features of Aluminum

Aluminum is an abundant metallic element which is widely used throughout the world for a wide range of products. Aluminum alloys are widely used in engineering structures and components where light weight or corrosion resistance is required [33]. General aluminum features are summarized as follows:

- Lightweight: Aluminum is one of the lightest available commercial metals with a density one third that of steel or copper.
- Resistance to Corrosion: Aluminum has excellent resistance to corrosion due to the thin layer of aluminum oxide that forms on the surface of aluminum when it is exposed to air.
- High Strength to Weight Ratio: The ratio of the tensile strength of aluminum is higher than any other metal.
- Strong: Mechanical properties can be increased by the addition of alloying elements and tempering.
- Easy to Work: It shows excellent machinability and plasticity ideal for bending, spinning, cutting, forging, drawing and roll forming operations.
- Electrical and Thermal Conductivity: Aluminum is an excellent conductor of both heat and electricity.
- Non-toxic: Aluminum is not only non-toxic but also does not release any odors which it is in contact. This makes aluminum suitable for use in packaging for foods.
- Strong at Low Temperatures: Steel becomes brittle at low temperatures, aluminum increases in tensile strength and retains excellent toughness.
- Easy Surface Treatment: Generally aluminum requires no protective or decorative coating; the surface supplied is entirely adequate without further finishing.
- Reflectivity: Aluminum reflects light and other forms of radiant energy.
- Easy to Recycle: Due to low melting temperature, it is economically recyclable.
- Shock Absorbing: Due to its low modulus of elasticity, aluminum is used for automobile bumpers.
- Sound Absorbing: Used for ceilings.

- Ductility: Aluminum is easy to cold work and fabricate.
- Cost-efficiency: Aluminum processing is inexpensive.

Aluminum is used in many applications. These applications include:

- Transport (automobile, ship, train ,subway ,aircraft, spacecraft),
- Food protection and packaging,
- Building and architecture (building coating systems, windows, doors, various construction),
- Insulation,
- Electricity industry,
- Machinery and equipment manufacturing,
- Chemical and food industry.

2.2.1.2 Aluminum Alloys Chemical Composition

Aluminum mixed with various metals to give a variety of features. Due to tensile strength of pure aluminum is not high, mechanical property can be markedly increased by the addition of alloying elements and tempering. Major alloying elements of aluminum alloy are shown in Table 2.6 and classification is made according to adding metals.

Table 2.6: Major Alloying Elements of Aluminum Alloy [34]

Alloy Groups	Major Alloying Elements
1XXX	Aluminum with 99.0 % minimum purity and higher
2XXX	Copper
3XXX	Manganese
4XXX	Silicone
5XXX	Magnesium
6XXX	Magnesium and Silicon
7XXX	Zinc
8XXX	Other Elements
9XXX	Unused Series

Besides unalloyed aluminum, a large variety of aluminum alloys can be hot forged. Effects of alloying elements are shown in Table 2.7.Examples of commonly hot forged aluminum alloys are:

- Pure or nearly pure aluminum alloys: 1285, 1070, 1050 and 1100.
- Nonhardenable aluminum alloys: 3003, 5152 and 5052.
- Hardenable aluminum alloys: 6063, 6053, 6082, 2017, 2024 and 7075.

Table 2.7: Effect of Alloying Elements ([35], [36])

Alloy Groups	Effect of Alloying Elements
1XXX	• Pure aluminum with a minimum 99% aluminum content by weight and can be work hardened.
2XXX	• Can be precipitation hardened to strengths comparable to steel. • Susceptible to stress corrosion cracking and are increasingly replaced by 7000 series in new designs. • Series do not have as good corrosion resistance as most other aluminum alloys.
3XXX	• Widely used as general-purpose alloys • Moderate-strength applications requiring good workability.
4XXX	• Aluminum-silicon alloys are used in welding wire and as brazing alloys where a lower melting point than that of the parent metal is required.

Table 2.7: Effect of Alloying Elements ([35], [36]) (Continued)

5XXX	• Alloys in this series possess good welding characteristics and good resistance to corrosion. • Magnesium is considerably more effective than manganese as a hardener, about 0.8% magnesium being equal to 1.25% manganese, And it can be added in considerably higher quantities.
6XXX	• The magnesium-silicon (or magnesium-silicide) alloys possess good formability and corrosion resistance, with medium strength. • Capable of being heat-treated • Easy to machine • Can be precipitation hardened, but not to the high strengths that 2000 and 7000 can reach.
7XXX	• Heat-treatable alloys of very high strength
8XXX	• Used for alloys not covered by the above series.

2.2.1.3 Material Selection

Cast aluminum alloys yield cost effective products due to the low melting point, although they generally have lower tensile strengths than wrought alloys. Chemical composition for aluminum alloy 6082 is shown in Table 2.8. The most important cast

aluminum alloy system is Al-Si, where the high levels of silicon (4.0% to 13%) contribute to give good casting characteristics.

Table 2.8: Typical Chemical Composition for Aluminum Alloy 6082 [5]

Element	%Present
Si	0.7-1.3
Fe	0.0-0.5
Cu	0.0-0.1
Mn	0.4-1.0
Mg	0.6-1.2
Zn	0.0-0.2
Ti	0.0-0.1
Cr	0.0-0.25
Al	Balance

6000 series alloys contain silicon and magnesium in approximate proportions to form magnesium silicate, thus making them capable of being heat-treated. The addition of a large amount of manganese controls the grain structure which in turn results in a stronger alloy. Though less stronger than most of the 2000 or 7000 alloys, the magnesium-silicon (or magnesium-silicate) alloys possess good formability and corrosion resistance, with medium strength. Alloys in the heat-treatable group may be formed in the T4 temper (solution heat-treated but not artificially aged) and then reach full T6 properties by artificial ageing.

Aluminum alloy 6082 is the alloy most commonly used for machining. It has the highest strength of the 6000 series alloys. Aluminum alloy 6082 has very good weldability but strength is lowered in the weld zone. Properties of aluminum 6082 are shown in Table 2.9 and typical fabrication response for aluminum 6082 is shown in Table 2.10.

Table 2.9: Properties of Aluminum 6082 [37]

Physical Properties	**Metric**	**English**	**Comments**
Density	2.7 g/cc	0.0975 lb/in³	Typical
Mechanical Properties	**Metric**	**English**	**Comments**
Hardness, Vickers	95	95	
Tensile Strength, Ultimate	290 MPa	42100 psi	wall thickness < 5 mm
Tensile Strength, Ultimate	310 MPa	45000 psi	wall thickness > 5 mm
Tensile Strength, Yield	250MPa	36300 psi	wall thickness < 5 mm
Tensile Strength, Yield	260MPa	37700psi	wall thickness > 5 mm
Elongation at Break	10 %	10 %	
Thermal Properties	**Metric**	**English**	**Comments**
Thermal Conductivity	170 W/m-K	1180 BTU-in/hr-ft²-°F	

Table 2.10: Typical Fabrication Response for Aluminum Alloy 6082 [38]

Process	Rating
Workability – Cold	Good
Machinability	Good
Weldability – Gas	Good
Weldability – Arc	Good
Weldability – Resistance	Good
Brazability	Good
Solderability	Good

In the T6 and T651 temper, aluminum alloy 6082 machines well and produce tight coils of scarf when chip breakers are used. Typical mechanical properties of aluminum alloy 6082 according to tempers are shown in Table 2.11. The most common tempers for aluminum 6082 are;

O-Annealed wrought alloy

T4-Solution heat treated and naturally aged

T6-Solution heat treated and artificially aged

T651-Solution heat treated, stress relieved by stretching and artificially aged [37]

Table 2.11: Typical Mechanical Properties of Aluminum Alloy 6082 according to Tempers [38]

Temper	O	T4	T6/T651
Proof Stress 0.2% (MPa)	60	170	310
Tensile Strength (MPa)	130	260	340
Shear Strength (MPa)	85	170	210
Elongation A5 (%)	27	19	11
Hardness Vickers (HV)	35	75	100

2.2.2 Tools and Tool Steels in Hot Forging

Tool steel in forging die has a number of general characteristics that will always be involved in forging operations. These are [39]:

- Steel must have improved physical properties.
- Steel must show adequate hardness and ability to keep this hardness at elevated temperatures - temper resistance (wear, plastic deformation, thermal fatigue cracking).
- Steel must have an improved level of hot tensile strength.
- Steel must have good toughness and ductility at low and elevated temperatures.
- Steel must have adequate hardenability (retention of wear resistance, etc., if the die is re-sunk).
- It is important that the die steel exhibits adequate toughness/ductility in all directions.
- Steel must have adequate fatigue resistance.

Selection of the tool steels in forging die basically depends on the type of forging operation. Classification for tool steels may be done as followings:

- **High Speed Steel (HSS):** HSS is a type of steel which is used in high speed applications, such as in drill bits and power saw blades. High speed steel is an alloy that combines several metals like tungsten, chromium, molybdenum, cobalt and others. Tungsten is the most common type of steel presently used in high speed steel products. Type of metals can provide a heat resistance that can keep the metal hard even under extreme temperatures.
- **High Nickel Alloy (Inconel 718):** Inconel 718 is a precipitation hardenable nickel-based alloy designed to show unusually high yield, tensile and creep-rupture properties at temperatures up to 1300°F. The slow age-hardening of alloy 718 permits annealing and welding without instinctive hardening during heating and cooling. Inconel 718 has excellent weldability when relative to the nickel-base superalloys hardened by aluminum and titanium.
- **Tungsten Carbide:** Tungsten carbide has excellent hardness between 68 to 81HRC,excellent wear resistance, high cutting speed, long service life and excellent hot working performance due to hardness could be remained at 60 HRC under 900~1000 ℃.
- **Hot Work Steels:** Hot work steels are medium, high-alloy type and most of them has relatively low carbon content (0.25 to 0.6%). Hot work steels should have several

physical characteristics that are resistance to deformation at the working temperature, resistance to shock, resistance to wear at the working temperature, resistance to heat treating deformation, resistance to heat checking and good machinability in the annealed condition.

Three types of hot work steel exist. These are chromium, tungsten and molybdenum hot work tool steels.

- **Chromium Hot Work Tool Steels:** This group of the H10 to H19 steels contain chromium with additions of tungsten, molybdenum, vanadium and cobalt. The carbon in this group is comparatively low, around 0.35-0.40 percent and this group has comparatively low total alloy content. This group provides good resistance to thermal softening and a variety of this group is available enabling hardness between 40 to 55 HRC. The tungsten and molybdenum promote good hot hardness.
- **Tungsten Hot Work Tool Steels:** This group of the H21 to H26 steels contains carbon, tungsten and chromium and in certain cases vanadium. The higher alloy content of these steels over the standard chromium hot work steels lead to improved resistance to thermal softening and abrasive wear and a variety of this group is available enabling hardness between 45 to 55 HRC. In the hot work tool steels in this group, toughness and thermal shock resistance are generally obtained by reducing the carbon content. So it is necessary to adjust the tungsten and vanadium, since these both reduce hardenability by holding too much carbon in complex carbides.
- **Molybdenum Hot Work Tool Steels:** This group of the H42 and H43 steels contains molybdenum, chromium and vanadium, together with tungsten and varying amounts of carbon. Advantage of this group of steels over the tungsten hot work steel is their greater resistance to heat checking, they must be heat treated to avoid decarburization.

2.2.3 Lubrication

Lubrication is one of the most significant parameters in hot forging processes, as die life, forming forces and surface quality of the workpiece depends on lubrication. Figure 2.8 shows number of variables and their inter-relationship with the lubrication and wear of the dies. Functions of metal working lubricants can be summarized as:

- Separate surfaces
- Protect surfaces

- Remain stable and durable
- Cools the materials
- Not health-hazard
- Inexpensive

There are three basic types of lubricants used for forging dies today. These types can be grouped as follows:

- **Graphite Containing Lubricants** (water-based, oil based, greases, etc.) It is the main category having graphite as the basic active solid lubricant in function of their ability to advance the functions needed for a forging lubricant which summarizing are :a) **Lubricate** – providing an even and smooth flow of the work piece to acquire a perfect filling of the die contour; b) **Release** – providing an easy removal of the work piece from the die (without damage to it); c) **Cooling** – providing heat removal of the die and assist to decreasing thermal cracking occurrences and die wear, and d) **Protection** – conserving the die integrity as much as possible in order to run economic and extended productive series of forging parts.
- **Synthetic Lubricants –** It is a category of products based on salts in which graphite is not used as the main component in their formulations. This type of forging lubricants based on salts have operational limitations in relation to graphite although some experimental forgings results(approximate 15% of the world total) of the lubricants based on salts obtained are equal to the results given by lubricants based on graphite. This type of lubricants has executed well where in the forging of flat and not complex forging occurs. The aim of their selection is to obtain clean and environmentally superior to products containing graphite.
- **Lubricants containing Molybdenum Disulphide, Boron Nitride, Glass and other components.** They are mostly used to forged titanium parts and other special alloys used in aerospace, defense and nuclear power.

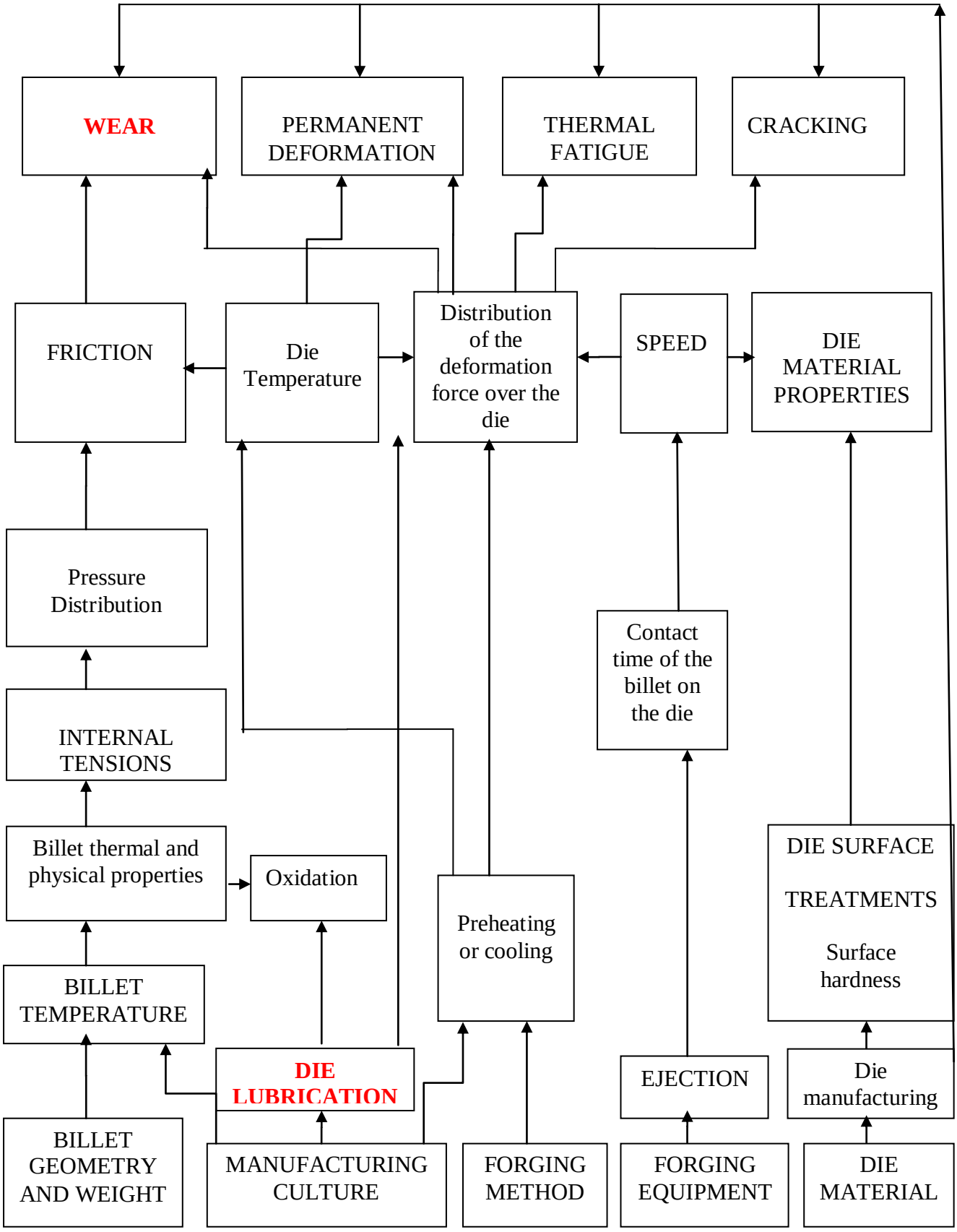

Figure 2.8: Schematic Diagram Shows Number of Variables and Their Inter-relationship with the Lubrication and Wear of the Dies [40]

2.3 Friction Analysis

Friction is an essential factor for determining the characteristics of metals as they are formed. Generally, excessive friction has a negative influence on die wear, product quality, product cost and productivity. Major factors affecting friction include normal stress along the die/workpiece interface, lubrication condition, relative velocity, temperature, roughness and mechanical properties of the material and the die. Hence, the frictional conditions at the die/workpiece interface greatly influence metal flow, formation of surface, internal defects, stresses acting on the dies and load-energy requirements.

The results of numerical FEM simulation of the process depend on the boundary conditions which are related to contact friction. Coefficient of Friction can be calculated with this formula:

$$\mu = \frac{F}{N} = \frac{\tau * A}{\sigma * A} = \frac{\tau}{\sigma} \qquad \textbf{(2.1)}$$

Friction coefficient can be reduced by several different ways. These are:

- Decreasing τ and/or increasing σ.
- Placing thin films of low shear strength over a substrate with high hardness is the ideal method for reducing abrasive friction.
- It is common to use various lubricants to reduce friction during the formation of metals.

2.3.1 Friction Models in Metal Forming

There are two laws that can be utilized for determining frictional stress. These are Coulomb friction law and shear friction law.

2.3.1.1 Amonton's and Coulomb's Friction Law

In Amonton's and Coulomb's model, the friction is proportional to the normal pressure q, and the proportionality measure is expressed through friction coefficient μ (Figure 2.9). It has importance only in areas of small normal pressures.

Frictional stress can be calculated with this formula:

$$\tau = \mu q \quad , \quad 0 \leq \mu \leq 0.577 \tag{2.2}$$

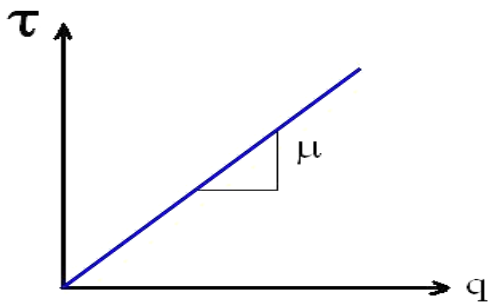

Figure 2.9: Coulomb-Amonton's Friction Model

2.3.1.2 Constant (Shear) Friction Law

Law of constant friction model assumes the constant tangential friction stress in contact surfaces, proportional to the friction factor m (Figure 2.10), is the case at existence of large normal pressures. Friction shear factor (m) values for metal forming operations are known for different applications and materials. These are presented in Table 2.12. Constant shear friction law has been widely used in simulations due to its theoretical simplicity and numerical rigidity. Frictional stress can be calculated with this formula:

$$\tau = m\, k \quad , \quad 0 \leq m \leq 1 \tag{2.3}$$

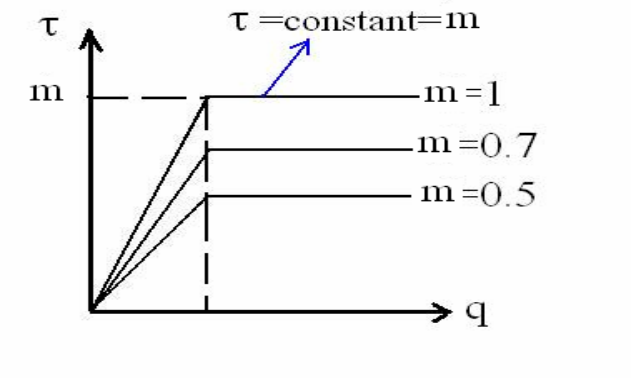

Figure 2.10 Constant (Shear) Friction Model

Table 2.12: Friction Shear Factors (m) According to Forming Conditions [36]

FORMING CONDITIONS	FRICTION SHEAR FACTOR
Cold forming of steels, copper and aluminum alloy with phosphate-soap lubricants	0.05-0.15
Hot forming of steels, copper and aluminum alloy with graphite-base lubricants	0.2-0.4
Hot forming of titanium and high temperature alloy with glass lubricants	0.1-0.3
Hot Rolling of plate and extrusion of aluminum with no lubricants	0.7-1.0

2.3.2 Effect of Friction Factor on Formability

Different coefficient of friction values for metal forming operations are known for different applications. These are presented in Table 2.13.

Table 2.13 Friction Coefficients for Forming Operations [37]

	Coefficient of Friction μ	
Process	**Cold**	**Hot**
Rolling	0.05-0.1	0.2-0.7
Forging	0.05-0.1	0.1-0.2
Drawing	0.03-0.1	-
Sheet-Metal Forming	0.05-0.1	0.1-0.2
Machining	0.5-2	-

Determination of the friction condition is important when obtaining flow curves for the material under formability investigations. Therefore, estimation of the friction condition is needed for this study.

2.3.3 Ring Compression Test

The ring compression test is a simple, inexpensive and reliable test to evaluate the friction condition in forging applications and it has been used since the 1960's. The high pressures and surface roughness in both the die and workpiece cause interfacial friction. The effects of surface roughness can be reduced by lubrication. The test uses rings of the forced material. Rings deformed under simulated forging conditions and the change in dimensions of inner diameter and height brought out the amount of interfacial friction. The ring compression test includes some assumptions which are constant interfacial shear factor represented by m and a constant rate of strain hardening for each material [1, 2].

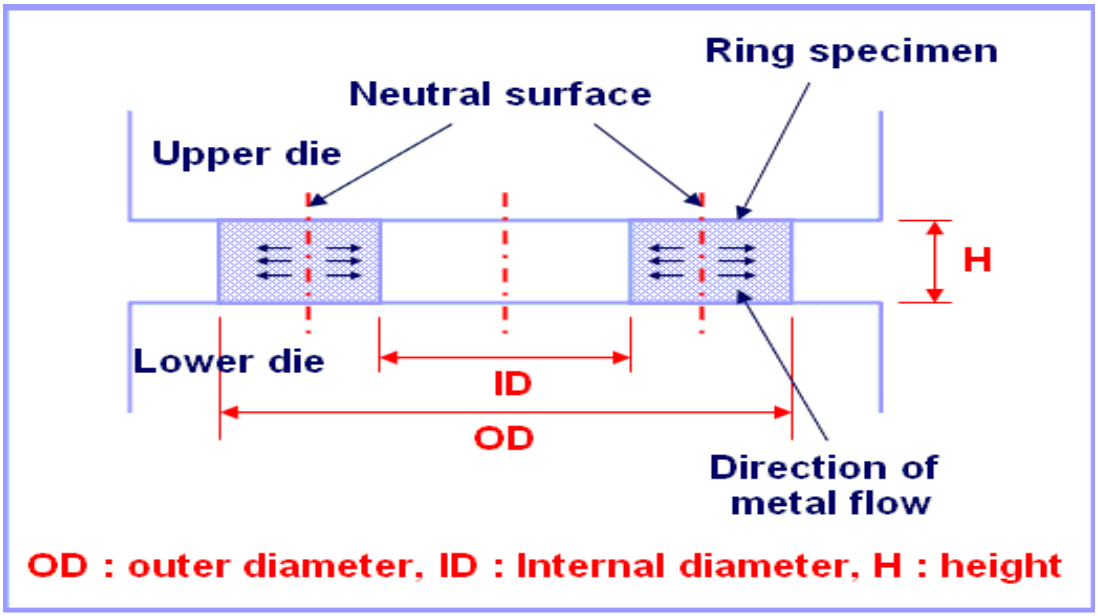

Figure 2.11: Principle of Ring Test [38]

For given conditions of temperature, strain and strain rate with the current values of the ring outer diameter, internal diameter and height measures; deformation of internal diameter of ring calculated and evaluated the magnitude of friction coefficient. Principle of ring test is shown in Fig. 2.11 schematically.

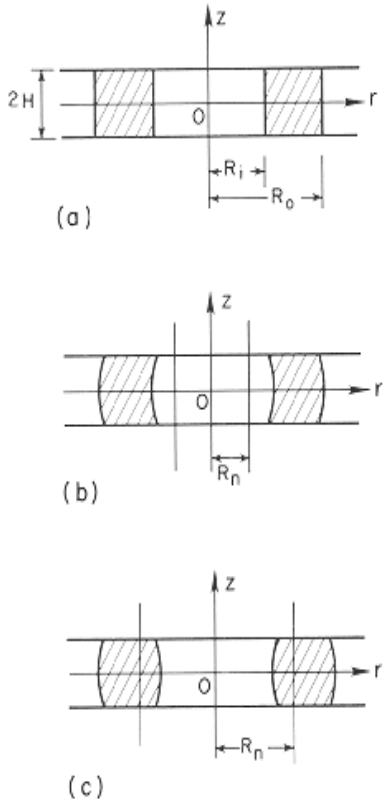

Figure 2.12: Geometrical Change and Friction Condition [39]

Ring sample is plastically compressed between two parallel planes (a), when friction coefficient is in low level, internal diameter increases and expanding of external diameter is large (b) and when friction coefficient is high level, internal diameter decreases and expanding of external diameter is small (c). (Figure: 2.12)

Graphic dependence between height strain and inner diameter strain, at various influences of friction, gives calibration curves for reading the value of coefficient/ factor of friction. Many authors were engaged in establishing these curves, by applying different methods. These methods are μ-friction, m-friction and f-friction model. Figure 2.13 shows friction calibration curves obtained from the ring compression test in terms of μ.

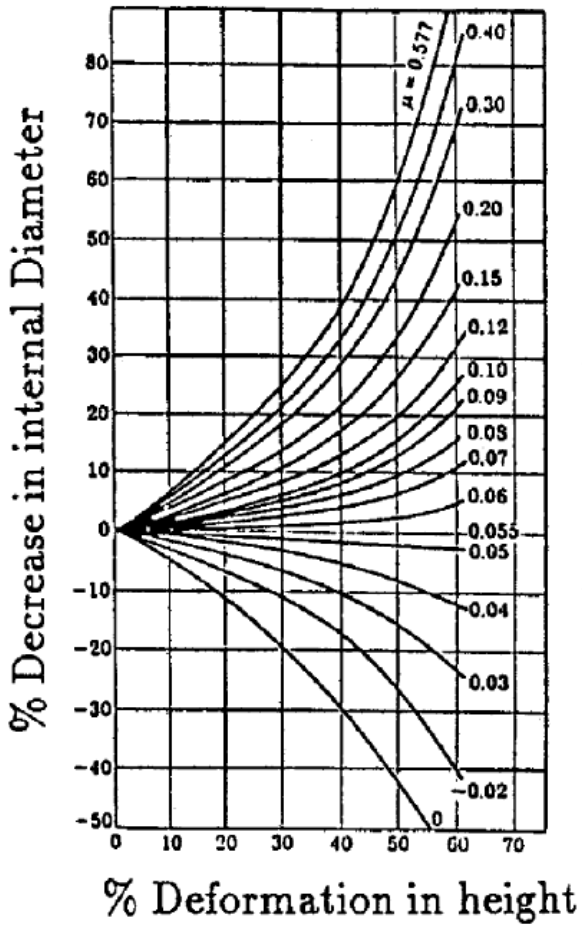

Figure 2.13: Friction Calibration Curves Obtained from the Ring Compression Test in terms of μ [41]

2.4 Object of Present Investigation

The main objective of the study took place at the request of the AYDINLAR A.Ş Forging Company from ATILIM University - Metal Forming Center of Excellence. AYDINLAR A.Ş Forging Company demanded an academic study which included determination of flow curves, friction tests and studies on internal structures of the forged part of forming of 6082 aluminum material with hot forging. Material requirement which is used in mechanical characterization tests are provided by AYDINLAR A.Ş. Forging Company. In this study following tests are performed;

1. Tests for Mechanical Behavior

Compression tests are performed using a dilatometer device in order to determine mechanical properties of AA 6082 in the range of 400 to 500 ° C temperature. Also material flow curve of aluminum alloy can be obtained by dilatometer test. The dilatometer test was performed at 0.1 1/s, 1 1/s, 10 1/s and 35 1/s strain rates at 400 °C, 450 °C and 500 °C temperatures for determining mechanical behavior of the material. Three repetitive tests are performed for all conditions.

2. Friction Analysis Tests

In the experimental study, the effect of different initial conditions such as temperature, press velocity, reductions of material and lubricant existence have been investigated. The characterization has been assisted by finite element simulation for these tests. Ring compression test are applied at 400 °C and 500 °C temperatures, %20 mm/s and %100 mm/s press velocities (%100 press velocity is approximately equals to 330 mm/s velocity), 2mm and 3,5 mm reduction of materials, dry or lubricated conditions and determining friction coefficients according to these parameters. The simulations show how temperature, press velocity, reduction of material and lubrication existence factors affect metal flow and ring geometry.

The aim of this study is to evaluate the ring test as a method for determining friction factors for aluminum under hot forging conditions. Simulation results of the various tests compared with experimental results and results are consistent with observed data.

CHAPTER 3

EXPERIMENTAL STUDY

3.1 Modeling of Experiments

The method of ring compression is the most widely applied method for determining contact conditions in bulk forming processes. The measurement of hole size after deformation reveals friction ring test calibration curves and it is used to determine the friction factor. In this experiment aluminum alloy 6082 is used which is machined into rings of appropriate dimensions of 10 mm height, 10 mm outer diameter and 5 mm inner diameter. 3-D Modeling of ring is shown in Figure 3.1.

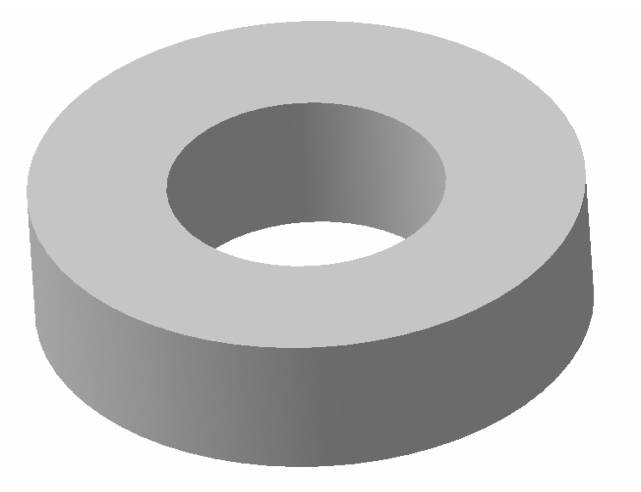

Figure 3.1: 3-D Modeling of Ring

Ring compression test is applied according to the change in four different parameters and determining friction coefficients according to these parameters. These parameters are;

1. Temperature: Performed in 400 °C and 500 °Ctemperature
2. Velocity of the Press : Applied %20 mm/s and %100 mm/s press velocity (%100 press velocity is approximately equals to 330 mm/s velocity)

3. Reduction of Material: 2mm and 3,5 mm (for 5mm height of rings)
4. Lubrication: Dry or lubricated

Figure 3.2: Samples of Ring Compression Test

There are three repetitive test applied for each condition. 48 ring samples were selected approximately the same size as shown in Figure 3.2. For each test run, a set of rings were heated in a resistive furnace to 400 °C and 500 ºC for 10 minutes (Figure: 3.3).

Figure 3.3: Pictures of Furnace

One ring at a time was removed from the furnace and placed between die and die holder. Then die was inserted on the press and press compressed the ring. Before compression, no attempt made to remove samples from servo press. Experiments are carried out on a Komatsu HIF80 OS Servo Press as shown in Figure 3.4.

Figure 3.4: Komatsu HIF80 OS Servo Press

3.2 Experimentation and Results

Aluminum alloy 6082 outer diameter, inner diameter and height are measured and averaged after deformation as show in the Table: 3.1.

Table 3.1: Inner, Outer and Thickness Dimensions after Forging Operation

Experiment no:	Sample no:	Temp. (°C)	Velocity (%)	Reduction (mm)	Lubricant	Inner Diameter (mm)	Outer Diameter (mm)	Thickness (mm)
1	1	400	20	3,5	+	2,36	14,59	1,55
	2	400	20	3,5	+	2,83	15,16	1,41
	3	400	20	3,5	+	2,31	15,04	1,46
Average						**2,5**	**14,93**	**1,47**
2	1	400	20	3,5	-	0	14,76	1,47
	2	400	20	3,5	-	0	14,64	1,50
	3	400	20	3,5	-	0	14,86	1,47
Average						**0**	**14,75**	**1,48**
3	1	400	100	3,5	+	2,79	14,42	1,58
	2	400	100	3,5	+	2,25	14,72	1,51
	3	400	100	3,5	+	2,85	14,80	1,51
Average						**2,63**	**14,64**	**1,53**
4	1	400	100	3,5	-	0	14,71	1,49
	2	400	100	3,5	-	0	14,75	1,48
	3	400	100	3,5	-	0	14,64	1,46
Average						**0**	**14,7**	**1,47**
5	1	400	20	2	+	4,51	11,57	2,80
	2	400	20	2	+	4,39	11,58	2,83
	3	400	20	2	+	4,34	11,53	2,84
Average						**4,41**	**11,56**	**2,82**

Table 3.1: Inner, Outer and Thickness Dimensions after Forging Operation (Continued)

Experiment no:	Sample no:	Temp. (°C)	Velocity (%)	Reduction (mm)	Lubricant	Inner Diameter (mm)	Outer Diameter (mm)	Thickness (mm)
6	1	400	20	2	-	4,03	11,39	2,81
	2	400	20	2	-	4,04	11,37	2,84
	3	400	20	2	-	4,04	11,44	2,81
Average						**4,03**	**11,40**	**2,82**
7	1	400	100	2	+	4,3	11,63	2,79
	2	400	100	2	+	4,37	11,55	2,80
	3	400	100	2	+	4,47	11,58	2,78
Average						**4,38**	**11,59**	**2,79**
8	1	400	100	2	-	3,93	11,52	2,76
	2	400	100	2	-	4,28	11,63	2,81
	3	400	100	2	-	3,98	11,71	2,77
Average						**4,06**	**11,62**	**2,78**
9	1	500	20	3,5	+	1,61	15,05	1,38
	2	500	20	3,5	+	2,45	14,88	1,52
	3	500	20	3,5	+	0,62	15,27	1,46
Average						**1,56**	**15,07**	**1,45**
10	1	500	100	3,5	+	1,43	15,01	1,46
	2	500	100	3,5	+	1,99	15,01	1,46
	3	500	100	3,5	+	1,92	14,80	1,52
Average						**1,78**	**14,94**	**1,48**
11	1	500	20	2	+	3,95	11,55	2,70
	2	500	20	2	+	4,01	11,54	2,73
	3	500	20	2	+	3,96	11,55	2,74
Average						**3,97**	**11,55**	**2,72**
12	1	500	100	2	+	3,93	11,59	2,78
	2	500	100	2	+	3,92	11,47	2,84
	3	500	100	2	+	3,95	11,54	2,76
Average						**3,93**	**11,53**	**2,79**

Reduction in height (%) on one axis and reduction of inner diameter on the other axis, with the corresponding curves that provided to determine the coefficient of friction for estimated coefficient of friction. The outer diameter measurements were not necessary for the calibration curves. Forging test could not be applied at 500 degrees without lubricant condition because of the mold and the workpiece sticking to each other. Experimental results show that inner diameter goes zero at dry with 3,5mm material reduction condition. Lubrication factor, increase of inner ring diameter occurs because the material slides over tool contact surface effortlessly.

3.3 Dilatometer Test

Material flow curve can be obtained by dilatometer as shown in the Figure 3.5. Dilatometer is an instrument used to measure the expansion of a sample with a temperature variation. Dilatometer is a very sensitive experimental tool to analyze the length (volume) changes and the kinetics of solid state phase transformations. The expansion signal Delta L or the coefficient of thermal expansion value are measured over temperature or time.

Figure 3.5: Pictures of Dilatometer

The specimen, 5mm in diameter and 10 mm in length, with a K type thermocouple in the center, is surrounded by the induction coil as shown in the Figure: 3.6. The electrically conductive solid specimen is heated by an induction coil at 400 ℃, 450 ℃, and 500 ° C temperatures and can be actively cooled by controlled inert gas flow. High heating and

cooling rates can be achieved using hollow specimens. Pictures of samples at different temperatures are shown in Figure 3.7.

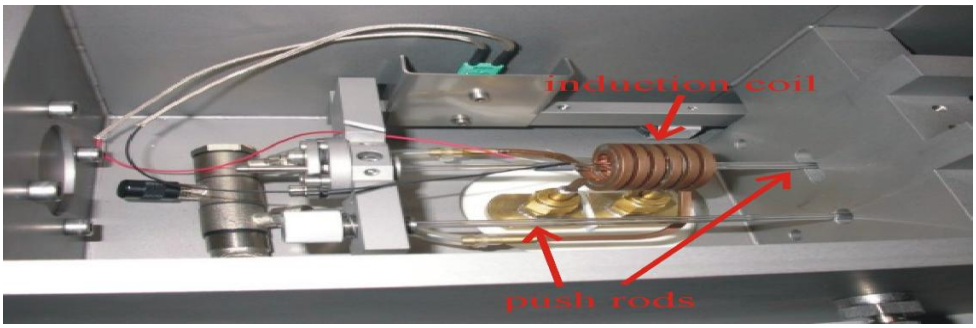

Figure 3.6: Detailed View of the Dilatometer

The dilatometer test was performed at 0.1 sn^{-1}, 1sn^{-1}, 10 sn^{-1} and 35 sn^{-1}strain rates and 400 ℃, 450 ℃, 500 ℃ temperatures. Three repetitive tests were performed for all condition. Sample dimensions measurement after dilatometer test for different strain rates and temperatures are shown in Table 3.2.

Table 3.2: Sample Dimensions Measurement after Dilatometer Test for Different Strain Rates and Temperatures

	T=400℃				T=450℃				T=500℃		
Strain rate (sn^{-1})	**Samp. No**	**h (mm)**	**ϕ (mm)**	**Strain Rate (sn^{-1})**	**Samp. No**	**h (mm)**	**ϕ (mm)**	**Strain Rate (sn^{-1})**	**Samp. No**	**h (mm)**	**ϕ (mm)**
ε̇=0.1	1	10,11	5,01	ε̇=0.1	1	9,99	4,99	ε̇=0.1	1	10,1	5,01
	2	10,15	5		2	10,1	5		2	10,09	5
	3	10,07	5,02		3	10,13	5,02		3	10,07	5,01
ε̇=1	4	9,88	5,02	ε̇=1	4	10,08	5	ε̇=1	4	10,15	5,01
	5	10,12	4,99		5	10,12	5,01		5	10,1	5,01
	6	10,09	5		6	10,08	4,99		6	10	5,01
ε̇=10	7	10,09	5	ε̇=10	7	10,05	5,01	ε̇=10	7	10,02	5,02
	8	10,01	4,99		8	10	5,02		8	10,13	5,01
	9	10,01	5,02		9	10,03	5,01		9	10,04	5
ε̇=35	10	5,04	5,02	ε̇=35	10	5,06	5,01	ε̇=35	10	5,05	5,01
	11	5,08	5,02		11	5,01	5,01		11	5,04	5
	12	5,04	5,01		12	5,05	5,01		12	5	4,98

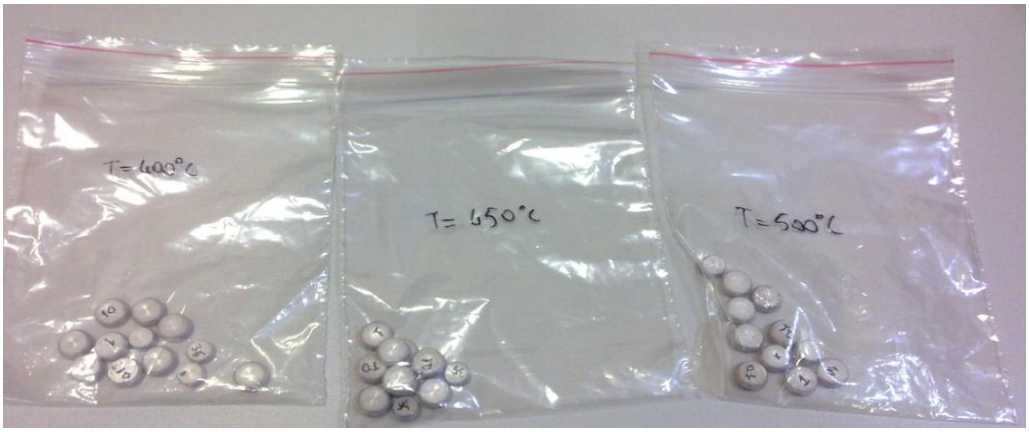

Figure 3.7: Pictures of Samples at 400 °C, 450 °C and 500 °C Temperatures

Several tests were performed at 500 °C temperature and 10 sn^{-1} strain rate in order to determine the effect of the waiting time on stress value for 1minute, 10 minutes and 100 minutes as shown in Figure 3.8. Due to not observation an explicit effect of the waiting time on stress values, all other thermo mechanical deformation tests were carried out at 1minute.

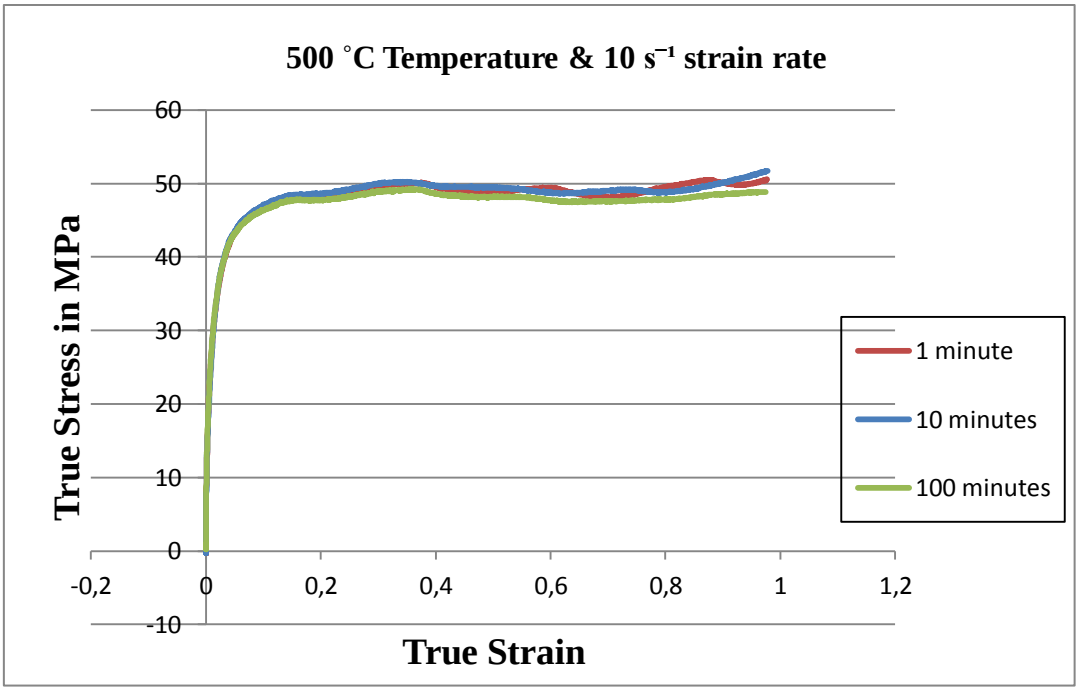

Figure 3.8: The Effect of the Waiting Time on Stress Values for 1 minute, 10 minutes and 100 minutes

3.4 Experimental Results of Flow Stress Measurement Test

At each temperature, three compression tests were conducted. In total, twelve compression tests were done. Now all the data necessary for the calculation of stress and strain are available.

True strain:
$$\varepsilon_{(u)} = \ln\left(\frac{h_u}{h_0}\right) \quad \textbf{(3.1)}$$

True stress:
$$\sigma_{f(u)} = \frac{F}{A_{(u)}} \quad \textbf{(3.2)}$$

Engineering strain:
$$\varepsilon_E = \frac{h_{(u)} - h_0}{h_0} \quad \textbf{(3.3)}$$

Engineering stress:
$$\sigma_E = \frac{F}{A_0} \quad \textbf{(3.4)}$$

By using these relations, true stress vs. true strain data was obtained and flow curves of Al 6082 at 400 °C, 450 °C, and 500 °C are presented. In Figs. 3.9, 3.10, 3.11, 3.12, 3.13, 3.14, 3.15, 3.16, 3.17, 3.18, 3.19 and 3.20 true strain-true stress curves are presented at different temperatures and different strain rates. Three different tests were done for each temperature.

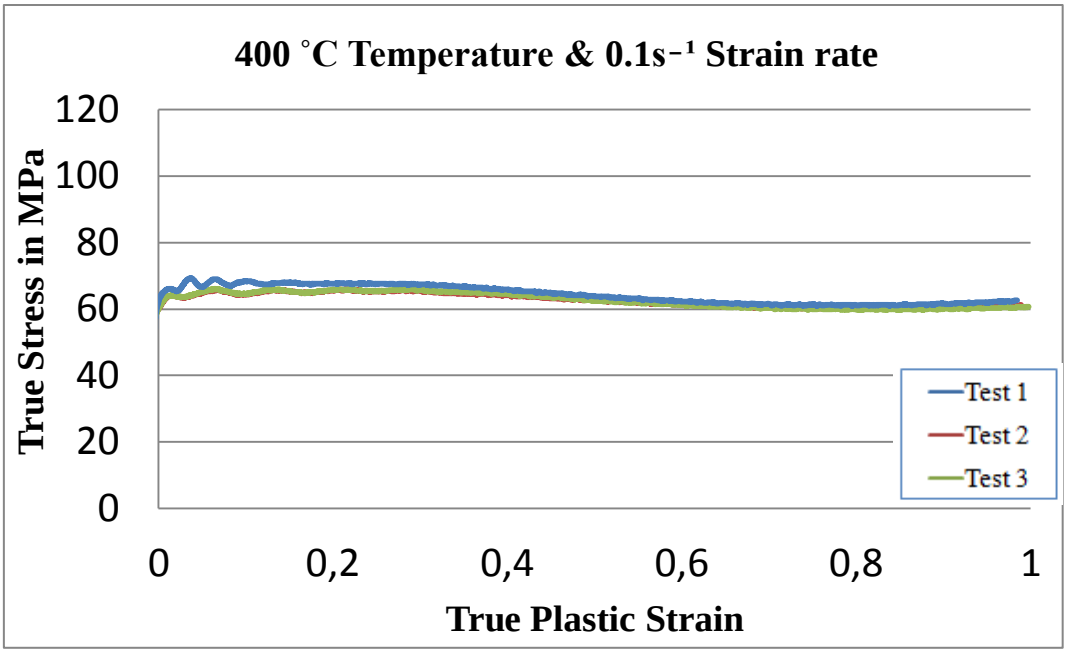

Figure 3.9: Flow curves of Al 6082 at 400 ˚C Temperature and 0,1 s⁻¹Strain Rate

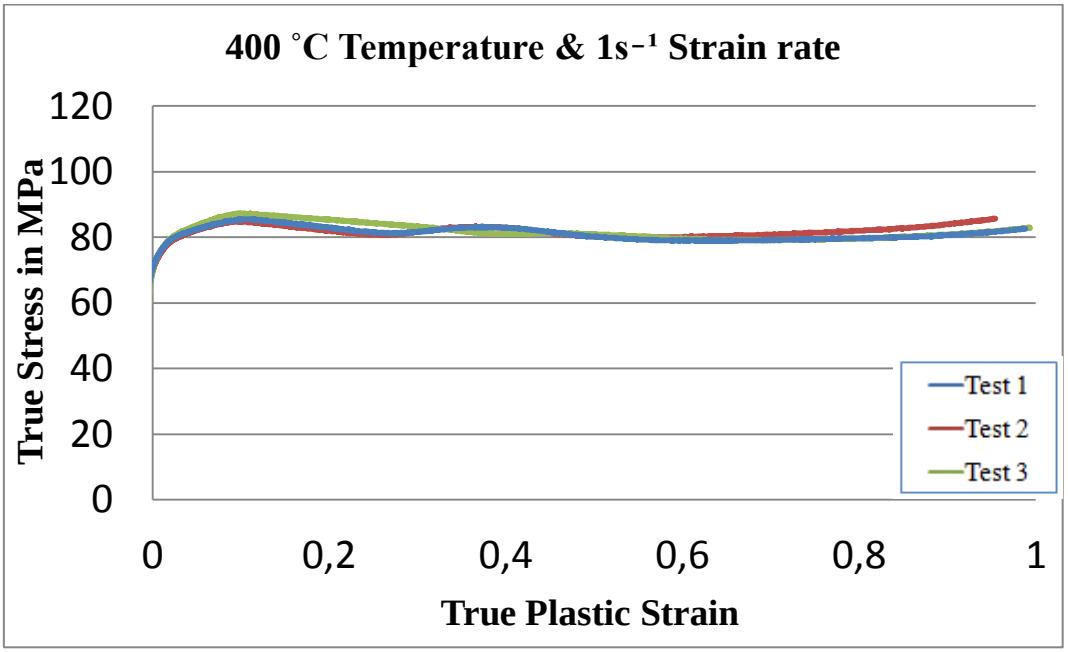

Figure 3.10 Flow curves of Al 6082 at 400 ˚C Temperature and 1 s⁻¹ Strain Rate

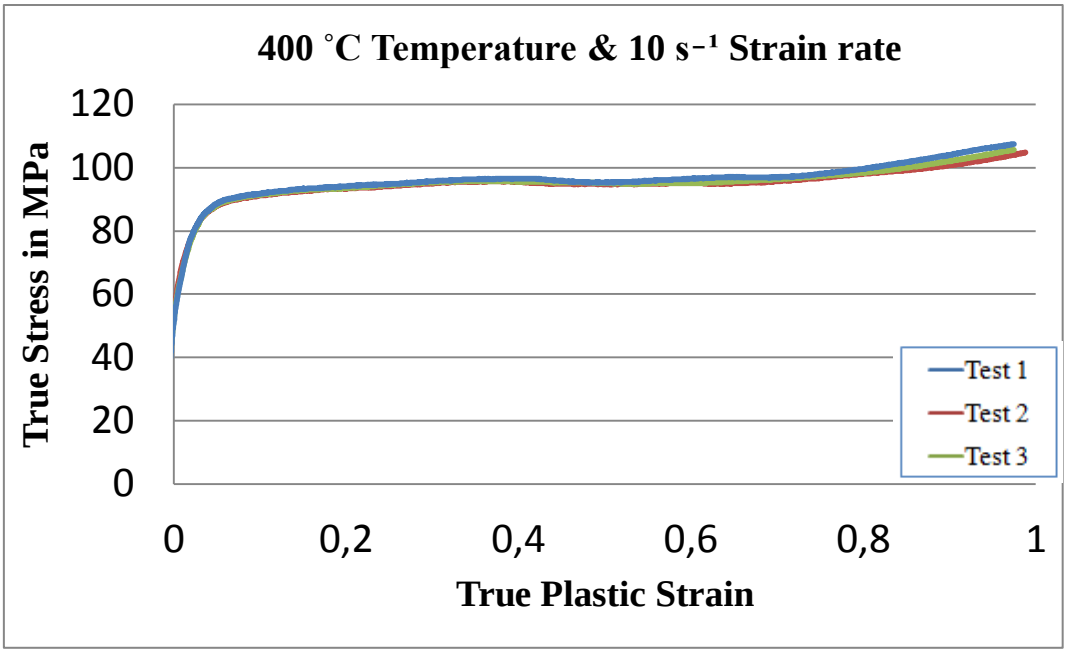

Figure 3.11: Flow curves of Al 6082 at 400 ˚C Temperature and 10 s⁻¹ Strain Rate

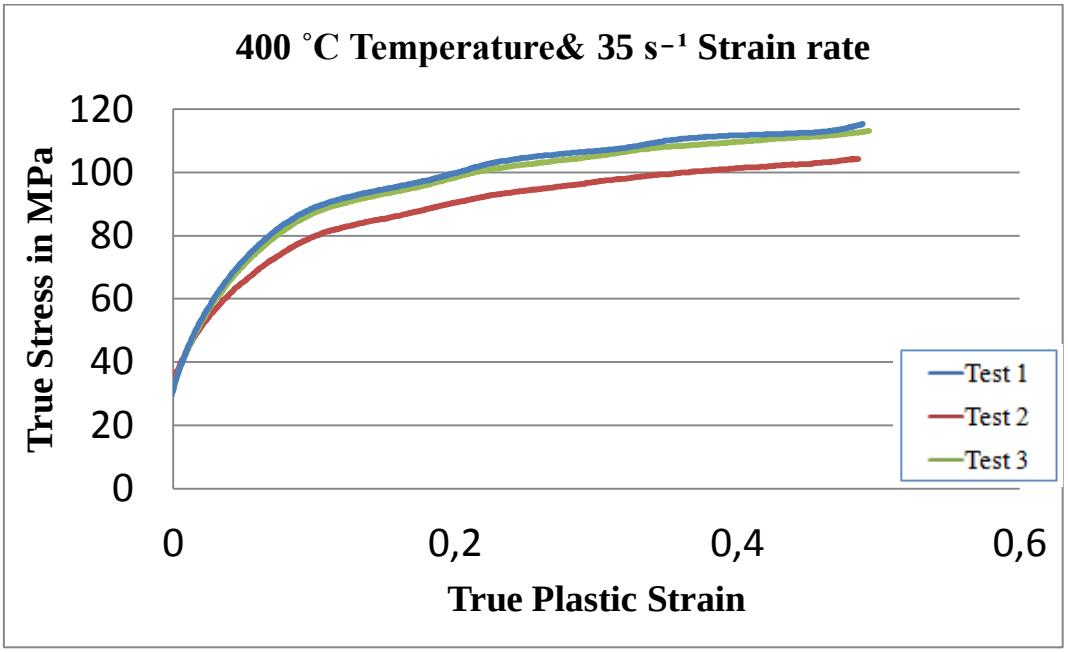

Figure 3.12: Flow curves of Al 6082 at 400 ˚C Temperature and 35 s⁻¹ Strain Rate

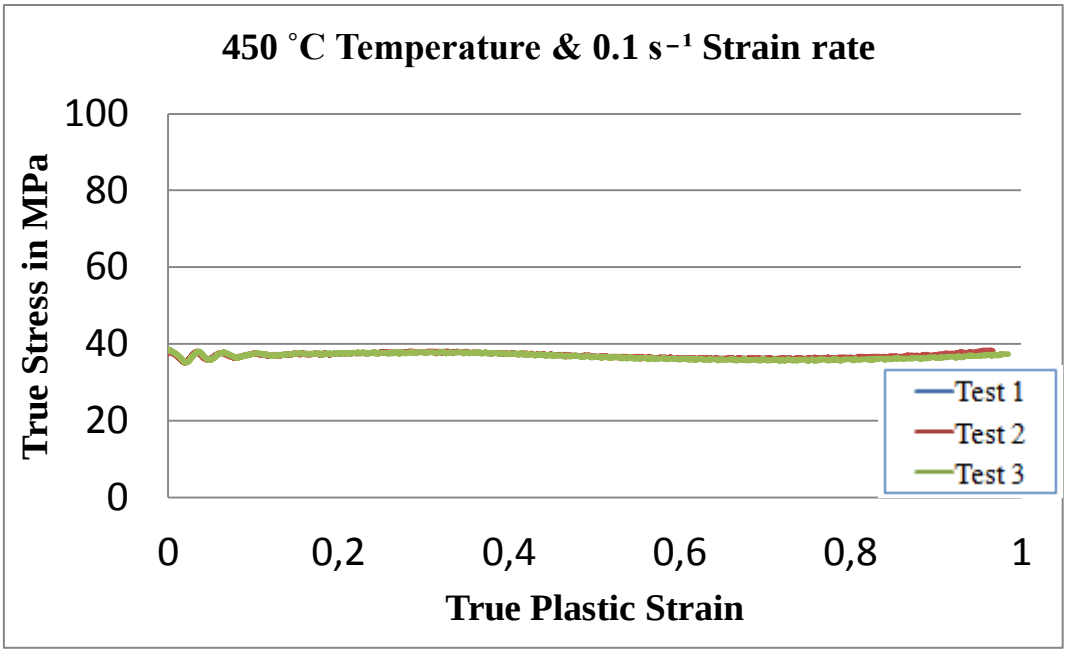

Figure 3.13: Flow curves of Al 6082 at 450 ˚C Temperature and 0.1 s⁻¹ Strain Rate

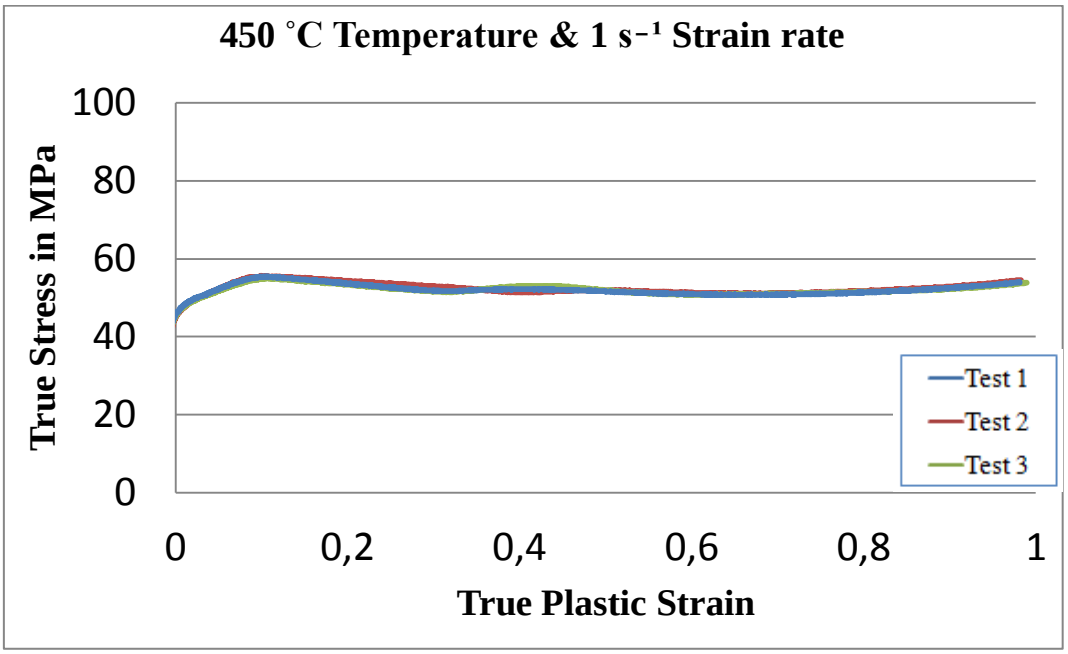

Figure 3.14: Flow curves of Al 6082 at 450 ˚C Temperature and 1 s⁻¹ Strain Rate

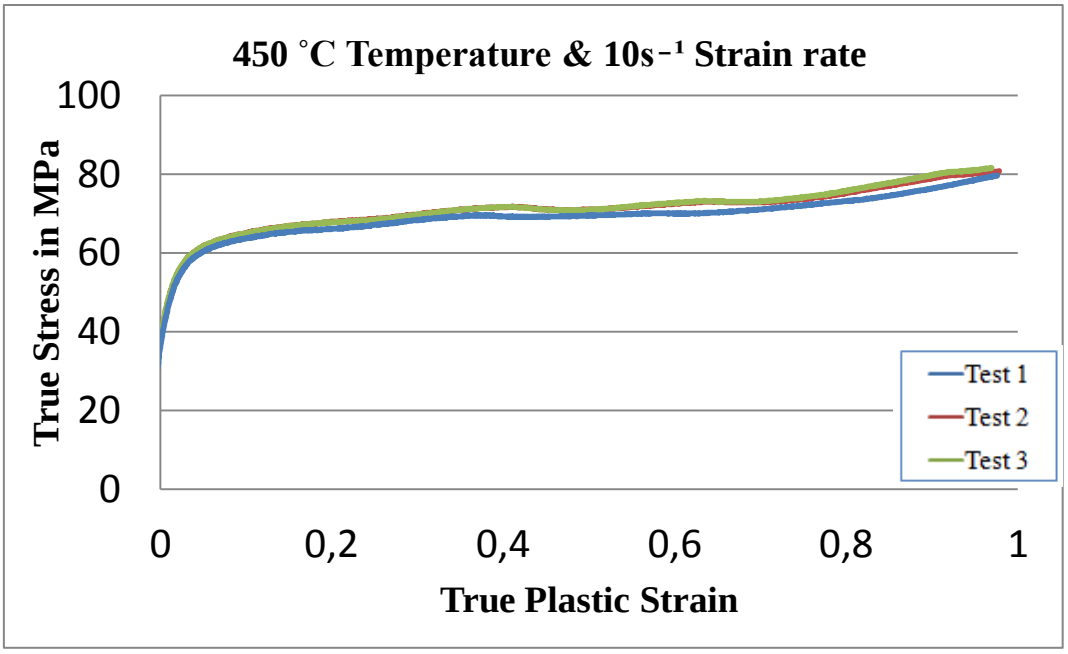

Figure 3.15: Flow curves of Al 6082 at 450 ˚C Temperature and 10 s⁻¹ Strain Rate

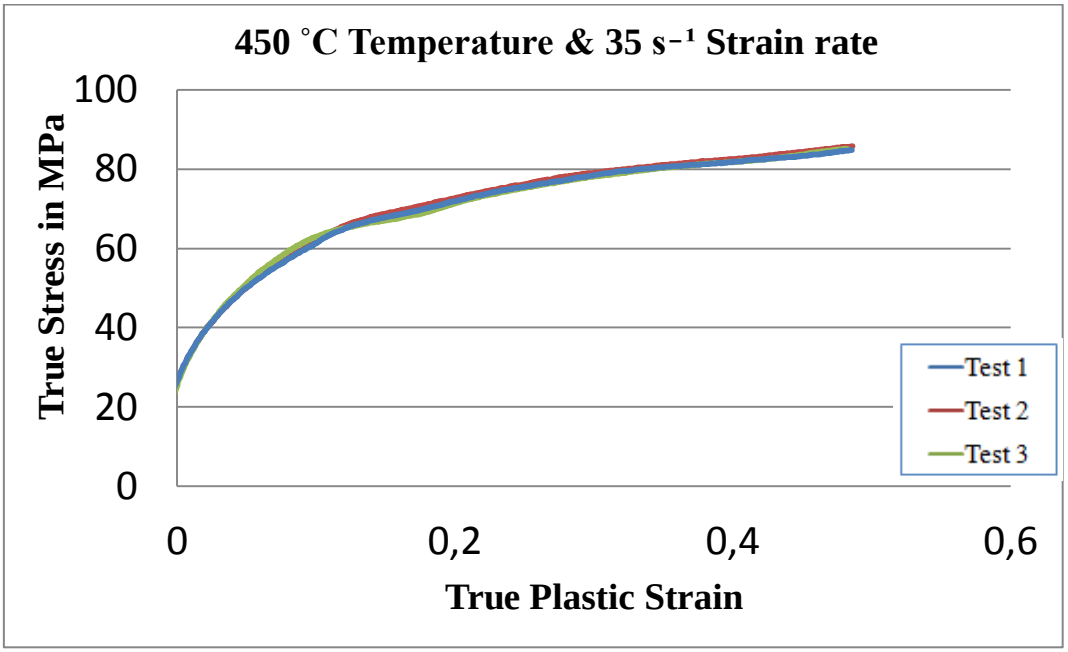

Figure 3.16: Flow curves of Al 6082 at 450 ˚C Temperature and 35 s⁻¹ Strain Rate

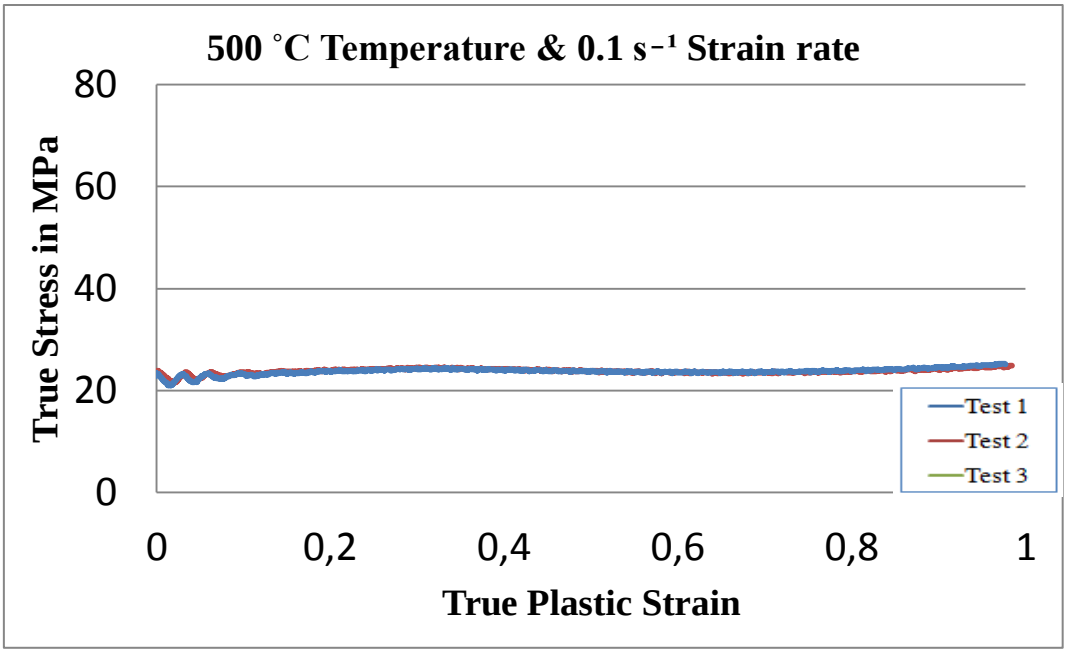

Figure 3.17: Flow curves of Al 6082 at 500 ˚C Temperature and 0.1 s⁻¹ Strain Rate

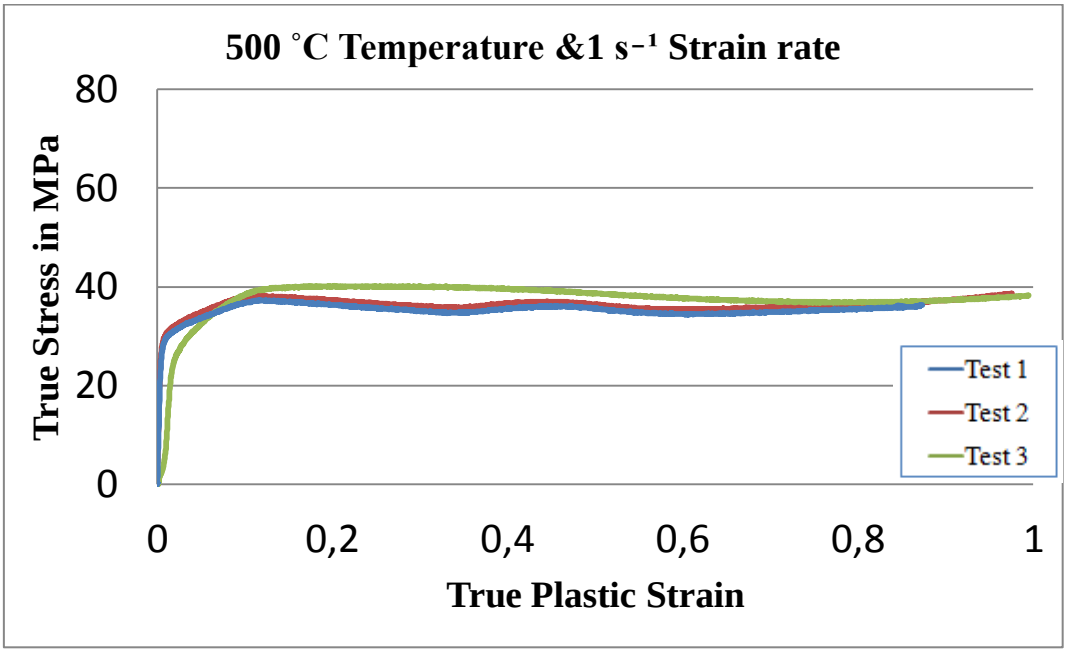

Figure 3.18: Flow curves of Al 6082 at 500 ˚C Temperature and 1 s⁻¹ Strain Rate

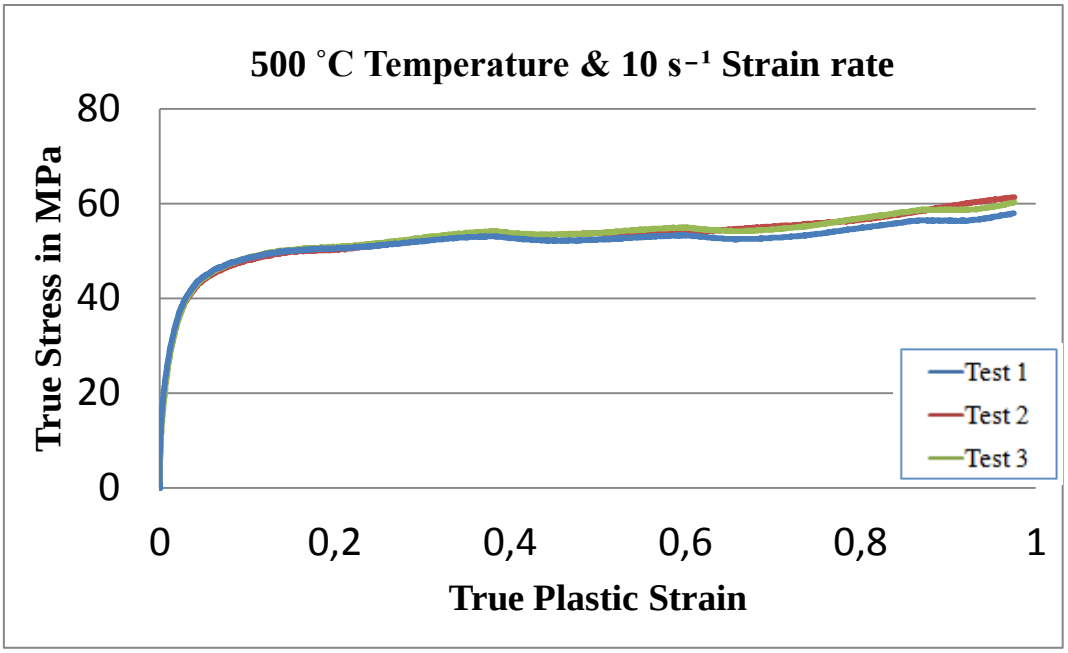

Figure 3.19: Flow curves of Al 6082 at 500 ˚C Temperature and 10 s⁻¹ Strain Rate

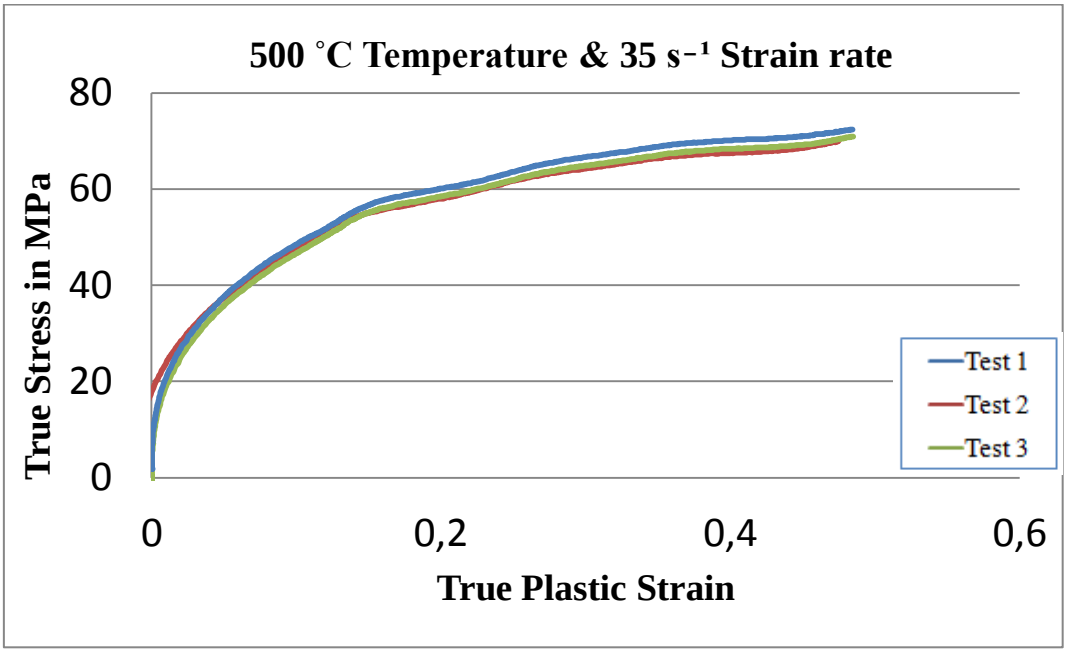

Figure 3.20: Flow curves of Al 6082 at 500 ˚C Temperature and 35 s⁻¹ Strain Rate

3.5 Evaluation of Measurement Result According to Various Equation

On the basis of experimental results of ring tests for aluminum alloys, models for calculation of flow stress were investigated according to three methods. Comparison of those methods leads to the conclusion that within a specific range of strain values they can be used for describing the measured curves. Available functions are applied for indicate the stress in the aluminum 6082 alloy at the strain rate of 0,1 sn^{-1},1 sn^{-1},10 sn^{-1},35 sn^{-1} and temperatures of 400 ˚C, 450 ˚C and 500 ˚C. The evaluation is based on the assumption of a uniaxial compression stress state within the strain range of 0 ≤e ≤0.7 [42].

3.5.1 Zehner-Hollomon (Tong) Equation

The first method used for calculation of stress value is the Zehner-Hollomon (Tong) equation. The basic equation is given in 3.5. Values of parameters are given in Table 3.3. By using this table equation 3.6 is derived from equation 3.5.

$$\sigma = A\, e^{\frac{Q}{R(T+273)}}\, \dot{\varepsilon}^{m} \qquad \textbf{(3.5)}$$

Table 3.3: Table of Materials Constant used in Zehner-Hollomon (Tong) Equation

A	Q	m	R
0,4302	29082	0,1012	8.314

$$\sigma = 0.4302\ \ e^{\frac{29082}{8.314(T+273)}}\ \ \dot{\varepsilon}^{0.1012} \qquad \textbf{(3.6)}$$

In Fig. 3.21, 3.22, 3.23, 3.24 comparisons of experimental and calculated results of stress-strain curves are presented at different temperatures and different strain rates.

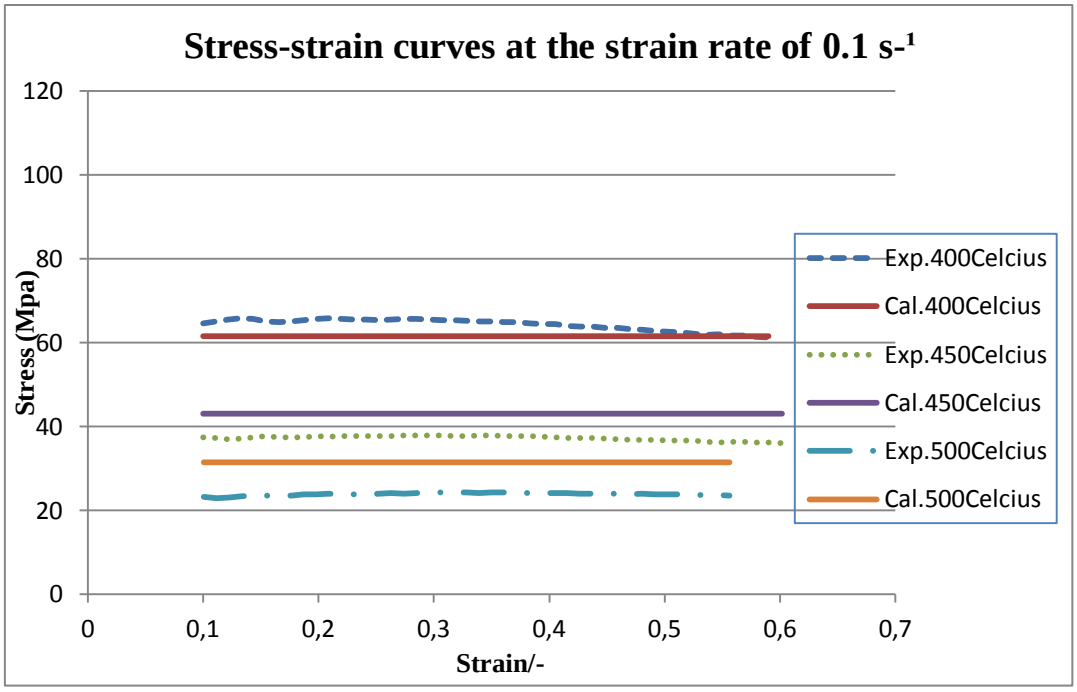

Figure 3.21: Comparison of Experimental and Calculated Results According to Zehner-Hollomon (Tong) Equation at the Strain Rate of 0.1 s^{-1}

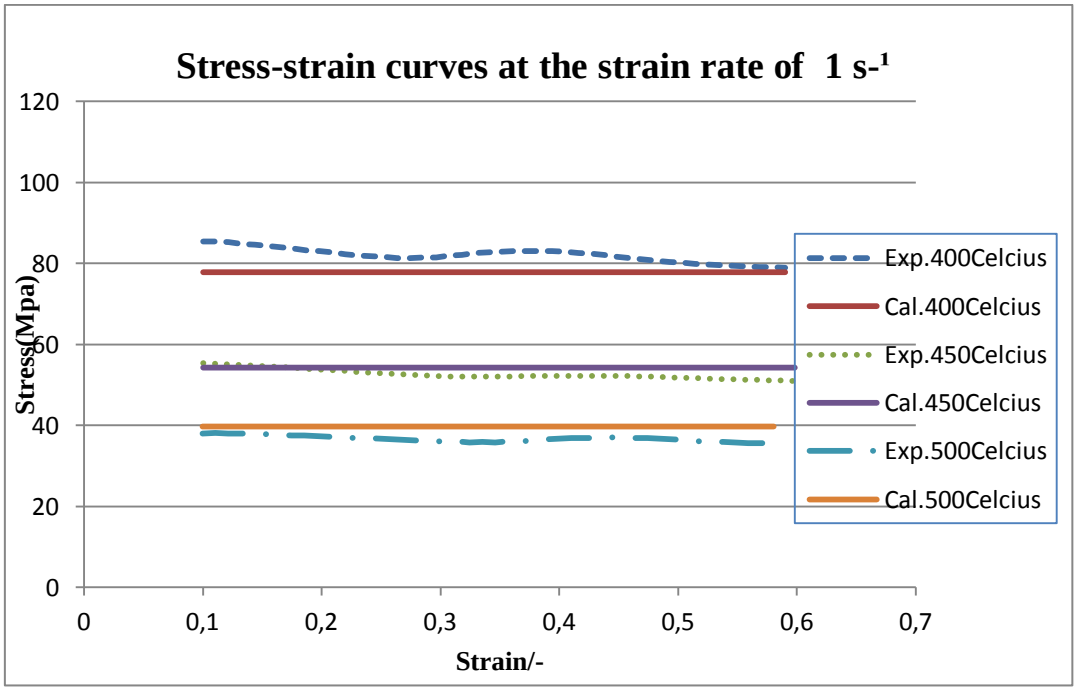

Figure 3.22: Comparison of Experimental and Calculated Results According to Zehner-Hollomon (Tong) Equation at the Strain Rate of 1 s^{-1}

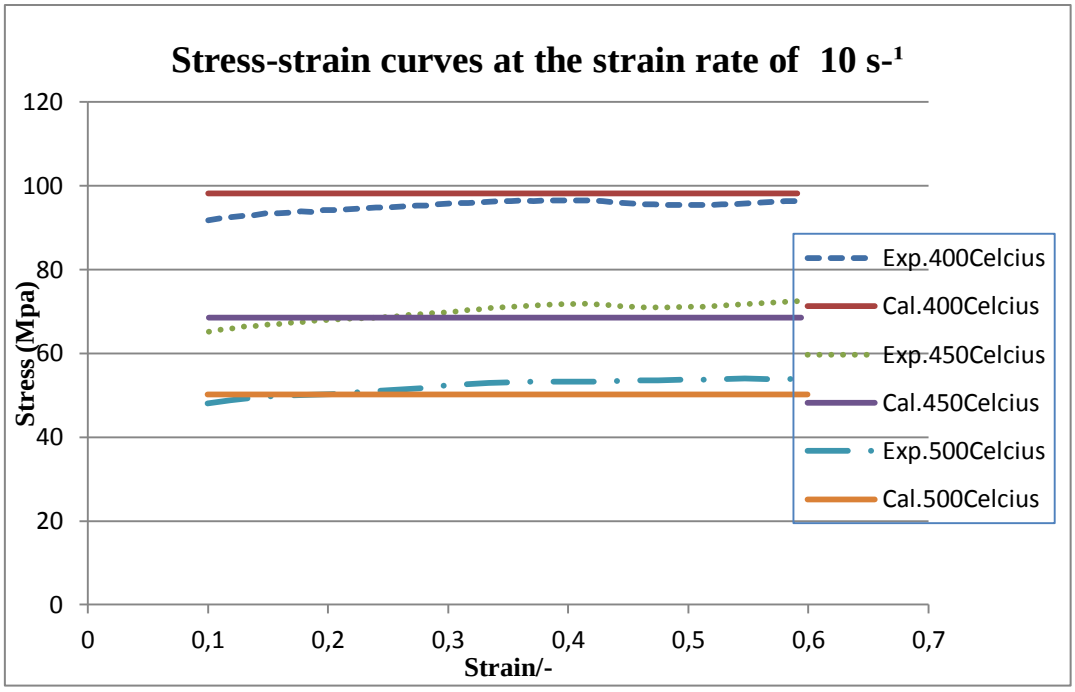

Figure 3.23: Comparison of Experimental and Calculated Results According to Zehner-Hollomon (Tong) Equation at the Strain Rate of 10 s^{-1}

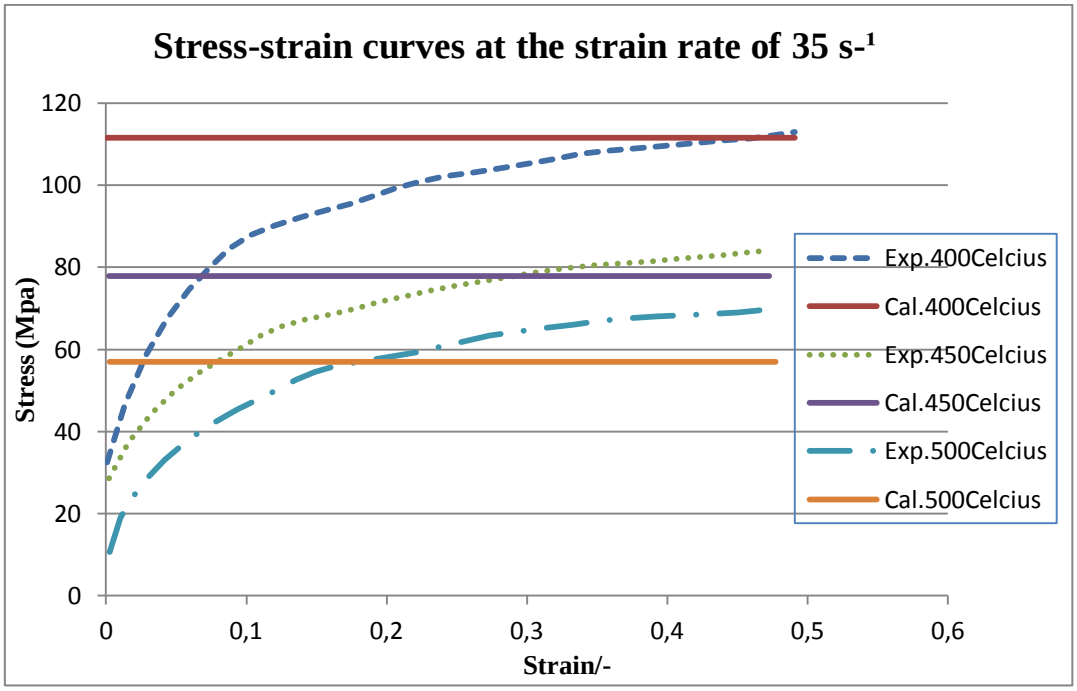

Figure 3.24: Comparison of Experimental and Calculated Results According to Zehner-Hollomon (Tong) Equation at the Strain Rate of 35 s^{-1}

3.5.2 Modified Zehner-Hollomon (Tong)

The second method used for calculation of stress value is the Modified Zehner-Hollomon (Tong) equation. The basic equation is given in 3.7. Values of parameters are given in Table 3.4. By using this table equation 3.8 is derived from equation 3.7.

$$\sigma = A\ e^{\frac{Q}{R(T+273)}}\ \dot{\varepsilon}^{m}\ (1-\beta e^{-N\varepsilon^{n}}) \qquad \textbf{(3. 7)}$$

Table 3.4: Table of Materials Constant used in Modified Zehner-Hollomon (Tong) Equation

A	Q	m	β	N	n	R
0,4302	29082	0,1012	0,7081	20,333	1,1144	8.314

$$\sigma = 0.4302\ e^{\frac{29082}{8.314(T+273)}}\ \dot{\varepsilon}^{0.1012}(1-0.7081\ e^{-20.333\varepsilon^{1.1144}}) \qquad \textbf{(3.8)}$$

In Fig. 3.25, 3.26, 3.27, 3.28 comparisons of experimental and calculated results of stress-strain curves are presented at different temperatures and different strain rates.

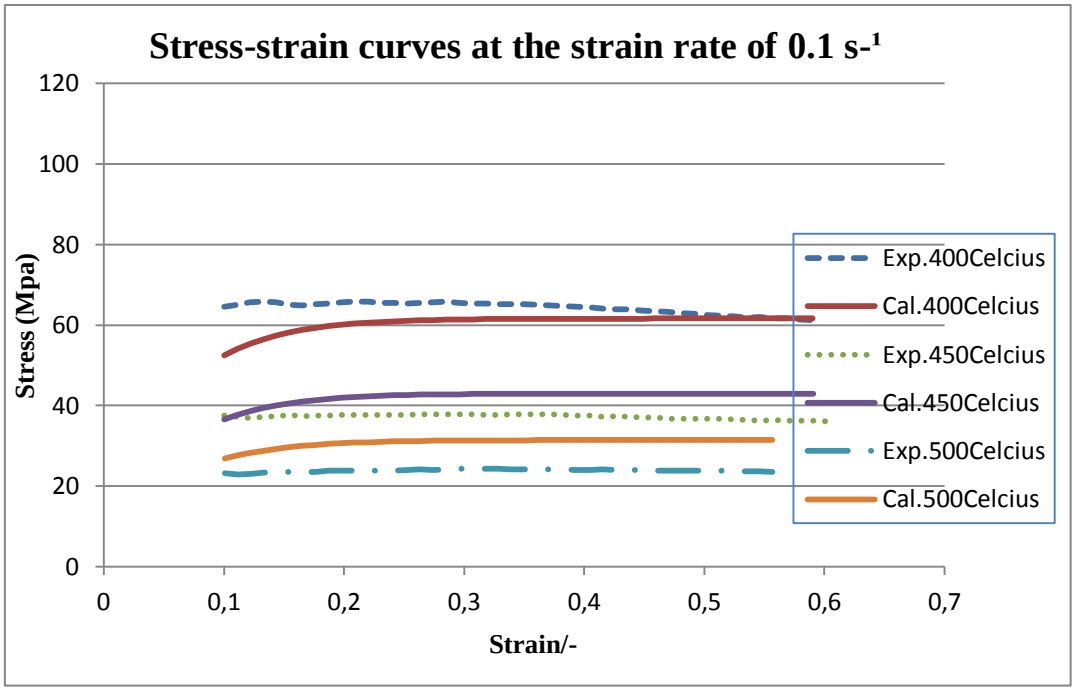

Figure 3.25: Comparison of Experimental and Calculated Results According to Modified Zehner-Hollomon (Tong) Equation at the Strain Rate of 0, 1 s^{-1}

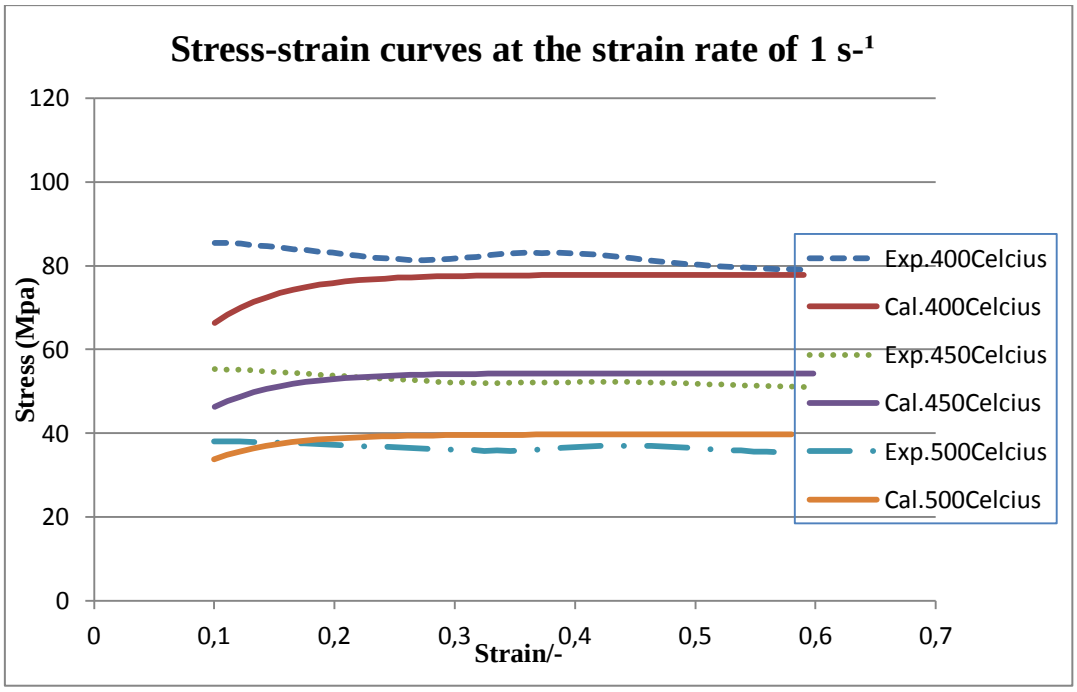

Figure 3.26: Comparison of Experimental and Calculated Results According to Modified Zehner-Hollomon (Tong) Equation at the Strain Rate of 1 s^{-1}

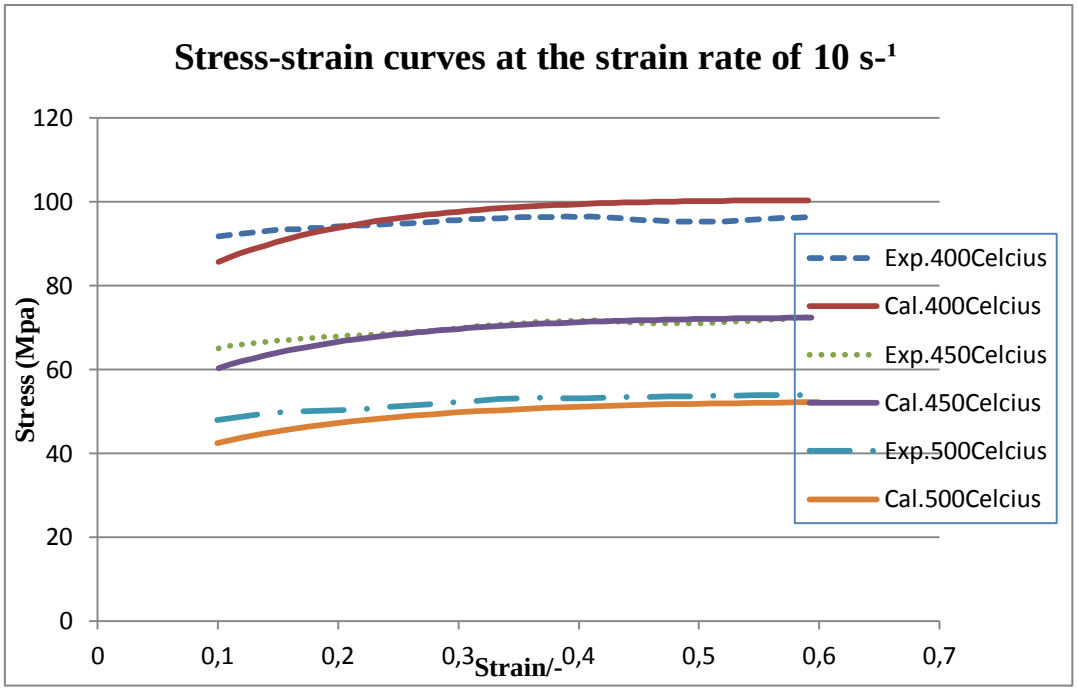

Figure 3.27: Comparison of Experimental and Calculated Results According to Modified Zehner-Hollomon (Tong) Equation at the Strain Rate of 10 s^{-1}

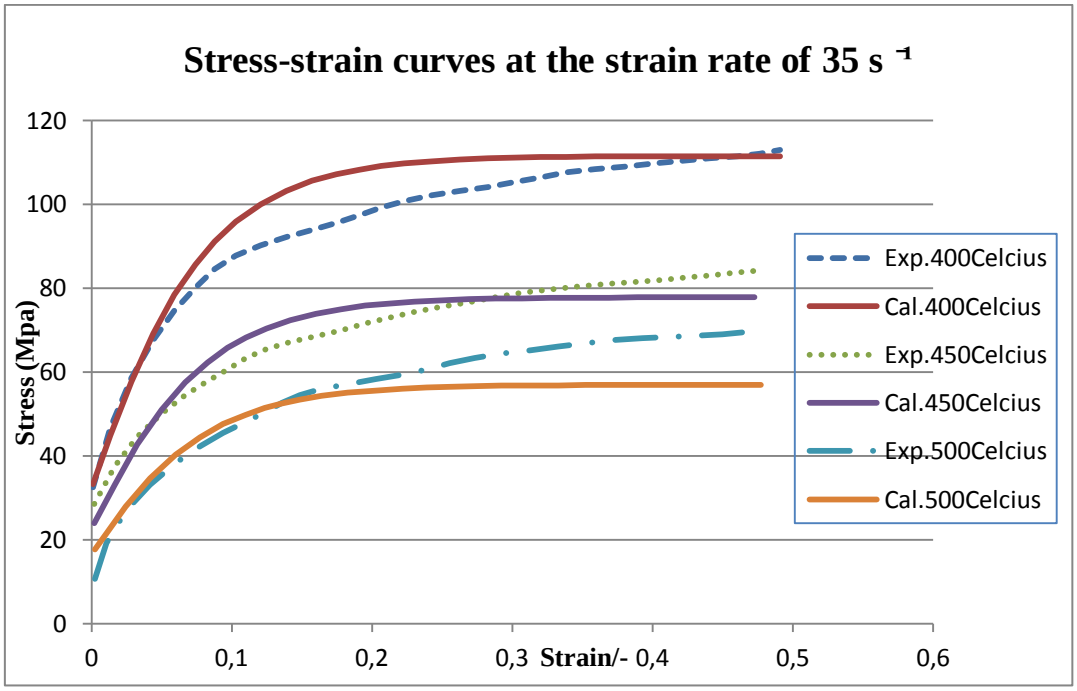

Figure 3.28: Comparison of Experimental and Calculated Results According to Modified Zehner-Hollomon (Tong) Equation at the Strain Rate of 35 s^{-1}

3.5.3 Power-Full MŞMM Equation

The other method used for calculation of stress value is the Power-Full MŞMM equation. The basic equation is given in 3.9. Values of parameters are given in Table 3.5. By using this table equation 3.10 is derived from equation 3.9.

$$\sigma = A\, e^{-m1(T+273)+\frac{-0.15}{\varepsilon}}\, \dot{\varepsilon}^{m3}\, (\varepsilon_0 + \varepsilon)^{\,m5(T+273)+m2+m6\dot{\varepsilon}} \quad \textbf{(3.9)}$$

Table 3.5: Table of Materials Constant used in Power-Full MŞMM Equation

A	m1	m2	m3	m4	m5	m6	ε_0
6061,6	0,0064	-1,659	0,154	-0,1499	0,0004368	0,06597	0,1632

$$\sigma = 6061.6\, e^{-0.0064(T+273)+\frac{-0.15}{\varepsilon}}\, \dot{\varepsilon}^{0.154}\, (0.163 + \varepsilon)^{\,0.0004368(T+273)-1.659+0.06597\dot{\varepsilon}} \quad \textbf{(3.10)}$$

In Fig. 3.29, 3.30, 3.31, 3.32 comparisons of experimental and calculated results of stress-strain curves are presented at different temperatures and different strain rates.

By observing all figures obtained by different equations, dynamic recryctalization can not solved at 35 s^{-1} strain rate and strain hardening takes place. However, dynamic recryctalization finds time to solve at 0, 1 s^{-1}, 1 s^{-1} , and 10 s^{-1} strain rates.

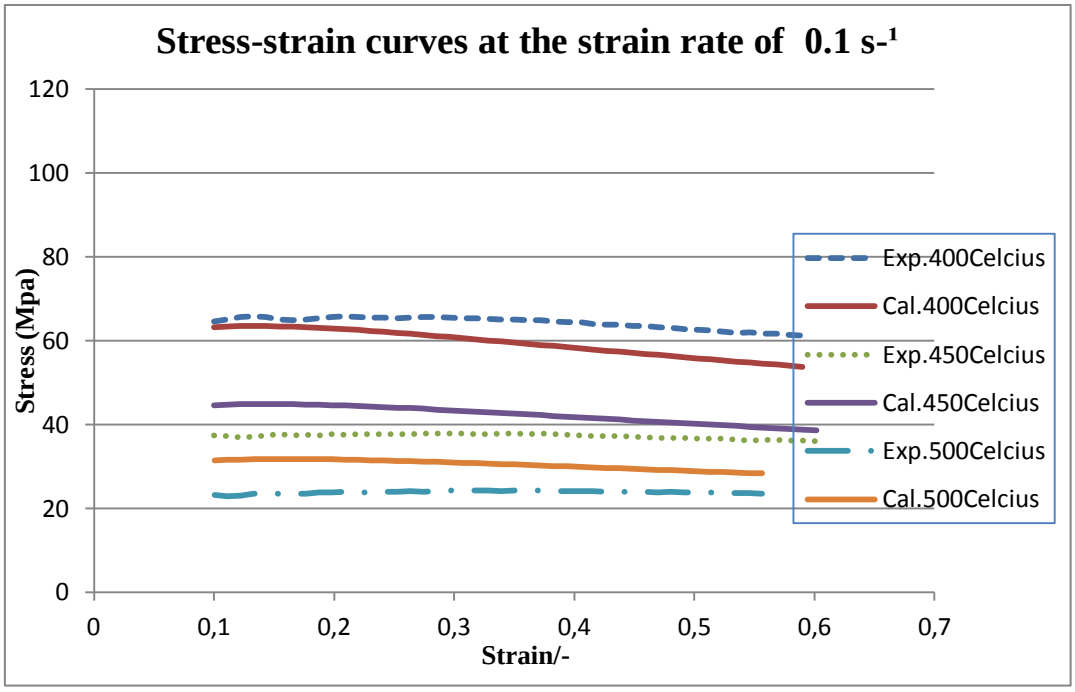

Figure 3.29: Comparison of Experimental and Calculated Results According to Power-Full Equation at the Strain Rate of 0.1 s^{-1}

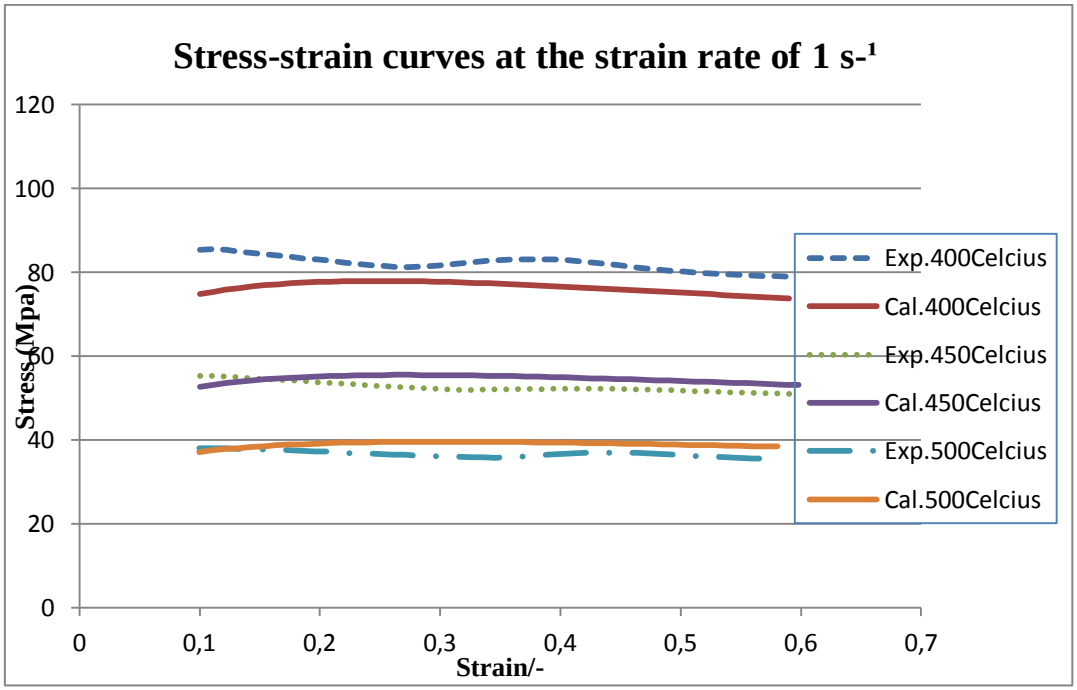

Figure 3.30: Comparison of Experimental and Calculated Results According to Power-Full Equation at the Strain Rate of 1 s^{-1}

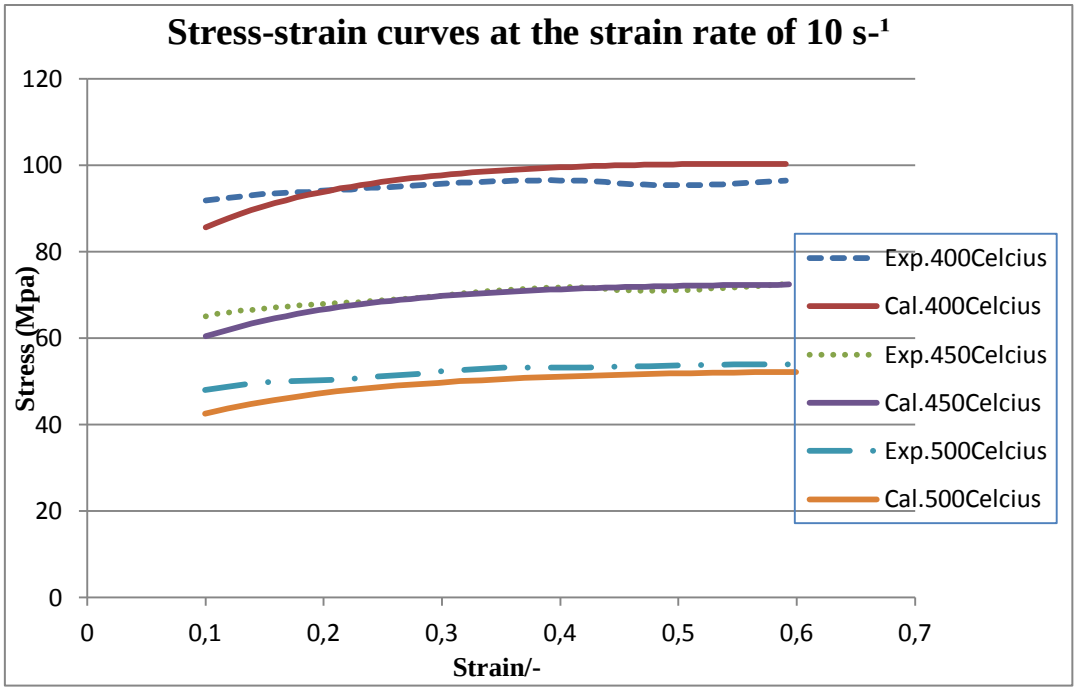

Figure 3.31: Comparison of Experimental and Calculated Results According to Power-Full Equation at the Strain Rate of 10 s^{-1}

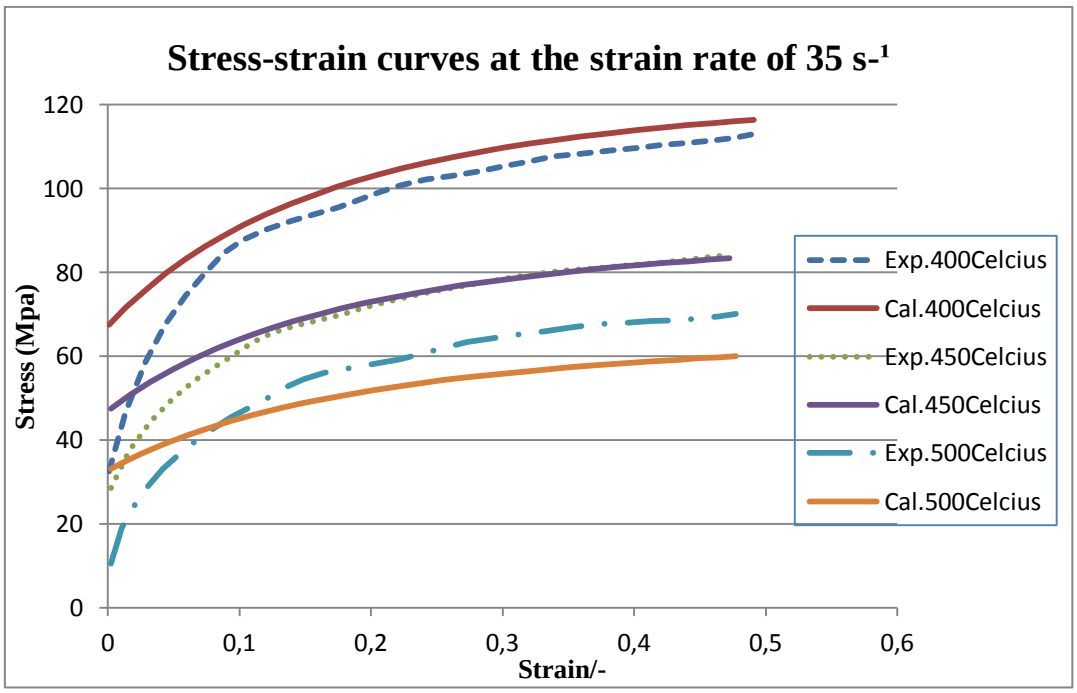

Figure 3.32: Comparison of Experimental and Calculated Results According to Power-Full Equation at the Strain Rate of 35 s^{-1}

CHAPTER 4

FINITE ELEMENT ANALYSIS OF THE FORGING PROCESS

In this chapter, a ring which is being hot forged in a forging company is analyzed by finite element method (FEM). The commercial Finite Element Analysis package; MSc. Marc 2010 is used in this study.

4.1 Simulation Process Parameters for Finite Element Method

In recent years, the finite element method (FEM) has been used to predict and analyze the material deformation during a metal forming operation. The following requirements should be executed to obtain successful finite element results [43].

1. Identify the physical problem
2. The idealization of this problem should be done correctly and assumptions and implications should be identified correctly.
3. Identify the correct spatial discretization conditions such as type of elements used, topology of element mesh, and the density of element mesh should be constructed according to the nature of problem.
4. Identify the boundary conditions applied in the simulation: friction, heat transfer, machines, dies etc.
5. Identify correct material laws and parameters such as flow curve, anisotropy, failure, etc.
6. Identify numerical parameters used in the simulation accordingly: penalty factors, convergence limits, increment sizes, remeshing criterion etc.
7. Optimization of the computational times, the time required to prepare the model and storage requirements of the model and the results are other important factors to obtain desired result. Also the simulation should be economical.
8. The results should be evaluated carefully and checked whether they are valid or not.

4.2 Choosing Analysis Type in FEM

There are generally two types of analysis that are used in industry: 2-D modeling, and 3-D modeling. 2-D FE simulation required much time to complete a simulation due to non-steady state metal flow with manual remeshing. Also 2-D simulation tends to yield less accurate results. 3-D FE simulation is necessary when dealing with asymmetrical complicated parts. When running all data on the fastest computers effectively, 3-D modeling produces more accurate results. The workpiece and dies are modeled by using MARC software, which allows analysis of two-dimensional, axisymmetric forging processes. Figure 4.1 shows modeling of punch, die, symmetry axis and workpiece. Only quarter of its profile was modeled by MARC.

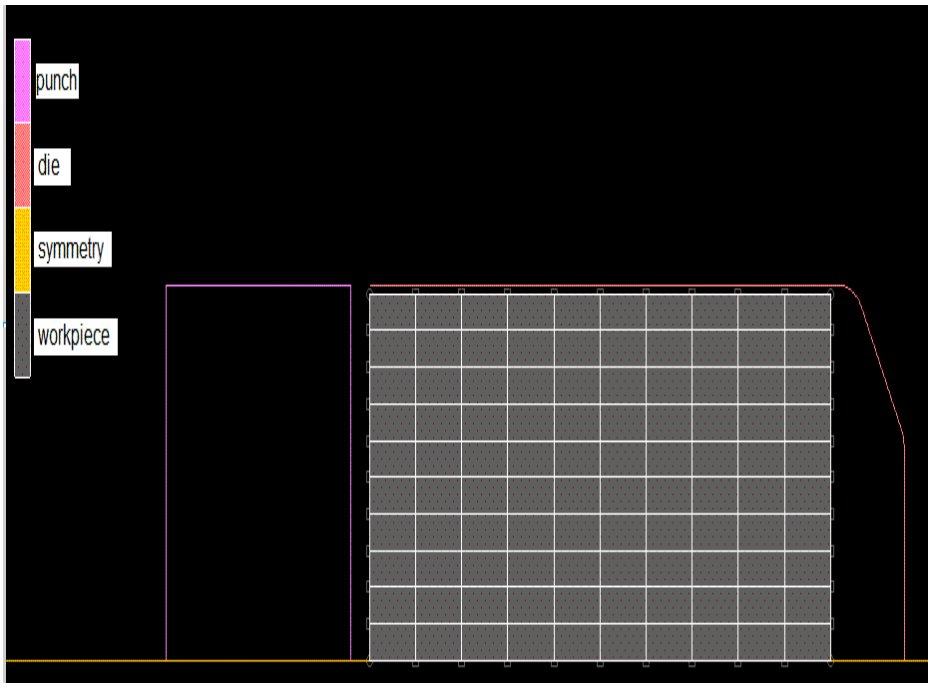

Figure 4.1: Modeling of the Ring, Die and Punch

4.3 Element Types Used in Analyses

The axisymmetric workpiece and dies are modeled by using 4 nodes full integration quadrilateral elements in the analyses. Initial billet have 550 quadrilateral elements with 4 nodes having 0.1 mm edge length. In case of high friction ($m \geq 0.5$) convergence could not be obtained. To eliminate this problem 4 nodes reduced integration quadrilateral are used instead

of full integration elements. It would be better to use 8 nodes (quadratic) elements with reduced integration but there is no remeshing support for 8 nodes in elements in MSc. Marc parameters and details of FEM simulations are tabulated in Table 4.1.

4.4 Remeshing and other Parameters

Remeshing is the process of replacing a distorted mesh with a new undistorted mesh. Meshes can also be classified based upon the dimension and type of elements present. For a 2D mesh, all mesh nodes lie in a given plane. In most cases, 2D mesh nodes lie in the XY plane, but can also be confined to another Cartesian or user defined plane. Most popular 2D mesh elements are quadrilaterals and triangular.

There are three types of remeshing procedures available for two dimensional problems in MSc. Marc Mentat:

- Overlay Quad produces a mesh of quadrilateral elements fitting deformed shape of the workpiece.
- Advancing Front generates quadrilateral elements, a mixed mesh containing both quadrilateral and triangular elements and a complete triangular mesh depending on the choice.
- Mapped mesher creates a mesh composed of only triangular elements.

In the analyses, “advancing front quad” remeshing procedure with completely quadrilateral elements is selected since the initial workpiece is meshed with QUAD (4) elements. Software offers five remeshing criteria to decide under what cases remeshing of the workpiece is performed. These cases are element distortion, tool penetration, increment, angle deviation, strain change and immediate. In the study “strain change” with a maximum value of 0.25 is given the predefined condition for remeshing. When the recorded strain change reaches the value 0.25, the new remeshing occurs**.**

Table 4.1: Parameters used in FEA of Hot Forging Process

ANALYSIS OPTIONS	FEA Program	MSc. Marc
	Material Plasticity Procedure	Rigid-plastic
	Die Material Type	Rigid
	Punch Velocity	According to kinematics of the servo press used
	Number of Steps	200
	Time per Step	0,001s
	Iteration Method	Newton-Raphson
	Remeshing	Global remeshing, advancing front type, depends on element distortion, strain change:0.25
	Max. Element Edge Length After Remeshing	0,1mm
	Number of Elements	Quarter model:550
CONTACT	Friction Model	Shear bilinear displacement
	Relative Sliding Velocity	Default (=0)
MATERIAL	Model	Modified Zehner-Hollomon $\sigma = A\ e^{\frac{Q}{R(T+273)}}\dot{\varepsilon}^{m}(1-\beta e^{-N\varepsilon^{n}})$

In forming simulation, due to the high contact stresses at the interface between workpiece and the die, the constant shear friction factor gives better results than the Coulomb friction coefficient, which is appropriate for use in sheet metal forming. The friction factor is taken in the range of 0.1 to 1.0. Modified Zehner-Hollomon material model is used due to

numerical results obtained in the simulations are in good agreement with the experiment results. Technical information of the machine is given in Appendix A.

4.5 Visualization of Finite Element Results

In order to simulate forging process of the ring, analyses have been performed in the range of 0.1 to 1.0 friction factors at 400 ºC and 500 ºC temperatures. Effective stress distribution and force-time curve results are examined in the postprocess.

4.5.1 Effective Stress Results

When effective stress distribution values given in Figs. 4.2 - 4.11 are examined, it can be seen that hot forging process at 400 C˚ temperature results in higher stress values than 500 C˚ temperatures. Therefore, hot forging process at 400 ˚C temperatures effective stress scale is taken between 50 MPa and 130 MPa. These figures show when shear factor increases, inner diameter of the ring decreases and closes the opening of the ring.

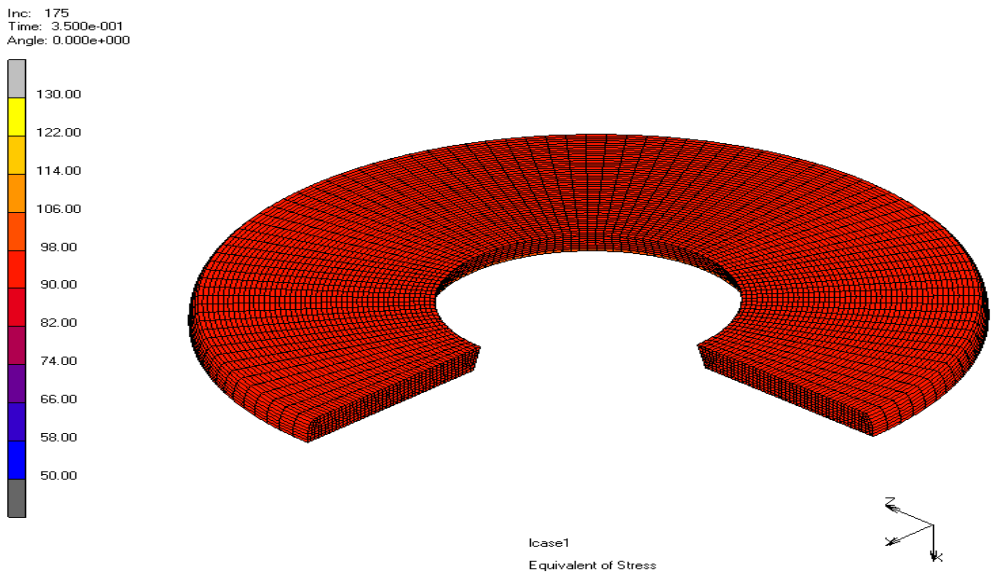

Figure 4.2: Effective Stress (MPa) Distribution of Forging Process at 400 °C with Friction Factor=0.1

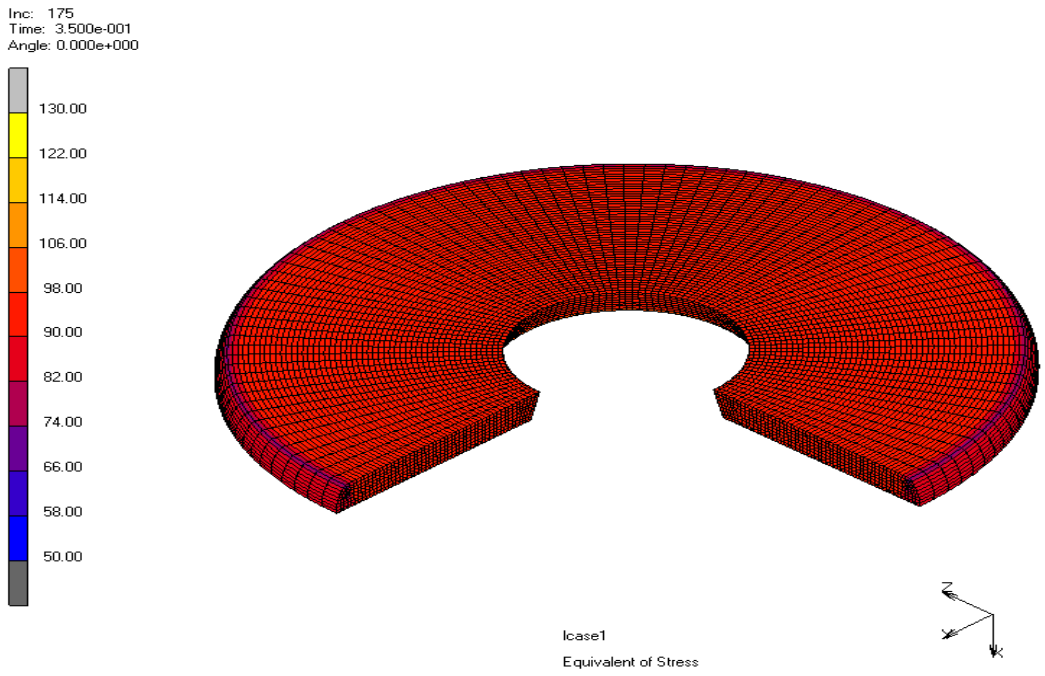

Figure 4.3: Effective Stress (MPa) Distribution of Forging Process at 400 °C with Friction Factor=0.2

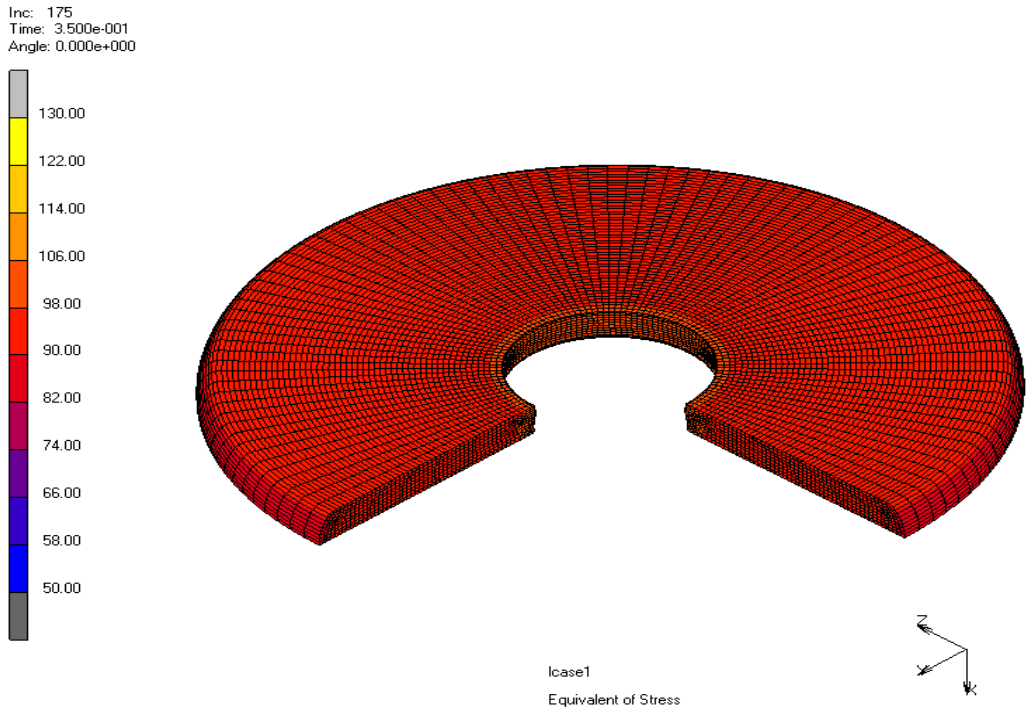

Figure 4.4: Effective Stress (MPa) Distribution of Forging Process at 400 °C with Friction Factor=0.3

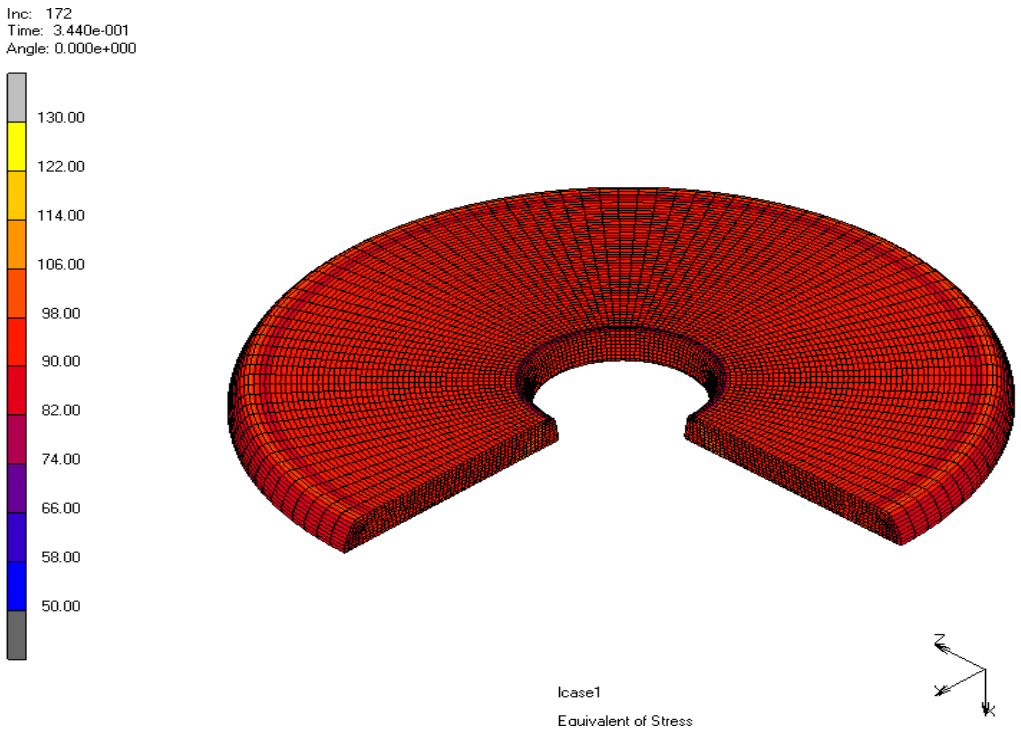

Figure 4.5: Effective Stress (MPa) Distribution of Forging Process at 400 °C with Friction Factor=0.4

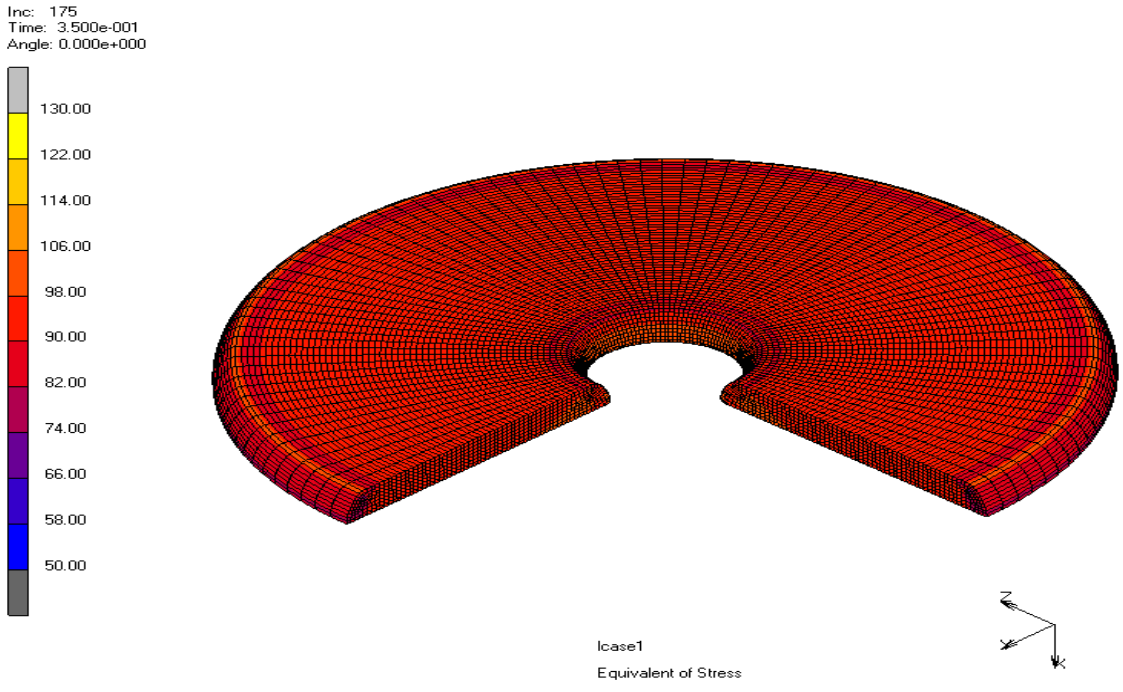

Figure 4.6: Effective Stress (MPa) Distribution of Forging Process at 400 °C with Friction Factor=0.5

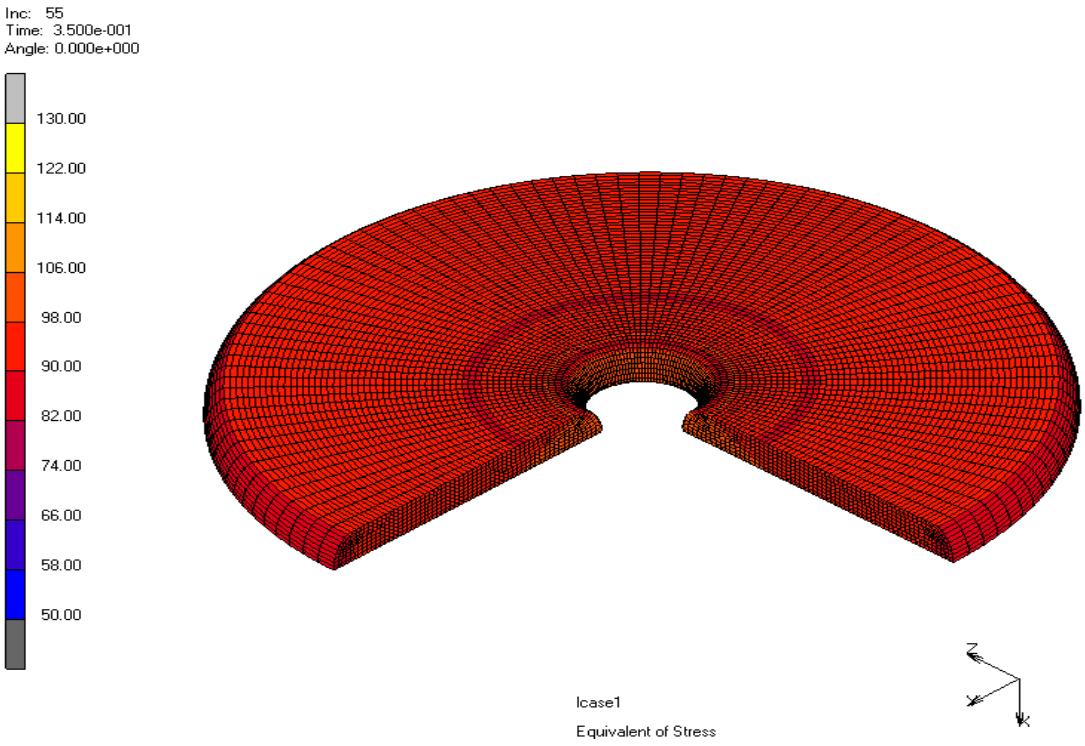

Figure 4.7: Effective Stress (MPa) Distribution of Forging Process at 400 °C with Friction Factor=0.6

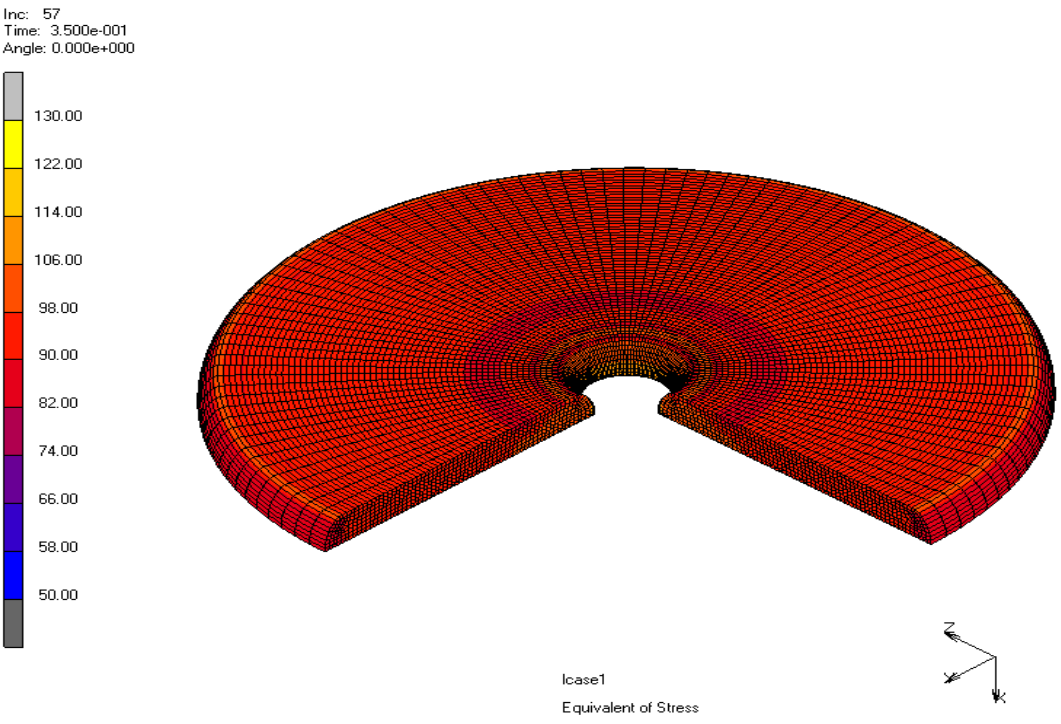

Figure 4.8: Effective Stress (MPa) Distribution of Forging Process at 400 °C with Friction Factor=0.7

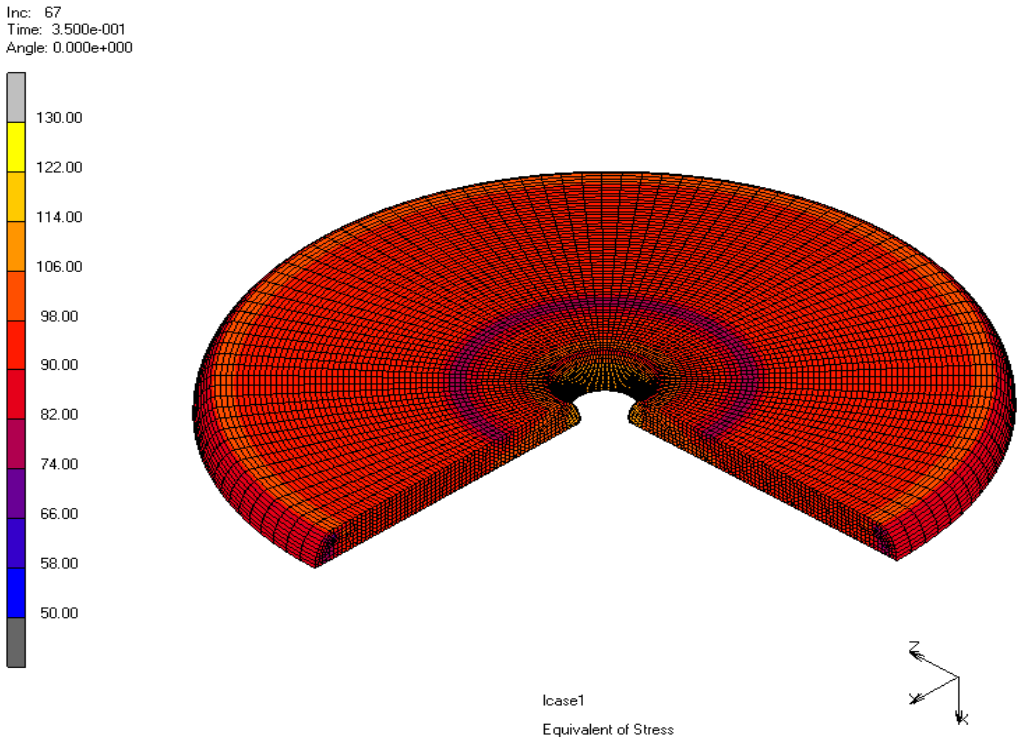

Figure 4.9: Effective Stress (MPa) Distribution of Forging Process at 400 °C with Friction Factor=0.8

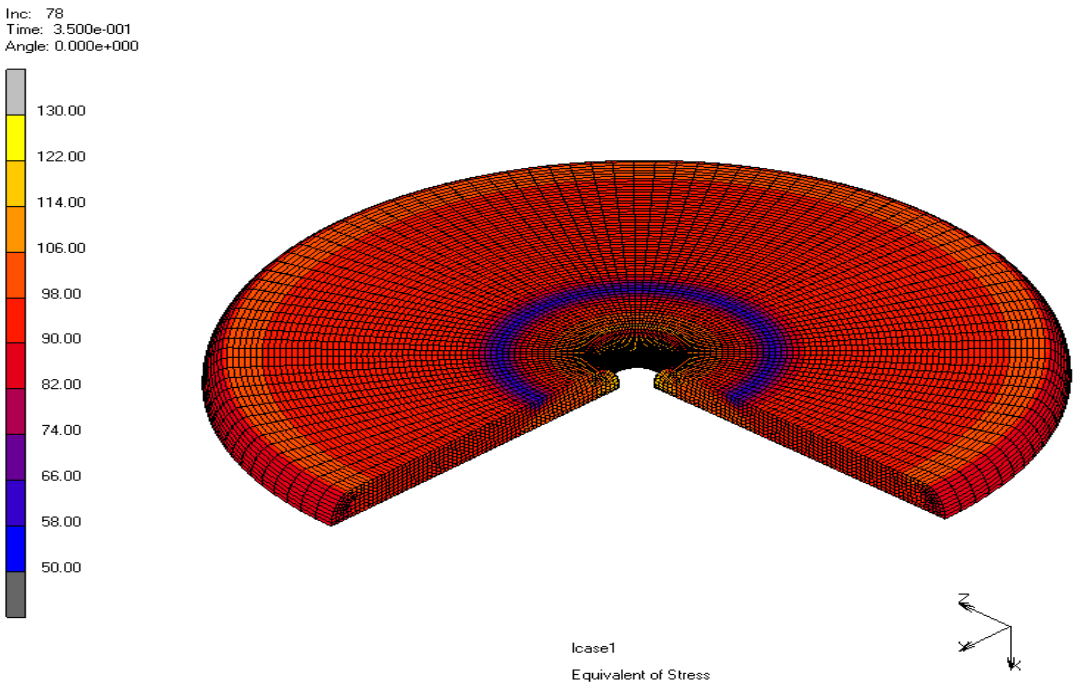

Figure 4.10: Effective Stress (MPa) Distribution of Forging Process at 400 °C with Friction Factor=0.9

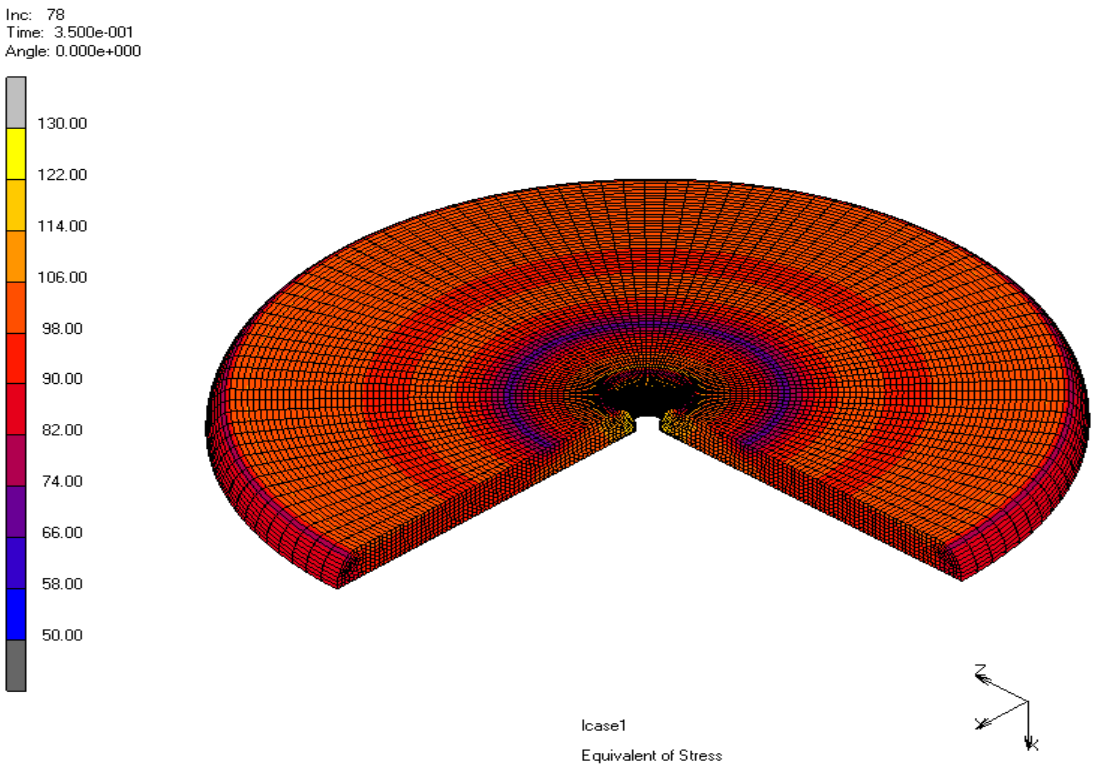

Figure 4.11: Effective Stress (MPa) Distribution of Forging Process at 400 °C with Friction Factor=1.0

Hot forging process at 500 ˚C temperature effective stress scale is taken between 30 MPa and 70 MPa. Effective stress distribution values given in Figs. 4.12 - 4.21 are examined, it can be seen that when friction coefficient is low level, internal diameter increases and expansion of external diameter is large and when friction coefficient is high level, internal diameter decreases and expanding of external diameter is small.

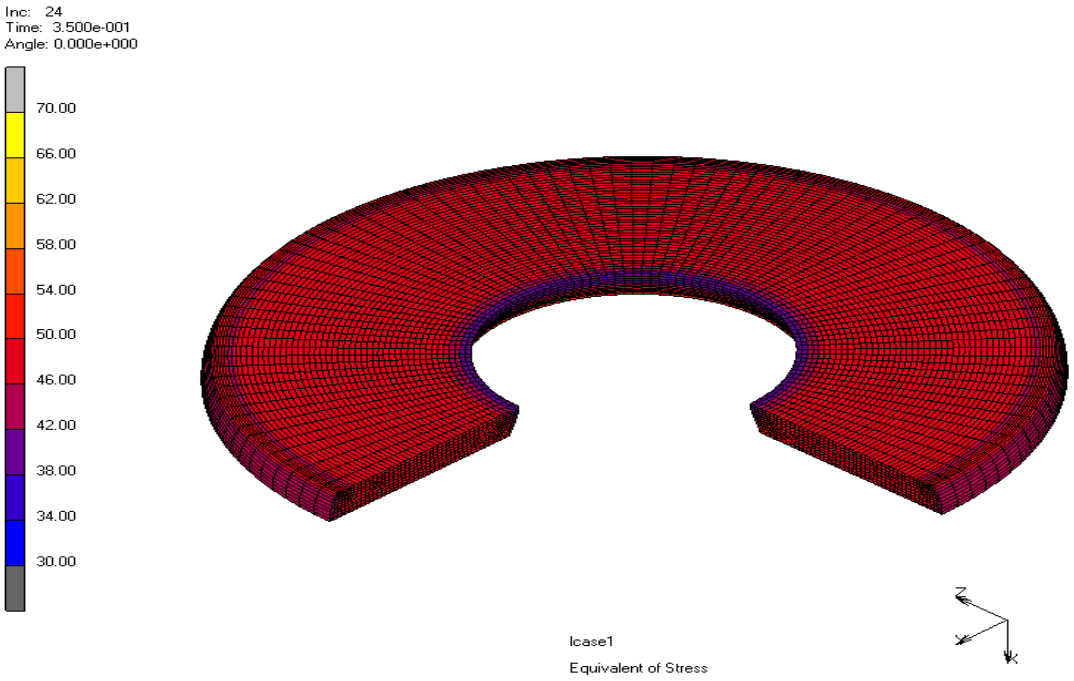

Figure 4.12: Effective Stress (MPa) Distribution of Forging Process at 500 °C with Friction Factor=0.1

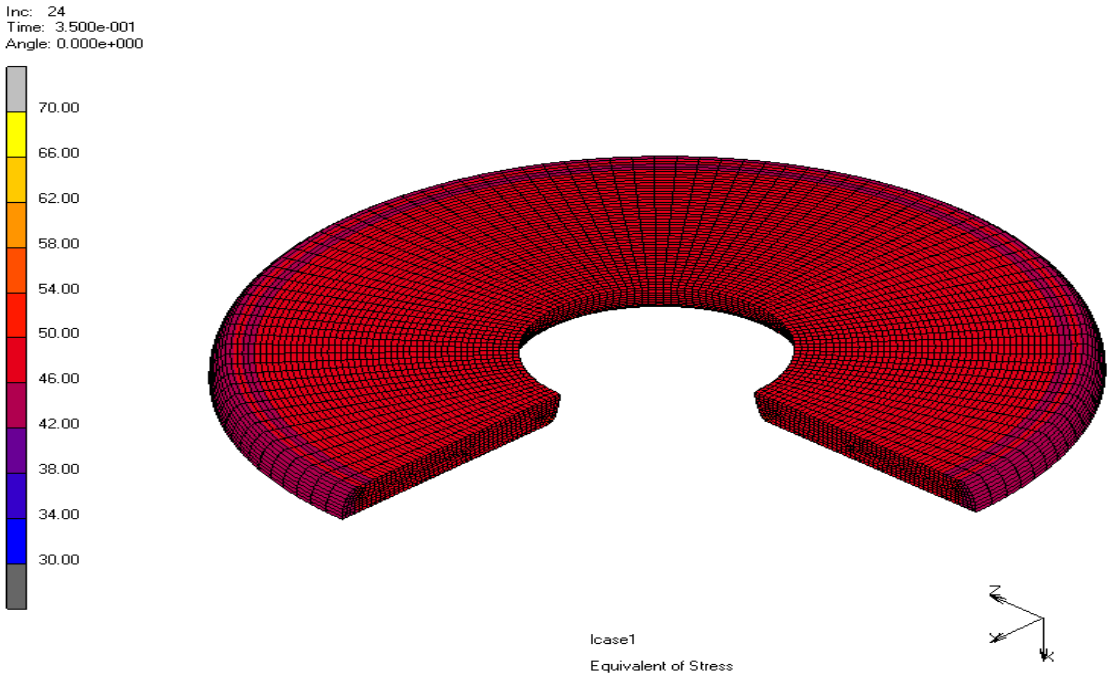

Figure 4.13: Effective Stress (MPa) Distribution of Forging Process at 500 °C with Friction Factor=0.2

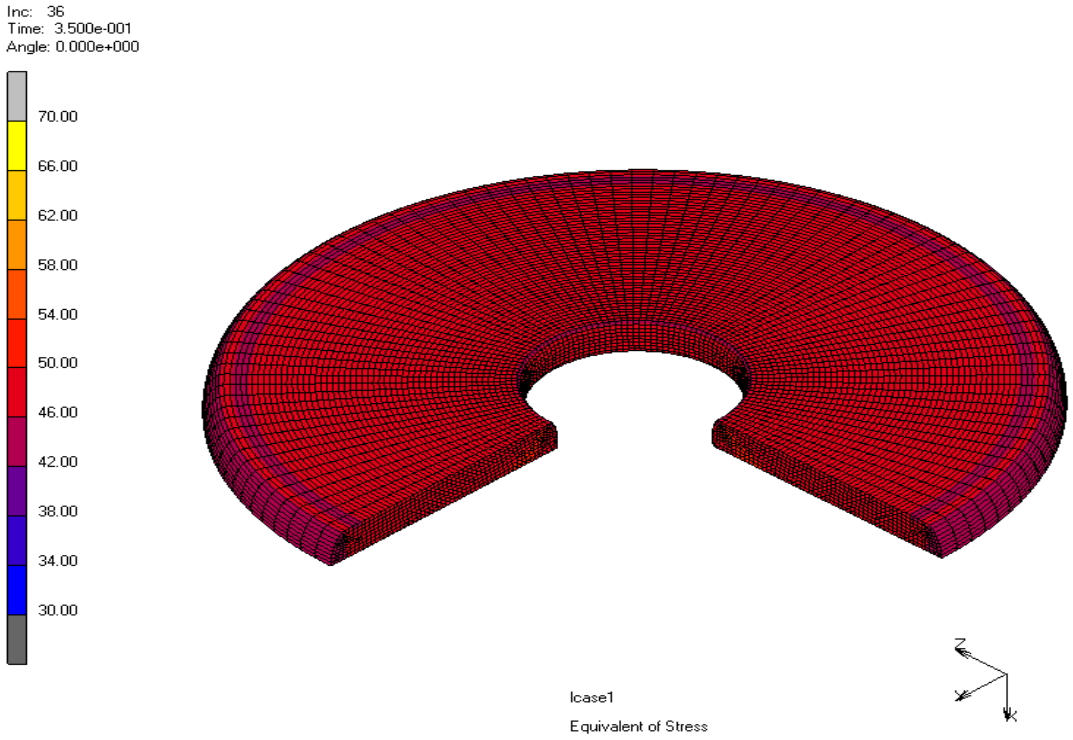

Figure 4.14: Effective Stress (MPa) Distribution of Forging Process at 500 °C with Friction Factor=0.3

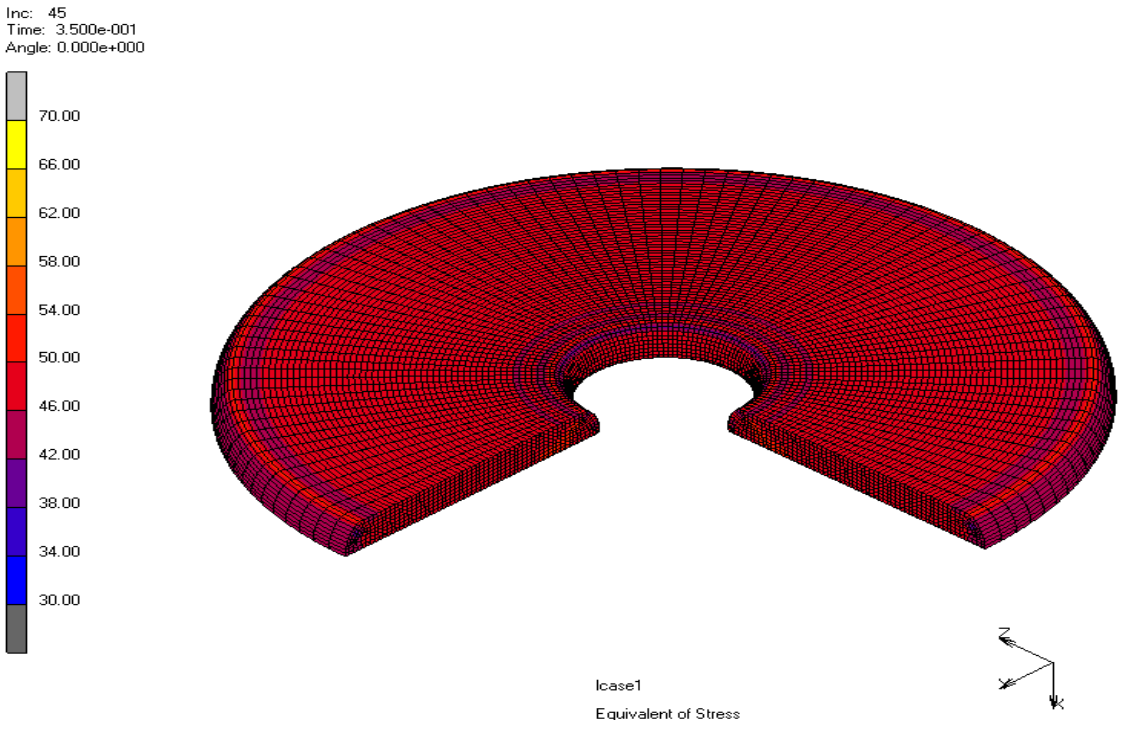

Figure 4.15: Effective Stress (MPa) Distribution of Forging Process at 500 °C with Friction Factor=0.4

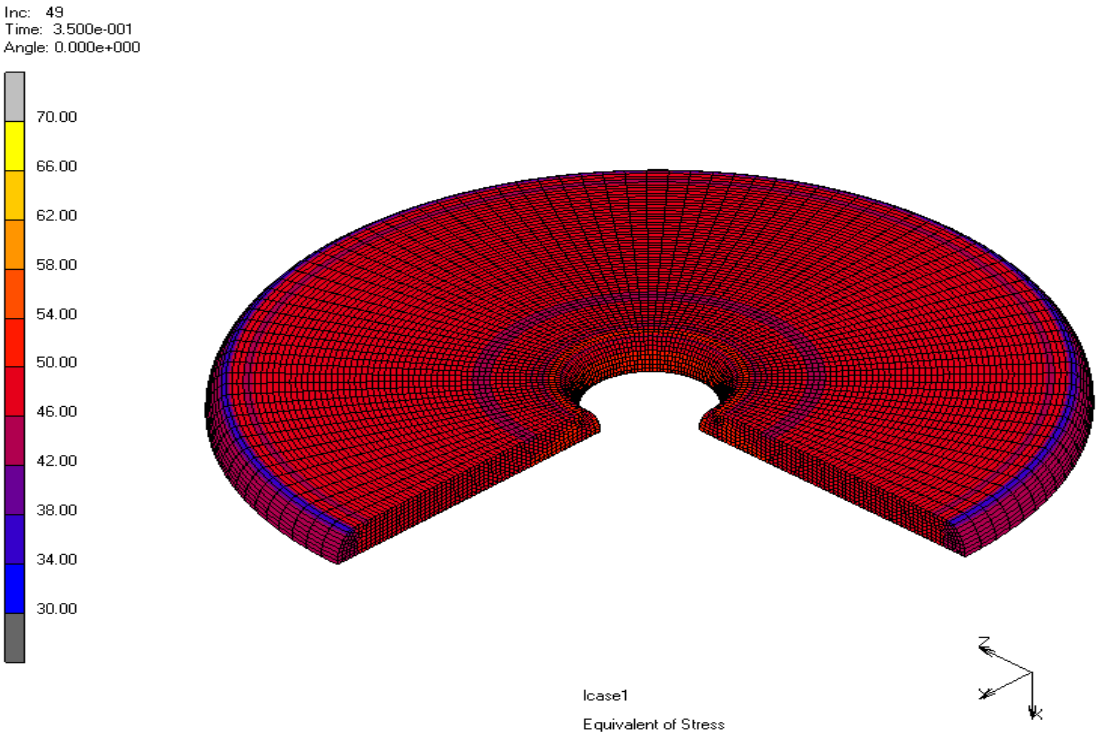

Figure 4.16: Effective Stress (MPa) Distribution of Forging Process at 500 °C with Friction Factor=0.5

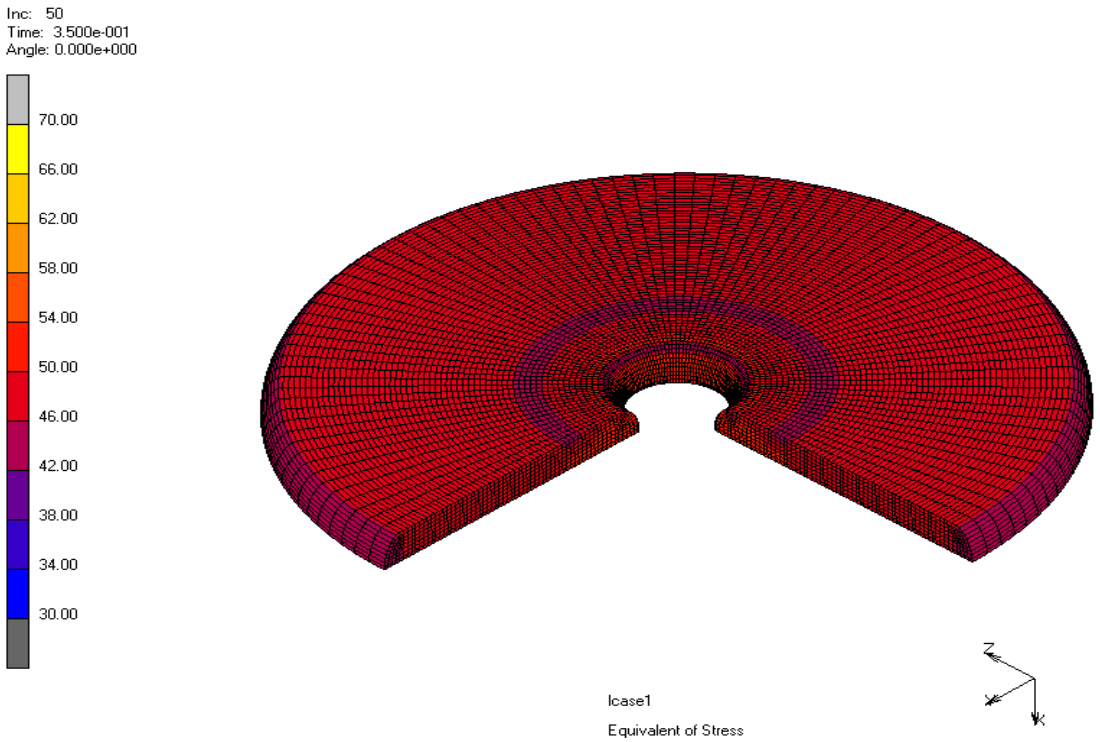

Figure 4.17: Effective Stress (MPa) Distribution of Forging Process at 500 °C with Friction Factor=0.6

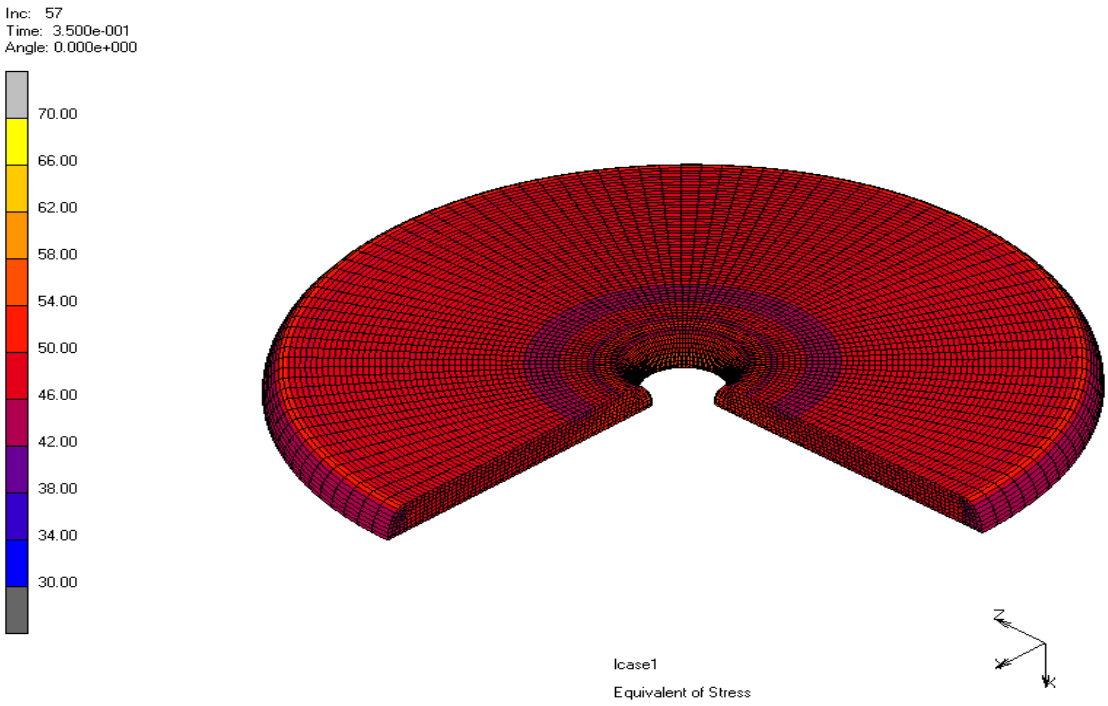

Figure 4.18: Effective Stress (MPa) Distribution of Forging Process at 500 °C with Friction Factor=0.7

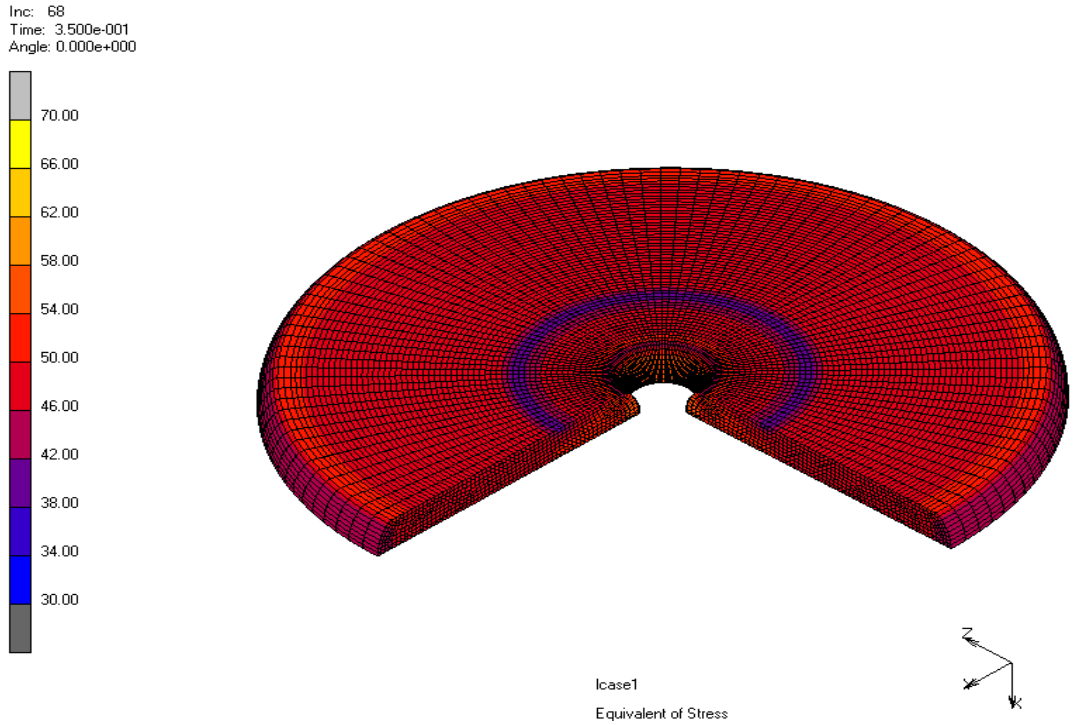

Figure 4.19: Effective Stress (MPa) Distribution of Forging Process at 500 °C with Friction Factor=0.8

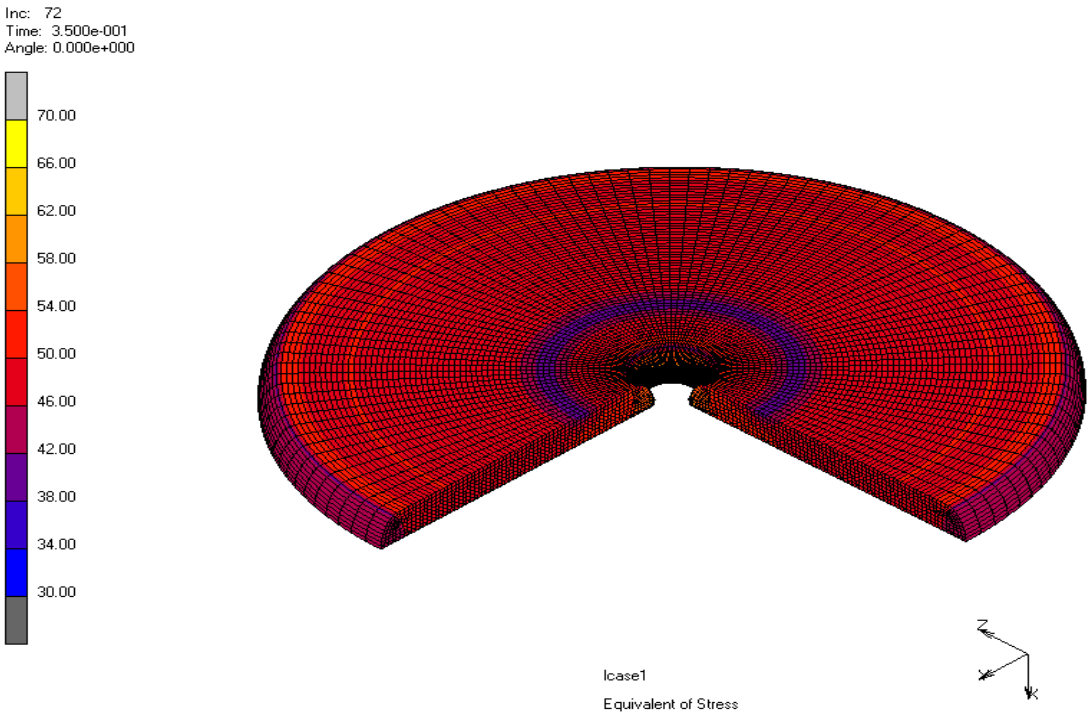

Figure 4.20: Effective Stress (MPa) Distribution of Forging Process at 500 °C with Friction Factor=0.9

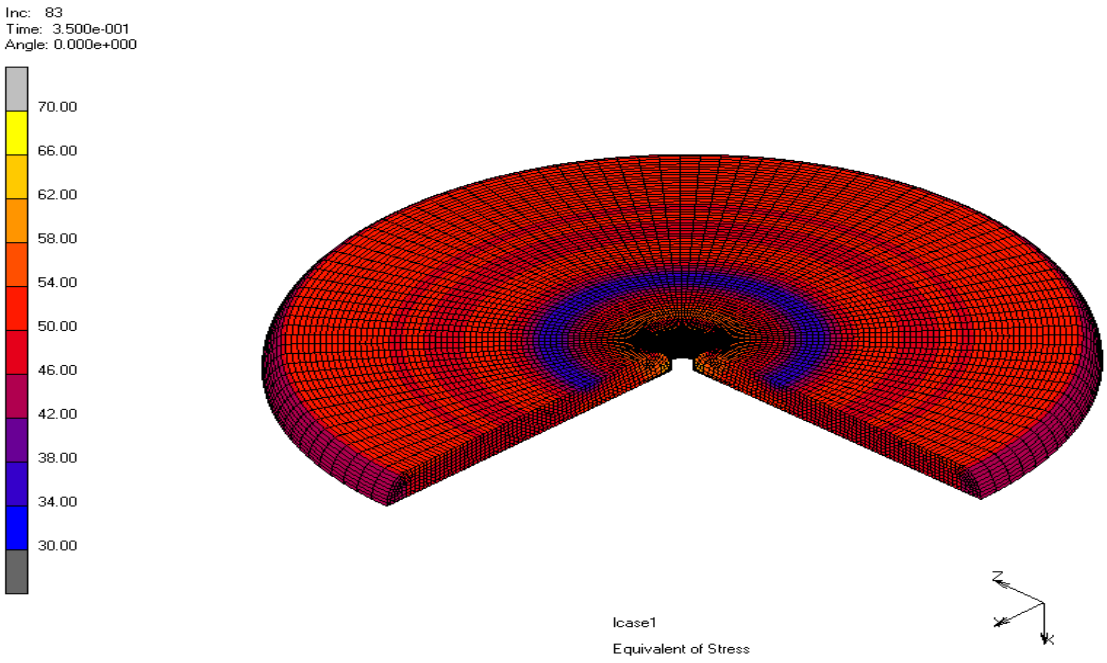

Figure 4.21: Effective Stress (MPa) Distribution of Forging Process at 500 °C with Friction Factor=1.0

4.5.2 Punch Force Results

The required force transmitted from punch to workpiece during deformation is also an important parameter to be observed. Force (N) vs. Time (sec) graph is shown in Figure 4.22 and 4.23. The die forces obtained in hot forging process at 400 ˚C temperature increases according to shear factor value. Therefore, at lower temperatures higher capacity presses are needed to deform the material. Force (N) vs. Time (sec) graph has been performed in the range of 0.1 to 1.0 friction factors at 400 ºC and 500 ºC temperatures.

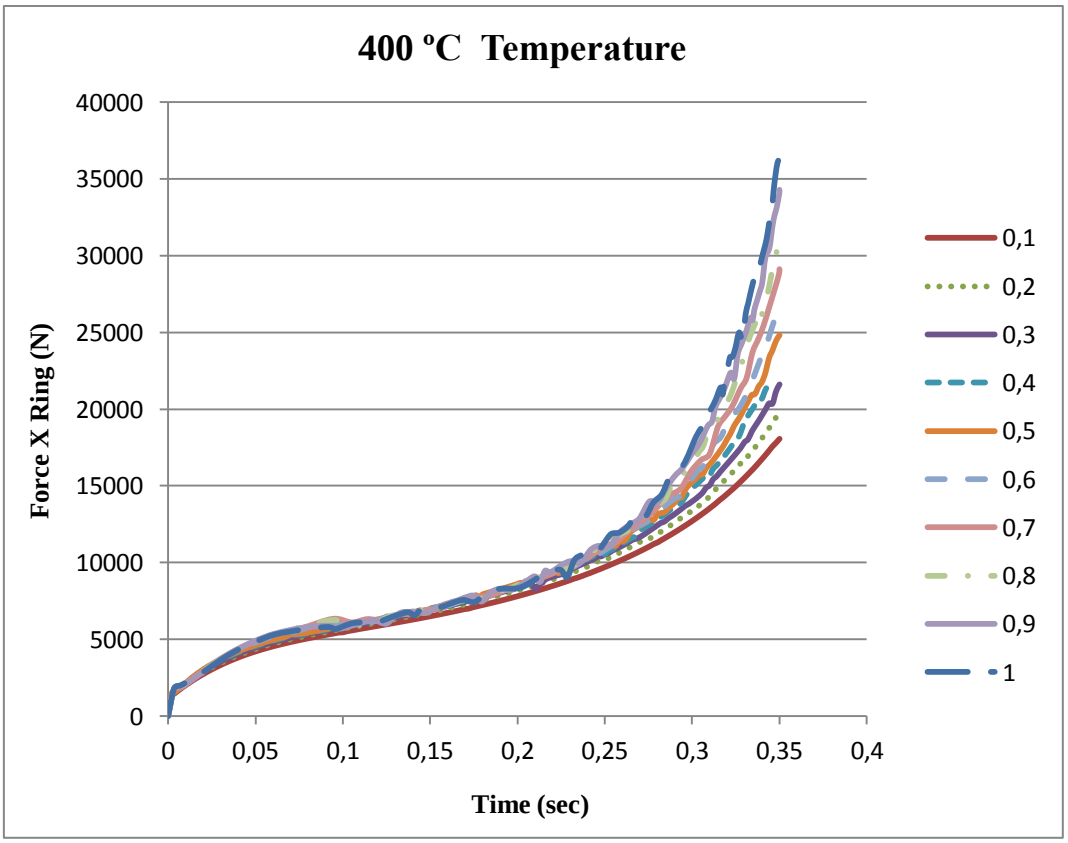

Figure 4.22: Punch Force (N) vs. Time (sec) Diagram for Forging Process at 400 °C Temperature in the range of 0.1 to 1.0 friction factors

The variation at the punch forces may be explained by the differences in the facial clearance values which were determined from the experiments.

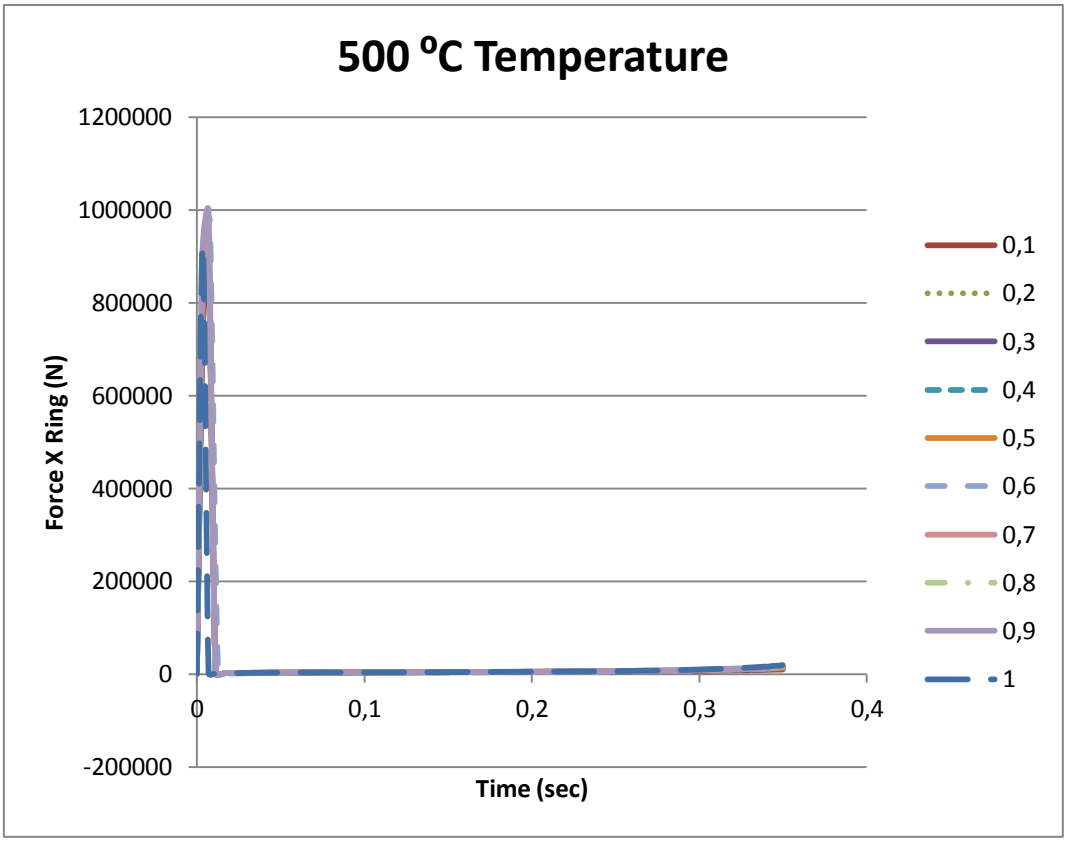

Figure 4.23: Punch Force (N) vs. Time (sec) Diagram for Forging Process at 500°C Temperature in the range of 0.1 to 1.0 friction factors

4.6 Discussion of Finite Element Results

Finite element analyses are performed at 400 and 500 ˚C temperatures within the range of 0.1 to 1.0 friction factors. Effective stress distribution and force-time curve results are examined. Two critical parameters of the analyses which are maximum required punch forces and maximum equivalent stresses of the workpiece for 400 ˚C temperature are listed in Table 4.2.

Table 4.2: Results of Analyses of Max. Values at 400 ˚C Temperature

Shear Factor (m)	Max. Force (kN)	Max. Equivalent of Stress (MPa)
0.1	1.80	102.25
0.2	1.95	101.21
0.3	2.16	101.23
0.4	2.16	100.99
0.5	2.48	105.32
0.6	2.69	104.29
0.7	2.91	107.90
0.8	3.11	112.13
0.9	3.43	119.13
1.0	3.63	124.59

Two critical parameters of the analyses which are maximum required punch forces and maximum equivalent stresses of the workpiece for 500 ˚C temperature are listed in Table 4.3.

Table 4.3: Results of Analyses of Max. Values at 500 ˚C Temperature

Shear Factor (m)	Max. Force (kN)	Max. Equivalent of Stress (MPa)
0.1	9.06	53.15
0.2	9.92	52.36
0.3	1.08	52.57
0.4	1.18	52.38
0.5	1.25	52.79
0.6	1.36	53.06
0.7	1.48	55.08
0.8	1.61	57.30
0.9	1.70	60.39
1.0	1.87	63.23

The maximum effective stress values and required forces are increasing with increased shear factor value because of increasing deformation. The maximum equivalent stress becomes 124.6 MPa and maximum required force becomes 3.63 kN at the 400 ºC temperature as seen in Table 4.2. However, the maximum equivalent stress values of the workpiece are lower than the yield strength of proposed material for punches, forming dies and counterpunches. These show that, the plastic strains are not expected on the die sets during the processes. The maximum equivalent stress becomes 63.23 MPa and maximum required force becomes 9.92 kN at the 500 ºC temperature as seen in Table 4.3. As seen from the results when temperature increases effective stress decreases.

CHAPTER 5

DISCUSSION OF RESULTS

In this study, initially, forging process of ring shaped parts which is currently produced at the hot forging temperature range has been analyzed. The analysis results by FEM simulation provide determination of the friction factor and better products in dimension and quality.

Ring compression test are applied at 400 ºC and 500 ºC temperatures, %20 mm/s and %100 mm/s press velocities (%100 press velocity is approximately equals to 330 mm/s velocity), 2mm and 3,5 mm reduction of materials, dry or lubricated conditions. Friction coefficients are determined according to these parameters. The dilatometer test is performed at 0.1 1/s, 1 1/s, 10 1/s and 35 1/s strain rates and 400 ˚C, 450 ˚C and 500 ˚C temperatures. There repetitive tests are performed for all conditions.

Two dimensional finite element analyses have been performed to simulate the hot forging process of rings. In order to simulate forging process of the ring, analyses have been performed in the range of 0.1 to 1.0 friction factors at 400 ºC and 500 ºC temperatures. The simulations show how temperature, press velocity, reduction of material and lubrication existence factors affect metal flow and ring geometry. Equivalent stress distribution and punch force vs. time graph for the workpiece have been given and the results of the analyses have been compared with the sample parts.

Following calibration curves at 400 ºC and 500 ºC have been obtained with respect to finite element simulations and experiments for this case study:

The friction values are consistently around 0.5 with lubricated condition and around 1.0 with dry condition at 400 °C, as can be seen in Figure 5.1. A value of 1 for m denotes that the material sticks on the surface, whereas 0 describes the perfect slip. This is a value indicating sticking friction, which would be expected for hot steel forging with no lubrication.

The friction values are consistently around 0.65 with lubricated condition and around 1.0 with dry condition at 500 °C, as can be seen in Figure 5.2. Comparison of these results with the calibration curves technique shows that the proposed method is quite acceptable.

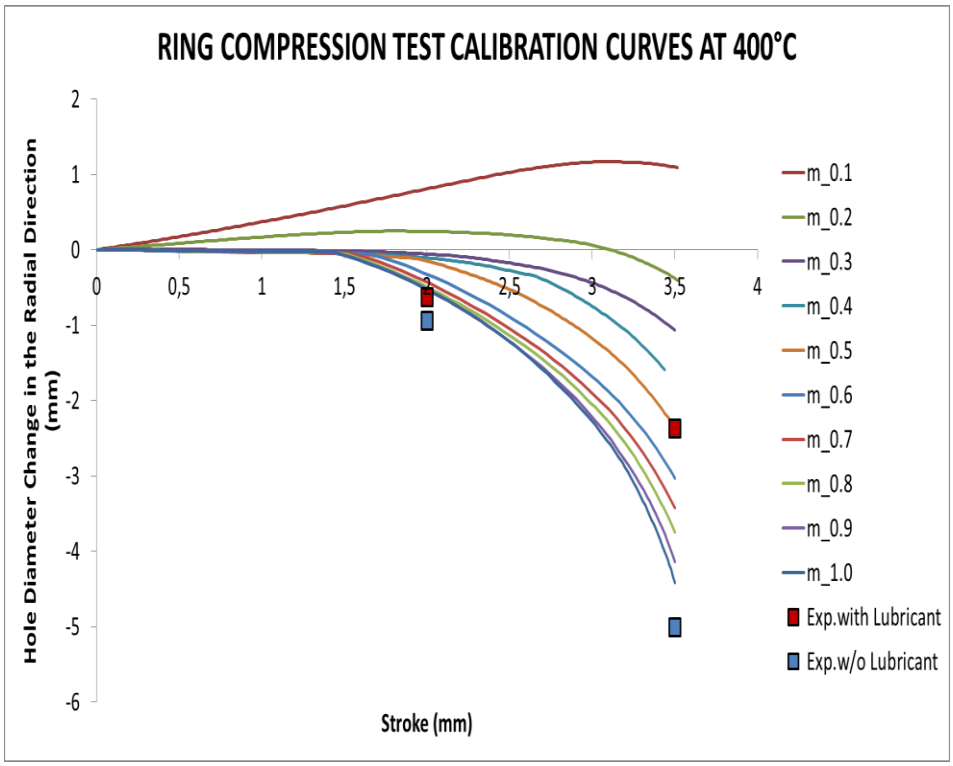

Figure 5.1: Ring Compression Test Calibration Curves with Experimental Results at 400 °C

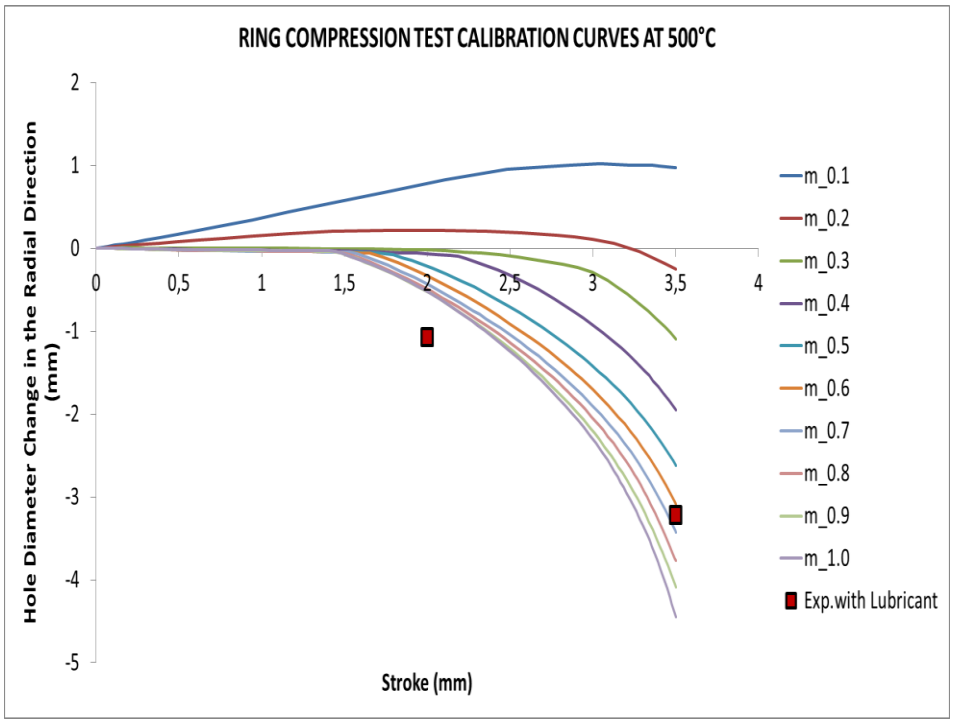

Figure 5.2: Ring Compression Test Calibration Curves with Experimental Results at 500 °C

CHAPTER 6

CONCLUSIONS AND FURTHER RECOMMENDATIONS

6.1 General Conclusion

In conclusion, following general results have been obtained with respect to finite element simulations and experiments for this case study:

1. Several tests are performed at 500 ˚C temperature and 10 1/s strain rate in order to determine the effect of the waiting time on stress value for 1minute, 10 minutes and 100 minutes. Due to no explicit effect of the waiting time on stress values, all other thermo mechanical deformation tests were carried out at 1minute waiting time.
2. Forging test could not be applied at 500 ˚C temperature without lubricant condition because of the mold and the workpiece sticking to each other.
3. In case of high friction ($m \geq 0.5$) convergence could not be obtained. To eliminate this problem 4 nodes reduced integration quadrilaterals are used instead of full integration elements. It would be better to use 8 nodes (quadratic) elements with reduced integration but there is no remeshing support for 8 nodes in elements in MSc. Marc
4. On the basis of experimental results of ring tests for aluminum alloys, models for calculation of flow stress are investigated according to three methods. Comparison of those methods leads to the conclusion that Modified Zehner-Hollomon method used for numerical results obtained in the simulations are in good agreement with the experimental results.
5. The maximum effective stress values and required forces are increasing with increased friction factor value because of increasing deformation.
6. The maximum equivalent stress becomes 124.6 MPa and maximum required force becomes 3.63 kN at the 400 ºC temperature. However, the maximum equivalent stress values of the workpiece are lower than the yield strength of proposed material for

punches, forming dies and counterpunches. These show that, the plastic strains are not expected on the die sets during the processes.

7. The maximum equivalent stress becomes 63.23 MPa and maximum required force becomes 9.92 kN at the 500 ºC temperature.
8. The variation in the punch force is due to different quantities of elements in material and facial clearance values used in the experiments.
9. The results of simulation show that, as temperature decreases the maximum effective stress and the required punch force values increase and it becomes difficult to deform the material.
10. It is observed that, as the temperature decreases the surface finish quality increases.
11. During finite element simulations, it has been observed that the effect of springback phenomena to the dimensions of the formed parts is negligible. This is also a reason of the condition that dimensions obtained from FEA models and measured from actual samples almost match with each other.
12. Any forging defects like folds, laps and unfilled regions related to flow of material have not been observed in the final product.
13. The friction values are consistently around 0.5 with lubricated condition and around 1.0 with dry condition at 400 °C.
14. The friction values are consistently around 0.65 with lubricated condition and around 1.0 with dry condition at 500 °C.
15. It is observed that, the numerical results obtained in the simulations are in good agreement with the experiment results.

6.2 Recommendations for Future Works

Recommendations for future works of this study are given as follows:

- Numerical analyses may be performed by different finite element programs.
- Die sets can be analyzed to see the effects of hot forging.
- Different types of aluminum alloy materials with different geometries of parts can be studied.
- Numerical analyses may be performed with different friction models. Other friction models that take the effect of sliding velocity, surface roughness into consideration are to be compared with the friction models used in this thesis.
- To improve productivity in mass production, tool life and wear analyses can be made for the dies.
- In hot forging operations where the contact pressures are high, different boundary lubrication conditions will be performed and the models can be used to predict the coefficient of friction.

REFERENCES

[1] Edward M. Mielnik, “Metalworking Science and Engineering”, McGraw-Hill Company, Inc., 1991.

[2] DeGarmo E. P., Black J. T., Kohser R.A., “Materials and Processes in Manufacturing”, Prentice-Hall International Inc., New York, 1997.

[3] T. Altan, G. Ngaile, G.Shen, “Cold and Hot Forging: Fundamentals and Applications”, ASM International, 2005.

[4] P.H. Kim, M.S. Chun, J.J. Yi, Y.H. Moon, “Pass Schedule Algorithms for Hot Open Die Forging”, Journal of Materials Processing Technology.

[5] Degarmo, E. Paul, Black, J T. & Kohser, Ronald A., “Materials and Processes in Manufacturing” (9th ed.), Wiley, 2003.

[6] Y.H. Kim, T.K. Ryou, H.J. Choi, B.B. Hwang, “An Analysis of the Forging Processes for 6061 Aluminum-Alloy Wheels”, Journal of Materials Processing Technology, 2002.

[7] T. Altan, F. W. Boulger, J. R. Becker, N. Akgerman, H. J. Henning, “Forging Equipment, Materials and Practices”, Battelle Columbus Laboratories Metalworking Division, Ohio, 1973.

[8] Lecture notes, Surananee University of Technology, 2007.

[9] George E. Dieter, “Mechanical Metallurgy”, McGraw Hill Kogakusha, Ltd., Tokyo, 1976.

[10] Ohiou.edu [On-Line], 2005, Available at:

http://www.ent.ohiou.edu/~raub/manufacturing/forging.htm.

[11] Forging Design Handbook, American Society for Metals, Ohio-USA, 1972.

[12] Z.Marciniak, J.L.Durcan, S.J.Hu, "Mechanics of Sheet Metal Forming".

[13] Moderncasting.com [On-Line], 2005, Available at: http://www.moderncasting.com.

[14] Vasquez. and Altan, T. "New Concepts in Die Design – Physical and Computer Modeling Applications", 2000, p. 212-223.

[15] A. Thomas, M. El-Wahabi, J.M. Cabrera, J.M. Prado, "High Temperature Deformation of Inconel 718", Journal of Materials Processing Technology 177 (2006) 469–472.

[16] B.-A. Behrens, "Finite Element Analysis of Die Wear in Hot Forging Processes", CIRP Annals - Manufacturing Technology 57 (2008) 305–308.

[17] William R.D. Wilson, Steven R. Schmid, Jiying Liu, "Advanced Simulations for Hot Forging: Heat Transfer Model for use with the Finite Element Method", Journal of Materials Processing Technology 155–156 (2004) 1912–1917.

[18] M.S. Joun, H.G.Moon, I.S.Choi, M.C.Lee, B.Y.Jun, "Effects of Friction Laws on Metal Forming Processes", Tribology International 42 (2009) 311–319.

[19] Hasan Sofuoğlu, "On the Measurement of Friction Coefficient Utilizing the Ring Compression Test", Department of Mechanical Engineering, Karadeniz Technical University, Volume 32, Issue 6, June 1999, Pages 327‑335.

[20] Kaguchı Shin, Tezuka Keıta, Yoshıno Fumıhero, Watanabe Shın'ıchı, Ouchı Kıyoshı, "In si-tu Measurement of Friction Coefficient by Ring Compression Test" Bulletin of Hachinohe Institute of Technology, Japan.

[21] Ishızuka Shızuo, Mızutanı Yoshısuke, "Influence of Surface Roughness on Friction Properties", Journal of Japanese Society of Tribologists, Japanese.

[22] Keith P. Savage, “Investigation of Friction Measurements at CSM for Hot Steel Forging Applications”, Department of Metallurgical and Materials Engineering, Undergraduate, Colorado School.

[23] S.B. Petersen, P.A.F. Martins, “Friction in Bulk Metal Forming: A General Friction Model vs. the Law of Constant Friction” N. Bay, Journal of Materials Processing Technology 66 (1997) 186- 194.

[24] Y.G. An, H. Vegter, “Analytical and Experimental Study of Frictional Behavior in Through-Thickness Compression Test”, Journal of Materials Processing Technology 160 (2005) 148–155.

[25] Prof. Dr.-Ing. Bernd-Arno Behrens, Dipl.-Ing. Falko Schäfer, Dipl.-Ing. André Hundertmark, Dr.-Ing. Anas Bouguecha, “Numerical Analysis of Tool Failure in Hot Forging Processes”, 17th International Scientific and Technical Conference, “Design and Technology of Drawpieces and Die Stamping” Poznań-Wąsowo, 22-24 September 2008.

[26] R.S. Lee, J.L. Jou, “Application of Numerical Simulation for Wear Analysis of Warm Forging Die”, Department of Mechanical National Cheng Kung University, Taiwan, Journal of Materials Processing Technology 140 (2003) 43–48.

[27] Lirio Schaeffer, Alberto M.G.Brito, Martin Geier, “Numerical Simulation using Finite Elements to Develop and Optimize Forging Processes”, Metal Work Laboratory, Universidad Federal do Rio Grande do Sul, Porto Alegre, Brazil.

[28] Prof. A. Erman Tekkaya, “A Guide for Validation of FE-simulation in Bulk Metal Forming”, Department of Manufacturing Engineering, Atılım University, The Arabian Journal for Science and Engineering, Volume 30, Number 1C.

[29] Nefissi N.; Bouaziz Z. &Zghal A., “Prediction and Simulation of Axisymmetric Forging Load of Aluminum”, Advances in Production in Engineering &Management, 2008.

[30] J.Horsinka, J.Kliber, K.Drozd, I.Mamuzıc, “Approximation Model of the Stress-Strain Curve for Deformation of Aluminum Alloys”, Faculty of Metallurgy and Materials Engineering, Metalurgija 50 (2011) 2, 81-84.

[31] Vesna Mandić, Milentije Stefanović, “Friction Studies Utilizing the Ring-Compression Test-Part1”, Department of Mechanical Engineering, University of Kragujevac, 8 th International Tribology Conference , Beograd, 8. -10. Oktobra 2003.

[32] K. Fisher, H. Schweiger, J. Hasenberger and H.Dremel, “New Tool Steel for Warm and Hot Forging”. The Use of Tool Steels: Experience and Research, Proceedings of the 6th International Tooling Conference, Karlstad, Sweden, September 10-13, 2002, pp.129-139.

[33] I. J. Polmear, Light Alloys, Arnold, 1995.

[34] K. Siegert, D. Ringhand and R. Neher, “Designing of Forgings”, University at Stuttgart, 1994.

[35] [On-Line] Available at: http://www.precisionsheetmetal.com/home/materials.htm, Retrieved 2009-07-26.

[36] Degarmo, E. Paul; Black, J T.; Kohser, Ronald A., “Materials and Processes in Manufacturing”, (9th ed.), 2003.

[37] Source: Mat Web, the Online Materials Database.

[38] [Online] Available at: http://www.azom.com/RapraBooks.aspx http://www.azom.com/books-a-z.aspx.

[39] [Online] Available at: www.forgemag.com, Forging-Die Material Development from Research to Implementation.

[40] Gustavo G. Schiuma, “Die Lubricants for Hot Forging”, FORGELUBE.

[41] Sofuoğlu, H., Gedikli, H., Rasty, J., "Determination of Friction Coefficient by Employing the Ring Compression Test", Transactions of ASME, Journal of Engineering Materials and Technology, Vol. 123, 2001, pp. 338-348.

[42]V. Ĉernik, "Determination of Stress-Strain Curves of Aluminum Alloys by Compression Test", Thesis, Ostrava, 2000.

[43] İsbir, S. S., "Finite Element Analysis of Trimming", M.S. Thesis, 2002, p.24, Middle East Technical University, Ankara.

APPENDIX A

TECHNICAL DATA OF THE PRESS

Specifications		Unit	Nominal
Capacity		kN	800
Capacity generation position		mm	5
Slide stroke		mm	130
Max. speed		1/min	75
Die height		mm	320
Slide adjustment amount		mm	80
Slide dimensions	L-R	mm	550
	F-B	mm	450
Shank hole dimension		mm	50.5
Bolster dimension	L-R	mm	800
	F-B	mm	600
	Thickness	mm	140
Main(servo)motor		kW	15
Balancer capacity		kg	190